EXPERIMENTAL TECHNIQUES FOR THE ISOLATION OF PANCREATIC STELLATE CELLS

M. JALALI

MPhil **2012**

EXPERIMENTAL TECHNIQUES FOR THE ISOLATION OF PANCREATIC STELLATE CELLS

Thesis submitted in accordance with the requirements of the University of Liverpool for the degree of Master of Philosophy

By

Mehdi Jalali

May 2012

CONTENTS

MAY 2012

DECLARATION & STATEMENT OF ORIGINALITY

I hereby certify that this thesis is the result of my own work. The material within this thesis has not been presented wholly or in part for any other degree or qualification.

The research was undertaken in the Department of Molecular and Clinical Cancer Medicine, Liverpool Cancer Research UK Centre, University of Liverpool.

H/E stains of patient tissue sections were provided by Dr Fiona Campbell, Department of Pathology, The Royal Liverpool University Hospital. All other procedures were carried out by myself.

ABSTRACT

Experimental Techniques for the Isolation of Pancreatic Stellate Cells Mehdi Jalali

Background: Two decades ago the pancreatic stellate cell (PSC) was identified as the cell type predominantly responsible for the 'desmoplastic reaction' associated with pancreatic cancer. PSCs have since been found to exhibit a great deal of interaction with cancer cells in vitro and in vivo. This feature, combined with their contribution to the stromal reaction, makes PSCs fundamental to pancreatic cancer progression. Understanding the mechanisms which mediate the transformation of stellate cells from their non proliferative quiescent state, to their tumour promoting activated state is vital, since inactivation of stellate cells in pancreatic tumours should reduce the mass of fibrotic tissue in and around the tumour, and enable better delivery of chemotherapeutic agents.

Methods: Attempts were made to isolate PSCs from pathological human pancreatic tissue using an 'explant' method. Cells which grew from the tissue were propagated and characterised according to morphology and the fluorescent expression of stellate cell markers: alpha SMA, GFAP, desmin, vimentin.

Results: Primary cells were isolated from 10 patients who possessed a variety of pancreatic diseases. Characterisation revealed three distinct cell types, one of which most closely resembled the PSC due to its morphology and expression of cell markers. However, several difficulties encountered during characterisation, particularly the lack of suitable cell controls, meant that it was not possible to identify these primary cells as PSCs.

Alpha SMA and GFAP were expressed in the primary cells, and antibody binding was specific according to isotype control stains. Unfortunately, the immortalised PSCs that were utilised as a positive cell control failed to exhibit alpha SMA. Furthermore, numerous epithelial cancer cell lines unexpectedly expressed GFAP, desmin, and vimentin. Around eighty flasks of primary cells were cryopreserved for use in future experiments. Two of the primary cell samples, along with the immortalised PSC line were taken forward for preliminary investigations of microRNA-29 expression. However, this yielded inconclusive data.

Discussion: A subsequent literature search revealed several studies which also demonstrated the mesenchymal characteristics of epithelial cancer cells. This suggests that specific binding may well have taken place in our experiments. As a result of the work described in this thesis,

there are now stocks of tumour derived- and inflammatory derived primary pancreatic cells, which following complete characterisation, will be ready to be utilised as an adjunct to the epithelial cancer cell lines frequently used for pancreatic cancer research in this laboratory.

ACKNOWLEDGEMENTS

I firstly wish to thank my supervisors Dr Eithne Costello-Goldring, Reader in Molecular Biology, and Dr Bill Greenhalf, Senior Lecturer in Molecular Biology, University of Liverpool, for their help and guidance throughout this degree.

I am very grateful to Dr Fiona Campbell, Department of Pathology, for dissecting pancreatic tissue samples for my primary cell culture, and also for providing H/E photographs which are displayed later on in this thesis. I would also like to thank Dr Margaret Roebuck for sharing her expertise regarding primary cell culture.

I am also grateful to the post-doctoral researchers within the Department of Molecular and Clinical Cancer Medicine, in particular Dr Claire Jenkinson for her advice throughout the year, as well as the other postgraduate research students for their help in teaching me various laboratory techniques, including Mr Paul Sykes for showing me how to carry out Immunofluorescence microscopy.

Finally, I have to thank the Royal College of Surgeons of England and the Jean Shanks Foundation for providing me with the necessary funds to undertake this postgraduate degree.

LIST OF ABBREVIATIONS

Bone marrow	BM
Bovine serum albumin	BSA
Bromodeoxyuridine	BrdU
Common bile duct	CBD
Complementary DNA	cDNA
Connective tissue growth factor	CTGF
Crossing point	Cp
Dulbecco's modified Eagle medium	DMEM
Dimethyl Sulfoxide	DMSO
Epidermal growth factor	EGF
Epithelial to mesenchymal transition	EMT
Ethylenediaminetetraacetic acid	EDTA
Extracellular matrix	ECM
Extracellular matrix metalloproteinase inducer	EMMPRIN
Endoscopic retrograde cholangiopancreatography	ERCP
Basic fibroblast growth factor	FGF2
Foetal bovine serum	FBS
Familial Pancreatic Cancer	FPC
Good clinical laboratory practice	GCLP
Glial Fibrillary Acidic Protein	GFAP
Head of pancreas	HOP
Hepatic stellate cell	HSC
Immunofluorescence	IF
Interleukin	IL
Iscove's modified Dulbecco's medium	IMDM
Laboratory information management system	LIMS
Liverpool Experimental Cancer Medicine Centre	LECMC
Major histocompatibility complex	MHC

MicroRNA	miRNA
Millilitre	mL
Messenger RNA	mRNA
Monocyte chemoattractant protein 1	MCP-1
Magnetic resonance cholangiopancreatography	MRCP
Neuropilin-1	NRP-1
Nucleotide	nt
Pancreatic intraepithelial lesion	PanIN
Pancreatic ductal adenocarcinoma	PDAC
Pancreatic stellate cell	PSC
Protease activated receptor-2	PAR-2
Phosphate buffered saline	PBS
Platelet derived growth factor	PDGF
Precursor microRNA	pre-miRNA
Primary microRNA	pri-miRNA
Randomised Controlled Trial	RCT
Reactive oxygen species	ROS
Roswell Park Memorial Institute	RPMI
Royal Liverpool University Hospital	RLUH
Smooth muscle actin	SMA
Secreted protein acidic and rich in cysteine	SPARC
Standard operating procedure	SOP
Transforming growth factor beta	TGFβ
Tumour necrosis factor alpha	TNFα
Terminal deoxynucleotidyl transferase dUTP nick end labelling	TUNEL
Urokinase-type plasminogen activator	uPA
Tissue plasminogen activator	tPA
Vascular endothelial growth factor	VEGF
Vascular endothelial growth factor receptor	VEGF-R

CHAPTER 1:

INTRODUCTION

1.1 Anatomy and Physiology of the Pancreas

The pancreas is a retroperitoneal organ, approximately 15 cm in length. It can be anatomically split into the head, neck, body and tail [1]. The head, which contributes to around half the mass of the organ, is embraced on its right side by the C-shaped curve of the duodenum [2]. The neck is a slight constriction which connects the head to the body of the pancreas [4]. The body gradually tapers to form a tail, which lies in close proximity to the left colic flexure of the colon and the splenic hilum [1].

The postero-inferior surface of the stomach rests upon the anterior surface of the pancreas body, and the two organs are separated by omental bursa [2]. The pancreas body is devoid of peritoneum on its posterior side, and the aorta, superior mesentery artery, and left kidney are in close proximity. Lienal and pancreaticoduodenal branches of the hepatic and superior mesenteric arteries supply blood to the pancreas, and lienal and superior mesenteric veins drain the pancreas [4].

The cells which populate the pancreas can be split into two main histological cell types: exocrine and endocrine cells. The exocrine portion of the organ is involved in digestion and consists of a network of ducts, which at their terminal end expand into sac-like structures called acini [5]. These ducts carry a fluid consisting of proenzymes and bicarbonate solution called pancreatic juice towards the ampulla of Vater for entry into the duodenum. The endocrine cells group together within the exocrine tissue to make up the Islets of Langerhans, and these cells play a major role in sugar metabolism [6].

1.2 Pancreatic cancer

Pancreatic cancer is a highly aggressive disease, representing the most lethal type of digestive cancer and the fourth leading cause of cancer-related mortality in the developed world [7;8]. Its poor prognosis is epitomised by a 5 year survival of less than 5%. The poor prognosis is somewhat related to the anatomical site, by which patients tend to develop symptoms late on in the course of the disease, already having developed locally advanced or metastatic disease at the time of presentation [9].

1.2.1 Epidemiology

The cause of pancreatic cancer remains unknown although several risk factors have been implicated including smoking, a family history, advanced age, male gender, chronic pancreatitis, diabetes mellitus, and a diet high in meats and low in vegetables. The dominant risk factors that have been studied are smoking and family history. Resected pancreatic cancers from patients who smoke contain more genetic mutations than those from non-smokers [10], and the risk of pancreatic cancer in smokers is 2.5 to 3.6 times greater than that in non-smokers. This risk is dose dependent according to the amount of tobacco use and the length of time exposed to tobacco smoke [9].

Approximately, 7 to 10% of sufferers have a positive family history of pancreatic cancer and are diagnosed with familial pancreatic cancer (FPC) [11]. FPC is inherited in an autosomal dominant fashion, and can be defined as a family which harbours at least two first-degree relatives that have been diagnosed with pancreatic cancer [12]. A person who has one first degree-relative with pancreatic cancer is reported to be 9 times more likely to develop the disease [11]. The risk of getting FPC is over 50 times as high in families with 4 or more affected members in contrast to families with no affected members. Many cases of FPC have been identified throughout the world, though for the majority no disease gene has been identified [12]. The most common germline mutation to cause FPC is an alteration in a DNA mismatch repair gene called BRCA2, where 5-20% of families with FPC harbour this mutation [12;13].

1.2.2 Pathogenesis of pancreatic cancer

Pancreatic ductal adenocarcinoma (PDAC) accounts for over 90% of pancreatic cancers. Less common subtypes include mucinous cystic neoplasms, colloid carcinomas, adenosquamous PDAC, and neuroendocrine tumours [4]. Around 75% of ductal adenocarcinomas occur in the head of the pancreas, 15-20% occur in the body, and around 5-10% occur in the tail of the pancreas [8]. Ductal adenocarcinoma of the pancreas head manifests as a white/yellow, firm mass which frequently expands to obstruct the adjacent common bile duct or main pancreatic duct. Microscopically, these tumours vary in appearance according to the degree of tumour differentiation, where poorly differentiated tumours exhibit less gland formation and mucus production, but greater epithelial anaplasia. A dense fibrous matrix envelops the ductal adenocarcinoma, and surrounding tissue often displays regions of Chronic Pancreatitis (CP). These areas are characterised by fibrosis, atrophy of glandular tissue, and dilation of ducts [1;6]. Infiltration of ductal adenocarcinoma into vascular and perineural spaces, as well as intra and peripancreatic lymph nodes, is also commonly viewed [4].

Ductal adenocarcinoma has been proposed to evolve through several noninvasive precursor lesions each of which vary morphologically. These include pancreatic intraepithelial neoplasia (PanIN), mucinous cystic neoplasms (MCN), and intra-ductal papillary mucinous neoplasms (IPMN) [14].

MCNs are composed of mucin-producing epithelial cells with a distinctive ovarian-type stroma. The majority contain focal areas of atypia which may eventually develop into carcinoma [15]. Compared to the other two precursor types, MCNs are the least frequent precursor to pancreatic cancer. A relationship between MCN and ductal adenocarcinoma is based on a studies which found invasive adenocarcinoma in around one-third of resected MCNs, and detected common genetic mutations between the two diseases (KRAS2, TP53, and SMAD4) [16;17]. However, these studies were observational and so do not provide direct evidence to demonstrate the progression of MCNs to PDAC. Furthermore, patients with ductal adenocarcinoma from resected MCNs have 5-year survival rates of around 60%, which is much higher than that associated with sporadic pancreatic cancer. Therefore, adenocarcinoma from MCN should be considered separately to adenocarcinoma from sporadic PDAC.

IPMNs are large mucin-secreting neoplasms (>5 mm). They are usually located in the exocrine tubes of the pancreas. This is unlike MCNs, which are found distant from the pancreatic ductal system, and only occasionally communicate with it through the creation of erosions or fistulae [15]. There is similar controversy regarding the role of IPMNs as a precursor lesion to PDAC. Research findings which link IPMNs to PDAC have also stemmed from observational studies. These included histological and genetic analyses, with the latter revealing common germline mutations including KRAS2, p16, TP53, and SMAD4 [17;18].

The most common neoplastic precursors to invasive adenocarcinoma of the pancreas are PanINs. These lesions are microscopic and so are not directly visible by pancreatic imaging. Molecular profiling studies have revealed a high number of common genetic alterations between PanINs and PDAC, including KRAS2, p16, TP53, and SMAD4 [19]. The prevalence of common somatic genetic alterations increase as the amount of cytological and architectural atypia in PanINs increase [11]. Therefore, the development of PanINs can act as a useful model to demonstrate pancreatic cancer progression.

PanIN development may be separated into 3 stages, beginning with ductal cell hyperplasia (PanIN-1A and 1B), followed by atypical hyperplasia (PanIN-2), and the formation of carcinoma in situ (PanIN-3) [14]. Low-grade PanINs (PanIN-1) are common in the elderly population, and PanIN-3 lesions are frequently present adjacent to PDAC on histological examination of resected tissue [20].

Activation of the KRAS2 oncogene, along with telomere shortening are believed to be the earliest known genetic abnormalities recorded during ductal adenocarcinoma formation, and have been detected in PanIN-1A and 1B lesions. The KRAS2 gene is up-regulated in over 90% of advanced ductal adenocarcinomas resulting in subsequent atypical activation of the signalling pathways controlling cell proliferation and cell survival [9]. Telomere shortening has been linked to chromonsomal instability [11].

CDKN2A inactivation has been noted in PanIN-2 lesions, and occurs in 95% of invasive ductal adenocarcinomas. This mutation activates proliferative signalling through loss of p16, a protein involved in the control of the G1 to S phase transition during the cell cycle [11;14]. TP53 and SMAD4 inactivation has been detected in advanced precursor lesions (PanIN-3). TP53 is a gene that regulates the function of DNA damage checkpoints, which usually

monitor the growth of regular cells. Therefore, its down-regulation which is present in 50-75% of pancreatic tumours results in genomic instability. SMAD4 expression is lost in approximately half of pancreatic tumours, resulting in aberrant signalling by TGFβ, a growth factor with a multitude of roles in pancreatic cancer [4;9].

Hence, almost all patients with fully established pancreatic cancer carry one or more of these four genetic defects. More recently, Jones et al [21] performed a comprehensive genetic analysis of 24 early pancreatic tumours. The results suggest that the genetic basis of pancreatic cancer is extremely complex and heterogeneous. Each tumour contained an average of 63 genetic alterations which could be organised into a core set of 12 signalling pathways. However, key mutations in each pathway varied between tumours from different patients, and not all tumours harboured alterations in all pathways.

Somatic mutations can be utilised as molecular markers in order to observe the evolution of pancreatic cancers. Studies have shown that an initial precursor neoplastic clone such as PanIN-1 will take more than 10 years to become malignant, and a further few years to metastasise. Analysis of molecular alterations revealed that almost all of the driver genes are mutated by the time a primary pancreatic cancer has developed into an invasive adenocarcinoma. These results highlight the potential benefit of screening patients during this 10 year period in which a primary cancer may reside in the pancreas before becoming locally invasive [22;23].

1.2.3 Clinical features, diagnosis and staging

As mentioned above the majority of pancreatic tumours arise in the head of the pancreas. When these tumours grow large enough they compress the common bile duct causing obstructive cholestasis, typified by jaundice, dark urine and pale stools. General symptoms of pancreatic cancer include nausea, and a deep, dull abdominal pain that broadly localises to the tumour area, as well as systemic manifestations such as weight loss and anorexia [9]. Signs on physical examination apart from possible jaundice may include hepatomegaly, a palpable Virchow's node, or palpable cervical lymph nodes [1].

Most people who present with symptoms attributable to pancreatic cancer have advanced disease, where the pancreatic tumour is typically large and has invaded beyond the confines of the pancreas [1]. One of the main reasons that pancreatic cancer has such a dismal prognosis is our inability to diagnose the disease at its earliest stages. The development of a highly sensitive and highly specific blood based biomarker for pancreatic cancer, which could be used to screen individuals is the current focus of many research efforts.

Currently, CA 19-9 is a biomarker used for therapeutic monitoring in pancreatic cancer, and early detection of recurrent disease in patients with known pancreatic cancer. Its use as a screening tool has had poor results however. Its limitations include a low specificity for pancreatic cancer, in that the levels of CA 19-9 may be raised in other diseases such as cholestasis as well [9]. As well as being highly sensitive and highly specific, an ideal biomarker for pancreatic cancer would exist in the blood at concentrations which correlate accurately with disease burden and response to treatment. Moreover, it would be measurable using a quick, easy to use and widely available assay. This would provide a more economical means of monitoring tumour burden than using standard imaging methods, thus benefiting the patient through reduced radiation exposure [7]. Screening pancreatic cancer for diagnosis in its early stages would not only offer potentially life-saving treatment for the patient, but also provide scientists with tissue samples of early stage pancreatic cancer that could be utilised for research. However, the benefit of screening must be balanced against the risk of false diagnoses whereby healthy individuals would be subjected to major surgery [12].

Helical computed tomography (CT) with intravenous administration of contrast media is the primary investigation of choice to assess a patient in whom pancreatic cancer is suspected. It can predict surgical resectability with 80 to 90% accuracy. Alternatively, if CT fails to reveal a pancreatic mass, endoscopic ultrasound is also an accurate means of investigation. It is also the preferred method for cytology sampling [9]. Endoscopic retrograde cholangiopancreatography (ERCP) can be used to conduct ductal brushings to aid diagnosis [4;14]. For patients who are unable to tolerate intravenous contrast for CT scanning, MRI can be used for disease staging [11].

Pancreatic cancer staging is undertaken using the TNM classification as depicted in Table 1.1. Attempts can be made to resect a tumour classified as stage I or II, whereas stage III

tumours which have engulfed the superior mesenteric artery or celiac axis, and stage IV tumours which have widely disseminated are considered non resectable [9].

Stage	Tumor Grade	Nodal Status	Distant Metastases	Median Survival†	Characteristics
				mo	
IA	T1	N0	M0	24.1	Tumor limited to the pancreas, ≤2 cm in longest dimension
IB	T2	N0	M0	20.6	Tumor limited to the pancreas, >2 cm in longest dimension
IIA	T3	N0	M0	15.4	Tumor extends beyond the pancreas but does not involve the celiac axis or superior mesenteric artery
IIB	T1, T2, or T3	N1	M0	12.7	Regional lymph-node metastasis
III	T4	N0 or N1	M0	10.6	Tumor involves the celiac axis or the superior mesenteric artery (unresectable disease)
IV	T1, T2, T3, or T4	N0 or N1	M1	4.5	Distant metastasis

Table 1.1 – TNM Staging of Pancreatic Cancer [9] where T denotes primary tumour, N regional lymph nodes, and M distant metastases

1.2.4 Treatment

1.2.4.1 Surgery

Around 15% of patients who present with pancreatic cancer are suitable for resection [24]. Two techniques are indicated for resecting cancer of the pancreas head. Pancreaticoduodenectomy (known as Whipple procedure), entails removal of the pancreas head, gall bladder, duodenum, proximal jejunum, part of the extra hepatic biliary tree, and distal stomach. The pylorus-preserving pancreaticoduodenectomy is identical to the classic Whipple procedure but with preservation of the pylorus. A recent review evaluated the results of seven randomised controlled trials which compared these two operative techniques. No differences were identified between them in terms of long-term survival, and mortality rates immediately following resection. The rate of complications such as pancreatic anastomotic leaks and delayed gastric emptying were similar with both procedures [11;25]. Conversely, operating time and blood loss were reduced with the pylorus-preserving pancreaticoduodenectomy [25]. More radical surgery involving extended retroperitoneal lymph node dissection has not proved successful either in terms of overall survival or in preventing local recurrence of pancreatic cancer, and therefore is not regularly practiced [26]. Ghaneh et al [27] summarised the results of three randomised trials comparing radical and standard resection, and concluded that radical dissections do not improve survival.

Prognosis following surgery can be predicted to some degree according to the presence of positive resection margins, tumour differentiation, the size of the tumour, and the involvement of lymph nodes [11]. Despite surgical intervention, 5-year survival remains as low as 10% with resection alone, and nearly all the patients who undergo a successful resection eventually relapse and die from the disease [24;28]. Adjuvant therapy in the form of chemotherapy and/or radiotherapy is provided in an attempt to improve survival and reduce disease recurrence [14].

1.2.4.2 Adjuvant therapy

During the past few decades several well powered randomised controlled trials of adjuvant treatment following pancreatic cancer resection have taken place, and these have established the current standard of care. One of the earliest investigations was the European Study Group for Pancreatic Cancer (ESPAC) 1 trial, which evaluated whether there was any benefit to adjuvant treatment following surgery to resect pancreatic cancer. The findings demonstrated a survival benefit for chemotherapy, but not for chemoradiotherapy [29].

The ESPAC 3 trial was later conducted to compare survival benefit of combined 5-fluorouracil and folinic acid, versus gemcitabine alone. No significant difference was found between these treatments in terms of progression-survival or quality of life scores, although gemcitabine was deemed safer [29]. On the contrary, another study reported a 1-year survival of 18% with gemcitabine, compared to only 2% with 5-fluorouracil [14]. Gemcitabine is now regarded as the optimal chemotherapy agent in the adjuvant and palliative treatment of pancreatic cancer. The ESPAC 4 trial is currently recruiting patients and aims to compare gemcitabine against a combination of both capecitabine and gemcitabine [24].

Other chemotherapy treatments have shown promise to act as adjuvant or palliative treatments. For example, treatment with a combination of fluorouracil, folinic acid, irinotecan, and oxaliplatin led to a median survival of 11 months, compared to only 6.8 months for gemcitabine alone. However, adverse effects were significantly raised with the combination treatments, including higher incidences of grade 3 or 4 neutropoenia, thrombocytopoenia, and sensory neuropathy [30]. Such aggressive multichemotherapy regimens should therefore be reserved for younger patients who possess higher performance statuses and can tolerate stronger treatment [8].

1.2.4.3 Neoadjuvant therapy

Research findings support the use of adjuvant therapy whereas neoadjuvant therapy has yet to be proven worthwhile. In fact, a recent meta-analysis found that whether or not neoadjuvant treatment is given, the proportion of patients who are eligible for resection is similar.

Furthermore, delaying surgical resection to provide neoadjuvant therapy could allow for disease progression, therefore after such therapy, patients should have their disease stage rechecked. Neoadjuvant therapy is mainly reserved for borderline resectable disease where it has been shown to evoke a partial response, thus changing disease from borderline resectable to resectable [11].

1.2.4.4 Investigational treatments for pancreatic cancer

The ineffectiveness and toxicity of using multiple chemotherapeutic drugs has encouraged researchers to turn their attention to novel agents, including targeted therapies which have had success in other cancers. The resilience of pancreatic cancer to chemotherapy may be due the multiple signalling pathways involved in its pathogenesis, thus suggesting that a single targeted agent is unlikely to be effective. Alternatively, the surrounding desmoplasia may contain cells that promote tumour growth, as well as providing a physical barrier between the tumour and the rest of the body [8].

Several targeted agents are undergoing clinical trials including PARP inhibitors, hedgehog inhibitors and multikinase inhibitors. An important phase III trial recently investigated the benefit of an epidermal growth factor receptor (EGFR) inhibitor named Erlotinib in adjuvant therapy. Unfortunately, when Erlotinib was combined with gemcitabine it was only modestly superior to gemcitabine treatment alone [31]. Immunological therapies such as an antitelomerase vaccine also hold considerable interest for further development [32]. The technique of using endoscopy to deliver chemotherapy or radiotherapy is now under investigation, though as yet no evidence exists that this method of delivery is as effective as standard methods [33].

1.2.4.5 Palliative therapy

A pancreatic tumour is inoperable if there is locally advanced disease, metastases, or the patient has a poor performance status [9]. Survival currently stands at approximately 9-10 months for patients with locally advanced disease [9], but only 3-6 months in patients with

metastatic disease [11]. Pain is the most common symptom which requires control and is usually dealt with using oral opiate preparations. However, if the pain originates from the coeliac plexus then infiltration with ablation of the plexus guided by ultrasound or CT can be performed. Radiotherapy may also be used to relieve pain from locally advanced disease [11]. Weight loss is common in advanced disease and can result from pancreatic insufficiency, common bile duct obstruction, or cachexia. Cachexia cannot be treated, though obstruction of the common bile duct is an indication for biliary stenting [9]. Pancreatic insufficiency results from either pancreatic duct blockage or sparse pancreatic tissue, and can be treated with pancreatic enzyme supplements and/or stenting [11].

1.3 The Tumour Microenvironment in PDAC

Surprisingly until very recently, the majority of research studies relating to pancreatic cancer have focused on the epithelial cell component of the tumour. This is despite it being recognised for a long time that malignant tumours comprise a heterogeneous mixture of cells from different lineages including mesenchymal, endothelial, and inflammatory cells. Therefore, after years of rigorous research into the genomic instability of cancer cells, our attention has now shifted to consider the tumour microenvironment (TME) as well.

In the context of PDAC, fibrosis stems from the accrual of surplus extracellular matrix proteins (ECM) in tissue, and is often referred to as tumour desmoplasia when associated with carcinoma [34]. The robust deposition of extracellular matrix during desmoplasia is directly related to the exuberant proliferation in mesenchymally and neuroectodermically derived cells [35;36]. Interestingly, the cell components in the TME are very similar to those that arise in response to tissue injury, hence various researchers have described the tumour as a wound that never heals [36].

Histological analysis of tissue sections excised from patients with PDAC reveals infiltrating carcinoma cells surrounded by a dense stroma comprising type I and III collagens, fibronectin and laminin. Collagen content is in fact 3-fold higher in the tissue of PDAC and CP compared to that of normal pancreas [37].

Breast and prostate cancers also have prominent desmoplastic reactions. In contrast to pancreatic cancer, research into epithelial-stromal interactions in these cancers was initiated several decades ago. Early studies relating to the breast cancer microenvironment discovered the mitotic activity of stromal cells to be significantly increased in the vicinity of epithelial components, thus implying an interaction between the cell types [38].

Furthermore, in breast cancer the presence of myofibroblasts is linked to a higher proliferative rate in tumour cells and a poorer prognosis [39]. The stromal influence on prostate carcinoma is also well documented. Surprisingly, one report has shown the that the degree of reactive stroma can predict prognosis and disease recurrence even as accurately as the established serum marker, prostate specific antigen [40].

Research into the pancreatic cancer microenvironment may have progressed more slowly than that of breast and prostate not only due to less funding, but also perhaps due to difficulties encountered in accessing tumour tissue samples for analysis [39]. Amongst the tumours expressing desmoplasia discussed above, pancreatic cancer displays the most extensive desmoplastic reaction, with stromal tissue accounting for up to 90% of the tumour volume [41]. PDAC, the most common variety of pancreatic cancer, is very similar to breast cancer in histological appearance. Tissue sections reveal a sparse duct-like structure with varying degrees of atypia surrounded by an intense desmoplastic reaction [35]. The identity of the different components of the TME, as well as their role in cancer initiation and progression is the focus of many current research efforts.

1.3.1 Which cells create the desmoplastic reaction?

Pancreatic cancer cells have the capability to produce ECM components as proven in both in vitro and in vivo studies [42]. However, the majority of reports demonstrate that the mass of fibrotic tissue associated with PDAC and CP originates in the stroma rather than the tumour.

Apte and colleagues [43] demonstrated that stromal areas of pancreatic cancer tissue sections stain intensely positive for collagen I, alpha SMA (Smooth Muscle Actin) and GFAP (Glial Fibrillary Acidic Protein), a molecular profile highly suggestive for activated pancreatic stellate cells (PSC). Using in situ hybridisation they demonstrated that procollagen messenger RNA (mRNA) expression localised to activated PSCs, implicating these cells as the predominant source of collagen in PDAC.

Data from Bachem and colleagues [37] reiterate these findings. Immunohistochemical analyses showed alpha SMA positive cells to correlate with collagen type I and fibronectin. Together, the ECM components and alpha SMA positive cells surrounded pan-cytokeratin positive carcinoma tissue. There was clearly no association between the ECM proteins and pan-cytokeratin staining. Interestingly, they also discovered pan-cytokeratin staining to correlate with expression of extracellular matrix metalloproteinase inducer (EMMPRIN). This implies that carcinoma cells have the ability to induce the formation of matrix metalloproteinases (MMPs) in neighbouring stromal cells.

A similar study of pancreatic fibrosis has revealed that pancreatic acinar cells adjacent to areas of fibrosis exhibit intense staining for transforming growth factor beta (TGFβ). This growth factor is a known activator and a profibrogenic mediator for PSCs. Pancreatic acinar cells remote from any areas of fibrosis did not stain positively for TGFβ. These results indicate the stimulation of PSCs by paracrine factors released from adjacent parenchymal cells [44].

1.3.2 The Pancreatic Stellate Cell

Pancreatic stellate cells exist in a periacinar location in the exocrine portion of the healthy pancreas. It is a cell type which comprises only 4% of the total number of cells in the organ [45]. In this location they exist in a quiescent state characterised by a star-like morphology and lipid droplets contained within their cytoplasm [46]. The lipid droplets contain vitamin A as evidenced by a rapidly fading blue-green fluorescence emitted on exposure to UV radiation [47]. The cells have a low rate of proliferation and a low capacity to produce ECM in this inactivated state.

PSCs can be identified through immunohistochemistry staining techniques. They express markers which are not specific to their own cell type, such as desmin and GFAP, both of which are cytoskeletal intermediate filament proteins also expressed by smooth muscle cells and astrocytes respectively [47]. Vimentin is a non-specific mesenchymal marker which has also been detected in PSCs.

During pancreatic injury, PSCs enter an activated state which is accompanied by morphological and functional changes. Cell morphology changes from a star shape to a 'myofibroblast-like' phenotype, and lipid droplets disappear from the cytoplasm [37]. Activated cells begin to express an additional marker, a cytoskeletal protein named alpha SMA. They also develop the capacity to secrete large amounts of ECM including collagens, fibronectin and laminin [39].

A diverse number of extra-cellular and intra-cellular molecules induce this activation during pancreatic injury. These include inflammatory cytokines such as IL-1 and IL-6, growth factors like TGFβ1 and TNFα, ethanol and its metabolites, and oxidative stress [37]. Furthermore, Schneider et al [48] have demonstrated that platelet derived growth factor (PDGF) induces PSC proliferation, and TGF β1 induces the synthesis of ECM proteins by PSCs. Other important factors that PSCs have been shown to produce include MMPs, as well as the inhibitors of these enzymes named tissue inhibitors of metalloproteinases (TIMPs). Hence, it is clear that PSCs play a major role in the maintenance of the surrounding stroma through both creation and degradation of the ECM [35].

As mentioned above, the number of PSCs in the normal pancreas amounts to only 4% of the total cell number. Conversely, in pancreatic cancer these cells can outnumber the malignant

epithelial cells, suggesting that they are recruited in large numbers and/or proliferate at a rapid rate [35].

Stellate cells are capable of sustaining their activated state through autocrine signalling. For instance, they generate growth factors such as TGFβ1, PDGF, connective tissue growth factor, as well as cytokines like IL1β, IL15, and endothelin 1 [49].

The persistent activated state of PSCs during CP and PDAC may also be partly explained by their ability to express the protease activated receptor-2 (PAR-2). It is speculated by Masamune and colleagues [50] that as part of a positive feedback loop, PAR-2 stimulates PSC proliferation and collagen synthesis. Interestingly, this protease only becomes active once it has been cleaved by trypsin, an enzyme which is highly abundant during pancreatic injury due to its leakage through the damaged exocrine ducts.

1.3.2.1 'Quiescent' state

During health, PSCs exist in the quiescent state and are thought to play a central role in the normal maintenance of ECM turnover. A recent study proposed that the PSC may even play role in normal exocrine function in the pancreas. Phillips et al [51] discovered that cholecystokinin (CCK) stimulates acetylcholine secretion by PSCs, which then induces acinar cells to secrete amylase. Hence, these findings have shown a new pathway by which CCK is able to stimulate exocrine secretion in the pancreas.

Quiescent PSCs also participate in temporary tissue repair processes following acute pancreatitis in both humans and rodents. Their exact role in this scenario remains to be clarified although the likelihood is that they lay down a provisional matrix at the site of injury to allow for subsequent cell proliferation, migration, and the assembly of new parenchymal cells. After the inflammation resolves the PSCs progressively disappear and may re-enter their quiescent state. However, it is the repeated pancreatic damage that can lead to chronic inflammation and the persistent activation of PSCs [52].

The periacinar location of quiescent PSCs, together with their long cytoplasmic processes which encircle the basal aspect of the pancreatic acinar cells could signify a role in the maintenance of pancreatic acinar cells, or perhaps the regulation of ductal pressures [47]. Additionally, their perivascular location suggests a possible role in the regulation of vascular functions [45].

The function of the lipid deposits which rest in the cytoplasm of the quiescent PSC is yet to be clarified. There is speculation that the vitamin A is required to maintain the quiescent state. Hence, loss of vitamin A may be essential for the activation of the PSC rather than a mere epiphenomenon [45]. In support of this theory, retinol which is a vitamin A derivative, has been shown to inhibit the activation of stellate cells, and has even managed to induce quiescence in culture-activated stellate cells [53]. This induction was recently shown to be mediated by Wnt–β-Catenin Signaling [46].

Clues to the function of PSCs can also be gleaned from research involving hepatic stellate cells (HSC) which have a very similar genotype. HSCs have been assigned several important physiological roles in the liver, including vitamin A storage, creation and turnover of ECM proteins, promotion of hepatocyte differentiation, and the regulation of ductal and vascular pressures in the liver [52].

1.3.2.2 Pancreatic cancer cells stimulate pancreatic stellate cells

High numbers of activated PSCs have been observed to localise around pancreatic cancer cells in human tissue sections of PDAC [43]. This has led some to question whether the PSCs are attracted towards the cancer cells, and essentially recruited from the tissues surrounding the tumour by the cancer cells. An alternative hypothesis is that cancer cells may be able to secrete growth factors or cytokines which increase stellate cell proliferation in the local vicinity of the tumour, leading to a greater number of stellate cells being detected around the cancer cells.

Bachem and colleagues [54] have investigated whether such paracrine signalling exists through a series of in vitro experiments. PSCs cultured in the supernatant of cancer cell lines had an

increased rate of proliferation, in comparison to those cultured in normal media. In a subsequent experiment, a PDGF neutralising antibody was added to the cancer cell supernatant which resulted in a reduction in PSC mitogenic activity. These results could indicate that PDGF controls proliferation of PSCs. However, it is also possible that the PDGF neutralising antibody bound with other receptors on the PSC in addition, or apart from the PDGF receptor, thus indirectly inhibiting proliferation through other pathways.

Wound healing assays and co-culture experiments have been performed by the same group. Cancer cell supernatant increased the rate of wound closure by PSCs, and during co-culture experiments, PSCs migrated towards the cancer cells. Pre-incubation of PSCs with neutralising antibodies to PDGF reduced their motility in both experiments [37].

Similar studies have been performed to investigate ECM production by PSCs. When cultured in cancer cell supernatant, they stained more intensely for collagens and fibronectin, compared with PSCs cultured in normal media. However, the addition of neutralising antibodies for TGFβ1 and basic fibroblast growth factor (FGF-2) to the cancer cell supernatant almost completely inhibited any matrix stimulating activity [37].

A further finding is that cancer cells are able to induce MMP-2 synthesis in PSCs. This through interactions with the PSCs via a glycoprotein called extracellular matrix metalloproteinase inducer (EMMPRIN), which is located on the cell surface of cancer cells. MMPs are another set of cells with critical roles in the development of pancreatic fibrosis, as well as the promotion of cancer cell invasiveness [55].

The cell signalling pathways that regulate PSC activation have not yet been fully elucidated. It has been established that PDGF interacts with PSCs through Src-dependent activation of the JAK2-STAT3 pathway and the MAP kinase pathway, extracellular-regulated kinases (ERK)1/2 and p38. Moreover, TGFβ1 has been shown to stimulate PSCs through SMADs 2, 3 and 4 as well as the MAP kinases [49]. Therefore, a few of the molecular pathways that regulate the mitogenic and fibrogenic activity of PSCs have already been elucidated. However, our understanding of these processes, especially those controlling the activation of PSCs need to be improved, so that targets can be identified for therapeutic interventions that will aim to prevent or even reverse the activation of PSCs.

1.3.2.3 Pancreatic stellate cells promote tumour progression

In an investigation by Vonlaufen and co-workers [56] conditioned medium of PSCs was shown to induce proliferation of pancreatic cancer cells at a significantly greater rate than that of cancer cells cultured in regular media. Subsequently, a neutralising antibody to PDGF was added to the supernatant which then inhibited these mitogenic effects. Migration and invasion were also induced in the cancer cells, as evidenced by Boyden chamber experiments and invasion assays respectively. Interestingly, PSC supernatant was also shown to reduce cancer cell apoptosis as measured by TUNEL staining. If the mechanisms by which PSCs inhibit cancer cell apoptosis could be elucidated, this could highlight favourable targets in the apoptotic pathway for which new pancreatic cancer therapies could be developed.

The same researchers created an orthotopic mouse model of pancreatic cancer in order to investigate the interaction between cancer cells and stellate cells in vivo. They found that mice injected with PSCs alone did not develop a pancreatic tumour. However, mice injected with cancer cells developed tumours, and mice injected with both cancer cells and PSCs developed even bigger tumours. Hence, PSCs alone do not have the potential to form a tumour, but instead play an important role in promoting the growth of cancer cells which are already present.

Interestingly, none of the mice injected with cancer cells alone exhibited obvious fibrous tissue, although some of the cells within the stroma stained faintly for alpha SMA. An explanation for this may be that the injected cancer cells recruited host murine PSCs at the tumour site. On further investigation, tumour sections from the mice that were co-injected with PSCs and cancer cells were also studied to elucidate the origins of the activated PSCs in the tumour site. They conducted immunohistochemical staining for alpha SMA and human nuclear antigen, the latter being a human cell-specific marker. The results revealed that some of the alpha SMA positive cells within the tumour resulting from co-injection also did not express human nuclear antigen. This implies that cancer cells managed to recruit and activate the PSCs belonging to the host species in order to enhance tumour growth.

A role for PSCs in the promotion of cancer cell dissemination has also been proposed by the same investigation. This is because a significantly higher proportion of the mice injected with a combination of PSCs and cancer cells developed distant metastases, compared to the

mice injected with cancer cells alone. Furthermore, serial sections of liver metastases stained positively for both αSMA and human nuclear antigen [56]. This indicates that the tumour cells and PSCs are disseminating through the bloodstream together, which is contrary to previous belief that the cancer cells recruit new stellate cells at the distant site of dissemination.

Hwang and colleagues [57] created a similar orthotopic mouse model of pancreatic cancer. They co-injected an immortalised PSC line with a cancer cell line. Primary tumour incidence, size and metastasis were all increased with co-injection compared to cancer cells alone. However, one must be cautious when interpreting these results due to the use of an immortalised PSC cell line instead of primary PSCs. These immortalised cells were reported to have altered characteristics to primary cultured PSCs including a doubling time in culture of only 12 hours.

In vitro studies by the same group reiterated the findings mentioned above, including the stimulation of tumour proliferation and invasion after culture of cancer cells in PSC supernatant. Anchorage-independent growth as measured by tumour colony formation on soft-agar was also increased with PSC supernatant. Furthermore, tumour cells treated with the conditioned medium of PSCs showed lower levels of apoptosis when subjected to both chemotherapy and radiotherapy [57]. However, these may have been indirect effects PSCs through their secretion of laminin and fibronectin, proteins which have previously been reported to have antiapoptotic effects [56].

In a different study, Bachem et al [54] injected PSCs alone into the left flank of nude mice, and co-injected PSCs and cancer cells into their right flank. All tumours that developed from co-injection grew faster and progressed to a significantly larger tumour volume. These results reiterate the findings from the vivo studies mentioned above, although the drawback of this investigation was that a xenograft mouse model was utilised rather than an orthotopic model. This does not allow for the assessment of tumour behaviour in its appropriate environment, as evidenced by the lack of metastatic pathways in that are available to a tumour in a subcutaneous model [39].

Fujita and colleagues [58] investigated the behaviour of cancer cell lines when they were co-cultured with PSCs. Interestingly, they discovered that the behaviour of the cancer cells varied between direct and indirect co-culture systems. Cancer cell proliferation was increased in direct culture with PSCs, compared to indirect co-culture. Indeed, indirect co-culture systems are generally more commonly used by researchers for in vitro studies, and

have eve been utilised for the co-culture experiments in most of the aforementioned studies. Direct co-culture also enhanced notch signalling pathways, whereas such induction was absent from indirect co-culture. This implies that there must be direct cell to cell contact regulatory mechanisms that exist between cancer cells and PSCs, in addition to the paracrine mechanisms already discussed above.

Xu and colleagues [59] have carried out a thorough investigation into the involvement of PSCs in tumour metastasis in pancreatic cancer. They performed a gender mismatch study with male PSCs and female cancer cells in a female orthotopic mouse model. Using fluorescent in-situ hybridisation they discovered that PSCs accompanied cancer cells during their journey from the primary tumour into the blood vessels and relocation to distant anatomical sites. These results support the findings made by Vonalufen et al [56] mentioned above, but are contrary to most previous beliefs that the cancer cells instead recruit new PSCs in the new metastatic site.

As well as facilitating local growth and metastases, PSCs are also able to directly stimulate angiogenesis through their secretion of vascular endothelial growth factor (VEGF) and periostin [41]. These effects and their implications for tumour progression will be discussed in a later section.

1.3.2.4 Origin of pancreatic stellate cells

It is widely agreed that PSCs play a fundamental role in pancreatic fibrosis, and many researchers are currently exploring the molecular mechanisms involved in the activation of these cells. In contrast, the origin of these cells and their turnover within the pancreas is still debated. It is commonly thought that most cancer associated PSCs arise from the existing pool of quiescent PSCs in the pancreas, although there is increasing evidence that there may be alternative sources [39].

The involvement of bone–marrow (BM) derived cells in organ fibrosis has been portrayed in a number of studies. A study conducted by Russo and colleagues [60] found that a large proportion of the myofibroblasts (70%) and hepatic stellate cells (68%) present during liver fibrosis had originated from the BM. The same process may occur in the pancreas during fibrosis although there is currently limited data to support this. However, the fact that PSCs and HSCs are 99.9% similar at the mRNA level suggests that they may even possess a common origin.

In a recent pancreatic study, Sparmann et al [61] compared the origins of isolated quiescent PSCs in normal rat pancreas, with those isolated from restored rat pancreas following an artificially induced episode of acute pancreatitis. The incidence of BM derived quiescent PSCs obtained from rat pancreas was approximately 7% from healthy pancreatic tissue, and 18% from the restored pancreas, a significant difference. The increased numbers of quiescent PSCs present in the pancreas after regeneration propose the enhanced recruitment of BM-derived cells to the pancreas, which have subsequently reverted back to their quiescent state after the resolution of the inflammatory process. To the author's best knowledge this is the first publication to reveal a BM origin for quiescent PSCs.

Mesenchymal stem cells (MSC), which originate from the bone marrow have been shown to localise to areas of pancreatic tumour growth [62]. More importantly, Direkze and colleagues [63] have shown that BM-derived cells MSCs also contribute to the myofibroblast population in a mouse model of insulinoma. Further investigations are needed to elucidate whether this is also the case in PDAC.

Contribution of endothelial cells to the myofibroblast cell population in pancreatic cancer has been reported by Zeisberg et al [64]. This phenomenon of endothelial to mesenchymal transition occurred through induction by TGFβ1 treatment, causing proliferating endothelial cells to convert phenotypically into fibroblast-like cells, with subsequent expression of mesenchymal markers.

The relative contributions of resident precursor cells, as well as BM-derived cells and MSCs, to the activated stellate cell population in the diseased pancreas requires clarification [52].

1.3.3 The extracellular matrix

The extracellular matrix (ECM) in healthy organs provides cells with a tensile scaffold necessary for appropriate assembly into three-dimensional macroscopic structures [65]. It is composed of collagens, non collagen glycoproteins, proteoglycans, and growth factors. There are also matricellular proteins within the matrix which lack a structural role, but instead act as modulators for the interactions between the cell components and the surrounding matrix [49]. These include connective-tissue growth factor (CTGF), secreted protein acidic and rich in cysteine (SPARC), thrombospondin and periostin.

1.3.3.1 Role of the ECM in tumour progression

The excess fibrous tissue found in and around the diseased pancreas was initially believed to be a host barrier against cancer invasion. In keeping with this belief, the development of a tumour suggested that cells had overcome the architectural constraints imposed by the matrix in order to multiply and survive, even in the absence of permissive interactions with the ECM [65].

Current evidence suggests that the matrix can modulate carcinogenesis by providing a supporting structure for tumour growth, as well as by acting as a reservoir for the storage of soluble signalling molecules. These can enhance cellular growth, differentiation, survival, and movement of the cancer cells [20].

Type I collagen, one of the most abundant collagens present in the ECM of pancreatic cancer, is secreted predominantly by PSCs. The collagen itself has been shown to increase the proliferation, migration and resistance to apoptosis of pancreatic cancer cells, mediated via signalling via its integrin receptors [66].

Armstrong et al [67] used tissue culture models to demonstrate that ECM proteins are able to enhance tumour growth. Cancer cell lines cultured on type I collagen showed higher rates of proliferation compared to those cultured on plastic. The degree of apoptosis was significantly

reduced in the cells cultured on type I collagen when all the cells were administered chemotherapy in vitro. These results were corroborated in multiple pancreatic cancer cell lines. Similar results were elicited in a small-cell lung cancer in vivo model which displayed how ECM proteins are able to protect cancer cells from apoptosis again mediated by integrin receptor signalling [68]. On the other hand, the results of these investigations may be seen as unconvincing if one assumes that cancer cells simply prefer to grow on a three-dimensional tissue matrix system which is more akin to their original environment, rather than the two-dimensional growth provided by a plastic coasted dish. This would explain the enhanced growth of cancer cells on the collagen surface.

As well as modulating carcinogenesis, the fibrotic matrix also serves as a protective barrier against potential therapeutic strategies such as chemotherapy and radiotherapy. The excessive matrix creates a hypoxic and hypovascular environment, making it difficult to access the tumour via the bloodstream. Olive et al [69] characterised tumour perfusion in a mouse model of pancreatic cancer, and evaluated intratumoural uptake of gemcitabine therapy. Their data highlighted inefficient tumoural uptake of gemcitabine as a direct result of poor vascularisation and perfusion within the tumour.

Growth factors like epidermal growth factor (EGF), fibroblast growth factor (FGF), PDGF and TGFβ exist within the matrix. These may be released through protease mediated digestion of the ECM which allows them to carry out their roles, one of which includes the activation of PSCs. Farrow and colleagues [70] have detected high expression of EGF specific to the stromal compartment, and high expression of EGFR specific to cancer cells. This implies that cancer cells are stimulated by their neighbouring stromal cells through EGF.

The expression of 'anti-adhesive' ECM proteins within the stroma can facilitate pancreatic cancer cell invasion. Such proteins include tenascin, vitronectin and versican. Versican is secreted by cancer cells as well as by activated stellate cells [70].

High levels of the SPARC expression originate from the stroma of the pancreatic tumour, and it has also been detected in the conditioned medium of PSCs [71]. The expression of this matricellular protein has been linked with a poor prognosis, and experimental studies have demonstrated the ability of this protein to increase pancreatic cancer cell invasiveness [49]. In contrast, other reports concluded that SPARC possesses tumour suppressing functions. For example, inhibition of endogenous SPARC in cultured cancer cells enhanced their

proliferation and migration [71]. Clearly further studies are required to elucidate the role of SPARC in pancreatic cancer.

Periostin is another matricellular protein that has been detected in the supernatant of PSCs. This expression is up-regulated in PSCs when they are co-cultured with pancreatic cancer cells. This protein seems to have a biphasic effect on cancer cell motility, where low concentrations suppress motility whereas high concentrations increase it [72]. Perhaps, the effects of SPARC are also dose-dependent like those of periostin. Finally, the role of thrombospondin has also been described. It has been associated with increased pancreatic cancer cell invasion, and its presence within the stroma is correlated with a poor prognosis.

1.3.3.2 Role of the ECM in tumour initiation

The studies mentioned above depict evidence for why the ECM is able to promote tumour progression in the pancreas. However, the role of the ECM in the oncogenic conversion of normal epithelial cells has also been suggested. The reduced physical compliance of the ECM, due to excessive deposition of collagen in tumours is apparently enough to initiate carcinogenesis. Changes in matrix rigidity are detected by surface receptors called integrins which connect to the cytoskeleton and translate this external information to the cell. Cell contractility is subsequently modified through the activity of Rho GTPases, a family of proteins involved in the regulation of a variety of cellular processes, such as the organization of the microfilamental network and cell-cell contact [65;73].

Paszek et al [74] cultured normal mammary epithelial cells on rigid substrates, which subsequently caused altered cell phenotypes with traits of neoplastic transformation. Such changes included disruption of cell to cell contacts, depolarisation, increased production of focal adhesions, and most importantly an increased receptiveness to proliferative signals from EGF stimulation. Interestingly, these changes could be repeated when Rho was artificially stimulated in normal mammary epithelial cells which were cultured in the absence of a stiff matrix. Furthermore, the authors discovered that mammary carcinoma cells spontaneously overexpress Rho, and inhibition of Rho or its downstream effectors could even reverse the phenotypic changes described above [65].

1.3.3.3 Interaction of the ECM with Pancreatic Stellate Cells

The ECM is believed to regulate PSC behaviour for several reasons. Firstly, experimental data has shown PSCs to revert to their quiescent state if cultured on a basal membrane-like matrix. Furthermore, in hepatic fibrosis, extensive degradation of the ECM has resulted in the apoptosis of HSCs presumed to be as a result of reduced survival signals being received from the ECM [75]. More recently, a mouse model was created which lacked plasminogen in order to represent impaired proteolysis of the ECM and a constant fibrotic matrix. This led to persistent PSC activation and accumulation of pancreatic collagens [52]. This implies that certain components in the ECM are promoting the proliferation or survival of PSCs.

Proteoglycans such as decorin, lumican, and versican are present in large quantities within the ECM in pancreatic cancer, and PSCs are thought to be the main source of these proteins. Versican stimulates cancer cell invasiveness and dissemination, whereas decorin and lumican seem to have tumour suppressing effects. Interestingly, PSCs cultured in the supernatant of pancreatic cancer cells increased their secretion of versican, but downregulated their expression of decorin and lumican. These results highlight the ability of cancer cells to manipulate their environment to make it less hostile and aid survival [49].

1.3.4 Matrix metalloproteinases

1.3.4.1 Role of MMPs and other proteases in tumour progression

Matrix metalloproteinases (MMP) are a large family of zinc-containing proteolytic enzymes directly involved in ECM remodelling [41]. One of the most important functions of MMPs is their ability to degrade type IV collagen, a component of the basement membrane. Digestion of this membrane allows cancer cells to invade local lymphatic channels and blood vessels, thus representing a critical step in tumour progression [35]. Invasion of the surrounding environment also brings malignant cells into contact with other ECM proteins such as collagen type 1, which can directly support cancer cell growth and contribute to their chemoresistance as mentioned in section 1.3.3.1 [20].

MMPs also regulate the bioavailability of growth factors and cytokines contained within the ECM. These molecules are released when MMPs digest the ECM, and their release subsequently has effects on tumour proliferation, angiogenesis and metastasis. Moreover, the transcriptional regulation of MMPs is regulated by these cytokines and growth factors contained within the ECM. For example, TGFβ1 has been shown to up-regulate collagens, MMP-2 and TIMP-1, whilst down-regulating TIMP-2, MMP-3, and interstitial collagenases such as MMP-1 and -13 secretion by fibroblasts [76].

The presence of MMP-1, -2, -3, -7, -9, -11, and -13 have all been reported in PDAC. MMP-2 and -9 are both highly expressed in cancer cells, but are also secreted by PSCs and macrophages [36]. As well as digestion of basement membrane collagen (Type IV), they also have the ability to digest the partially degraded collagens (Types I, III) [77].

Other than degradation of ECM components and release of sequestered growth factors, MMPs also promote tumour progression through complex signalling functions. For example, in vitro studies have shown that angiostatin, a potent angiogenesis blocker is cleaved from plasminogen by MMP-2, -3, -7, -9, and -12. Also, insulin like growth factor binding proteins and stromal cell derived factor are both cleaved and inactivated through MMP activity. Therefore, we must decipher which proteases are contributing to tumour progression, and

which are acting as part of the host defence. This is a necessary step in determining which MMPs are potential drug targets [78].

Research into squamous cell carcinogenesis has revealed that MMP-9 manifests proangiogenic activity in its ability to mobilise VEGF from the ECM [79]. On the contrary, MMP-9 is can cleave collagen IV to produce a proteolytic fragment named tumstatin, which possesses anti angiogenic properties [36]. The mixture of pro- and anti-tumourigenic roles of MMPs may account for the failure of MMP inhibitors in recent clinical trials. For instance, when combined with gemcitabine they displayed no superiority in outcome compared to the standard gemcitabine treatment alone [14;78]. TIMPs are also often overexpressed in tumours along with their target proteinases. This suggests that TIMPs probably have several roles in tumour promotion, rather than inhibition of MMPs alone [41].

MMP-7 also known as Matrilysin is expressed in PDAC, predominantly by epithelial cells in the invasive tumour front. Its expression in PDAC has been associated with an advanced pathological stage and poorer survival. Futhermore, MMP-11 (stromelysin-3) is also expressed in PDAC typically by stromal cells which are located adjacent to the tumour [36].

Apart from MMPs, various other proteases and their inhibitors exist within the TME. In a recent study researchers induced a cancer cell line to overexpress the protease inhibitor SERPINE2. They then compared local invasiveness between the tumours resulting from induced or non induced cells injected into the xenograft model. Pancreatic tumours developing from the induced cancer cells displayed greater local invasiveness which was accompanied by a striking increase in ECM deposition. Furthermore, they discovered that tumour growth was also increased in addition to local invasion, if the SERPINE2 overexpressing cells were co-injected with PSCs [80].

Urokinase plasminogen activator (uPA) and tissue plasminogen activator (tPA) are proteolytic enzymes regulated by the pancreatic cancer stroma, and their increased expression has been associated with an increase in pancreatic cancer cell invasion [70].

1.3.4.2 The role of MMPs in cancer initiation

A recent breast cancer publication has suggested that MMPs are able to initiate carcinogenesis [81]. A transgenic mouse model characterised by overexpression of MMP-3 expression demonstrated the appearance of premalignant lesions, followed by the development of overt mammary carcinomas. They managed to clarify the sequence of molecular events taking place. Firstly, EMT was induced by MMP-3 through the upregulation of Rac1b, a small GTPase with a role in the maintenance of the actin cytoskeleton. This upregulation led to the production of reactive oxygen species (ROS), specifically mitochondrial superoxide. Elevated levels of superoxide anions induced Snail expression, a transcriptional repressor of E-cadherin which is an epithelial cell to cell adhesion molecule. This explained the transformation from an epithelial to a mesenchymal phenotype [65].

It is fascinating that an enzyme previously believed to have a solitary role in digesting ECM has now been shown to cause genomic instability in normal cells. MMP-3 may be directly responsible for the acquisition of mutations in these epithelial cells, or alternatively it may provide a stromal environment which supports the survival of cellular clones bearing selected mutations [65].

1.3.4.3 Interaction of MMPs with pancreatic stellate cells

Pancreatic stellate cells are able to secrete both MMPs and TIMPs and therefore play a central regulatory role in pancreatic fibrosis by controlling matrix turnover.

EMMPRIN is frequently raised in various solid tumours including breast and ovarian cancer, in which its overexpression is correlated with tumour size, stage and prognosis [41]. It is also expressed on the cell surface and in the supernatant of several pancreatic cancer cell lines. PSCs cultured in the supernatant of the cancer cells have increased expression of MMP-1 and -2. However, if PSCs were cultured in supernatants depleted of EMMPRIN, this led to an inhibition of MMP expression [55]. These data imply that the cancer cells are stimulating

adjacent PSC secretion of MMPs in a paracrine fashion, as opposed to through cell to cell contacts.

In a different report, TGFβ1 has been demonstrated to reduce the expression of MMP-3 and -9 by PSCs. As mentioned in section 1.3.2.3, TGFβ1 is also expressed by PSCs themselves. Hence, PSCs may enhance fibrogenesis by inhibiting ECM degradation via autocrine signalling which inhibits their own production of MMP -3 and -9 [77].

1.3.5 Fibroblasts

Fibroblasts are derived from the primitive mesenchyme embryonic layer and stain positively for vimentin, an intermediate filament protein. In the healthy pancreas, fibroblasts form a fundamental part of residential connective tissue support. They are usually modest in number, but show proliferation in different forms of pancreatic injury including pancreatitis and pancreatic cancer [36].

The functions of quiescent PSCs are proposed to be analogous to those of fibroblasts in the healthy pancreas and have previously been discussed in section 1.3.2.1. Additional similarities between these cell types include their periacinar and periductal location, and the rapid production of ECM components upon activation, including type I, III, and V collagens and fibronectin [82]. Despite these similarities in function, it is now well accepted that PSCs are the main contributors of the excessive fibrotic tissue in the pancreas during disease states as explained in Section 1.3.1 [35].

Fibroblasts are elongated cells with extended cell processes that show a fusiform or spindle-like shape in profile. As well as vimentin, molecular markers include fibroblast specific protein 1 and CD90. However, the lack of a specific and reliable molecular fibroblast marker acts as a hindrance to studying these molecules in vivo. Myofibroblasts represent activated fibroblasts that are able to produce greater amounts of ECM, and can be distinguished from the normal fibroblast by their expression of alpha SMA [83].

Fibroblasts in mammals are highly heterogeneous, and a recent study has identified divergent gene-expression patterns between fibroblasts isolated from different anatomical sites within the same patient. Surprisingly, these disparities in gene expression were even as divergent as the variation between the lineages of white blood cells in the same patient [82].

The signals that mediate the transition of a normal fibroblast into a cancer associated fibroblast (CAF) are not yet fully understood. However, in vitro studies have shown that TGFβ can induce phenotypic features of CAFs in normal fibroblasts. This growth factor mediates these changes during fibrosis and wound healing. Further studies are needed to elucidate whether CAFs represent a unique subtype of the fibroblast, or merely a common phenotype of fibroblast activation during injury [82].

Several studies have demonstrated the role of fibroblasts in cancer initiation. For example, Kuperwasser and colleagues [84] demonstrated that over-expression of TGFβ by fibroblasts in their transgenic mouse model resulted in the initiation of breast cancer within the adjacent epithelial tissue. Similarly, another study compared primary fibroblasts isolated from normal tissue, to CAFs isolated from tumour tissue. Normal prostate epithelial cells were grafted into mice along with one of these fibroblast types. However, only the epithelial cells grafted alongside CAFs induced tumourigenesis [82].

Mesenchymal stem cells (MSC) are fibroblast-like progenitor cells. Their phenotypic markers include LNGFR and STRO-1, however no specific marker for the MSC has been discovered. They originate from the bone marrow and have the capacity for self renewal and to differentiate into several other cell types including osteocytes, chondrocytes and adipocytes. Their differentiation into PSCs has also been debated (Section 1.3.2.4). It is likely that they represent a subtype of fibroblasts due to similarities including a spindle shaped morphology and expression of the CD90 marker [85].

There are currently few if any studies which have discussed the role of MSCs in pancreatic cancer intiation and progression. However, Karnoub et al [86] investigated the effects of MSCs in tumour progression in a breast cancer xenograft mouse model. They injected a mixture of human bone-marrow MSCs and human breast cancer cells into several mice, and breast cancer cells alone into different mice. After 12 weeks the mice developed malignant tumours. However, distant metastases were only observed in mice injected with MSCs.

1.3.6 Immune cells

1.3.6.1 Lymphocytes

Dendritic cells regulate the production of functionally competent T cells. These cells are situated in tissues throughout the body and their designated role is to absorb antigens from their surrounding environment. Once loaded with antigens they migrate to the nearest lymphoid organ to present them to naive T cells. The T cells then become activated, which subsequently enables them to identify cancer cells that display cancer-specific antigens on their cell surface.

The Bone marrow (BM) is already known for its role as a primary lymphoid organ due to its ability to generate lymphocytes from immature progenitor cells. However, a recent study has shown that the BM is able to serve as a secondary lymphoid organ as well. The authors demonstrated that naive, antigen specific T cells in the blood home to the BM for priming. Additionally, they showed that $CD11c^+$ dendritic cells take up exogenous antigens from the blood and present them to resident T cells in the bone marrow. Hence, these two methods represent ways in which antigen specific T cells are able to undergo activation, proliferation and differentiation to form effector T cells that enter the bloodstream as a result of exposure to cancer antigens [87].

Another recent study has supported this notion. The BM was discovered to be imperative in producing $CD4^+$ and $CD8^+$ T cells that are specific to various antigens in PDAC. Primed memory T cells specific to cancer antigens were detected in all 41 of their patients with PDAC. Around a half of these memory T cells were also identified in the bloodstream of these patients [88]. Conversely, similar studies of melanoma and multiple myeloma patients identified primed memory T cells in the bone marrow of less than half of their patients [20]. However, the higher proportion of T cell responses discovered in PDAC could be attributed to its late clinical presentation meaning that greater quantities of cancer antigens are able to reach the BM by the time of diagnosis and BM sampling.

The type and extent of T cell response differs according to the antigens that are presented. For example, ECM breakdown products and type I interferons may encourage activation of T

cells in cancer tissues, whereas TGFβ and IL-10 have immunosuppressive effects. The latter are both produced in large quantities in PDAC by various cells in the TME including PSCs [89], macrophages, mast cells [90] and regulatory T cells [91].

In support of these findings, Von Bernstorff et al [91] analysed 116 patients suffering with PDAC and discovered mean concentrations of TGFβ and IL-10 to be significantly higher in the sera of PDAC patients to those of patient controls. Moreover, loss of CD3 in the T cells of patients with PDAC was elicited with immunohistochemical staining. CD3 is a membrane complex essential for signal transduction and subsequent activation of T cells. Its loss was also correlated with elevated concentrations of TGFβ and IL-10.

Freshly isolated $CD8^+$ T cells are able to recognise and lyse autologous pancreatic cancer cells in vitro. These primed $CD8^+$ T cells were also injected into a xenograft mouse model of PDAC which significantly delayed tumour progression [92]. These results are supported by the findings of Fukunaga et al [93] who reported a correlation between higher numbers of cancer-infiltrating $CD4^+$ and $CD8^+$ T cells and a better prognosis in PDAC.

As a result of the dense desmoplastic stroma surrounding pancreatic tumours, activated T cells may have difficulty accessing the cancer cells. In fact, a recent study found that tumour infiltrating lymphocytes became trapped in peritumoural tissues and were not able to reach the cancer cells in significant numbers [91]. This was seen in 28 of 33 dissected surgical specimens from patients with PDAC.

Cancer cells adapt in several other ways which help them remain undetected and to avoid being destruction by T lymphoctyes. For example, major histocompatibility complex (MHC) proteins and the fas receptor are both down-regulated in cancer cells, thus rendering them more resistant to the action of infiltrating T cells. The fas ligand is capable of inducing apoptosis in cells, and cancer cells also overexpress this. Furthermore, neoplastic cells have been shown to recruit and maintain local regulatory T cells, which act to inhibit both T cell activation and function [20].

Here one can conclude that pancreatic cancer is characterised by an abundance of cell mediated immunity. However, several mechanisms are in place to create a potent barrier and help protect the tumour from the action of activated T cells in situ. These alterations in the TME have been termed ‘tolerising’conditions. This represents the fact that neoplastic cells

are able to mimic signalling pathways of the immune system in order to propagate conditions that favour immune tolerance [94].

1.3.6.2 Inflammatory cells

Immunohistochemical analysis of PDAC sections by Aoyagi et al [95] revealed that a large number of neutrophils were located at the invasive front of the tumour. These cells expressed high levels of TGFβ which in turn correlated with large amounts of collagen production. Emmrich and colleagues [96] also used immunohistochemistry to demonstrate increased numbers of macrophages in the stroma in PDAC and CP, compared to that of healthy pancreatic tissue. Macrophages were the predominant subtype of immune cell in normal tissue, although in both PDAC and CP the predominant subtype was infiltrating T lymphoctyes.

Macrophages are derived from monocytes in the circulation which are drawn to tissues through the secretion of MCP-1, levels of which are raised both in PDAC and CP. The presence of the ECM component decorin is closely related to the expression of the MCP-1 protein [70]. Therefore, through mechanisms yet to be clarified, decorin may be responsible for drawing macrophages to the TME. Such an idea supports previous findings of the tumour suppressive functions of decorin. It also highlights that PSCs could indirectly affect immune processes through their ability to secrete decorin during pancreatic disease (See Section 1.3.3.3).

The presence of inflammatory cells within the stroma of PDAC has been correlated with increased angiogenesis, a recognised indicator of a poor prognosis [90]. Macrophages secrete proangiogenic growth factors such as VEGF, thus increasing both angiogenesis and metastatic potential. Macrophages are also able to secrete several interleukins which stimulate tumour local growth and invasion. For example, IL-1 decreases the adhesion between cancer cells and their surrounding basement membrane proteins including Laminin, thus promoting motility and cancer spread [35]. Moreover, IL-6 is released which activates PSCs, thus promoting tumour growth through greater ECM deposition as well as other effects previously discussed in Section 1.3.2.3. Finally, IL-8 secreted by macrophages has been

shown to increase the growth rate and likelihood of metastasis in an in vivo model of pancreatic cancer [70].

Cyclooxygenase-2 (COX-2), an enzyme that mediates inflammation in non-cancerous cells, has now been proposed as an important promoter of cancer cell invasion. Co-culture studies of pancreatic cancer cells with cancer associated fibroblasts have demonstrated upregulation of the COX-2 gene in both parties. Also, in vitro invasion assays revealed an increased invasive potential for the cancer cells during co-culture, an effect which was partially inhibited when a COX-2 inhibitor was added to the media [97]. This inflammatory enzyme can also affect PSCs, specifically their proliferative rate. Activated PSCs are capable of secreting COX-2, although when cultured in cancer cell supernatant this expression was significantly increased. The addition of an inhibitor of COX-2 to the media decreased proliferative rate, as well as reducing the PSC's own secretion of COX-2 [98].

1.3.6.3 The immune system and cancer initiation

Few T or B lymphocytes are detected in the scant stroma of the healthy pancreas. The situation in CP varies with substantial lymphocytic infiltration of the stroma and often K-ras mutation. Animal studies have demonstrated that K-ras mutation by itself cannot lead to PanINs or PDAC. However, animals induced with both CP and K-ras mutation are able develop PDAC [35].

A review by Farrow et al [99] explores how pancreatic inflammation, mediated by cytokines, reactive oxygen species, and upregulated pro-inflammatory pathways plays a key role in the early development of pancreatic malignancy. This is through increased cell cycling, disruption of cell differentiation, and the loss of tumour suppression with increased stimulation of oncogenic expression. According to van Heek and colleagues [100] increased intracellular ROS formation may lead to DNA damage and contribute to telomere shortening, changes which are widely observed in PanINs.

1.3.7 Vascular cells and angiogenesis

The main vascular cells which make up the TME include endothelial cells, pericytes, and vascular smooth muscle cells.

Pericytes are embedded within the basement membrane of blood microvessels adjacent to endothelial cells, both of which are important regulators of vascular development and remodelling [101]. They exist as precursor cells which demonstrate functional plasticity in their ability to differentiate further into vascular smooth muscle cells or collagen secreting stromal cells [36].

Endothelial cells are fully differentiated cells which are stimulated by the family of growth factors named VEGF. Their level of activity is determined by the dynamic balance between proangiogenic factors and endogenous angiogenic inhibitors [36].

VEGF promotes angiogenesis during embryonic development and is imperative to wound healing in healthy adults. During tumourigenesis, it is upregulated by oncogene expression, growth factors, inflammation and hypoxia to promote angiogenesis. Before a tumour can grow beyond 1-2 mm, it requires blood vessels for nutrients and oxygen. The release of VEGF and other growth factors prompts the formation of new blood vessels which allows the exponential growth of the tumour [4;102].

The blood vessels that form by VEGF secretion in tumours are irregular in terms of structure and function. They are leaky and haemorrhagic, and lack the organisation into venules, arterioles, and capillaries like in normal vasculature. The resulting blood flow is suboptimal, resulting in hypoxic conditions and further VEGF secretion [102].

Our knowledge relating to angiogenesis in PDAC is less advanced compared to that of pancreatic islet cell carcinogenesis. Using their mouse model of islet cell carcinogenesis, Hanahan et al. [103] proposed a multi-stage process in which angiogenesis is initiated in dysplastic tissues before the formation of any tumour. This has been termed the ‘angiogenic switch’. VEGF-A plays a key role in this progression, in addition to PDGF mediated signalling from endothelial cells to pericytes. The ’angiogenic switch’ is considered off when there is a balance between the effects of pro-angiogenic and anti-angiogenic molecules.

Pancreatic cancer tissues are hypoxic and have a low microvessel density unlike those found in islet cell tumours, and most other solid malignancies. However, this cancer, like all other cancers still depends on an angiogenic process [20]. Over-expression of VEGF and its receptors has been associated with a poor prognosis and increased metastatic potential in pancreatic cancer [41]. It has been demonstrated that the VEGF/VEGF-RII pathway regulates angiogenesis in PDAC. Genetic down-regulation of VEGF-RII has been shown to inhibit both local growth and the likelihood of metastases [104].

Abdollahi and colleagues [105] carried out transcriptional profiling to identify proangiogenic factors in a large number of human pancreatic tissue samples. They compared normal pancreatic tissue, chronic pancreatitis, and primary and metastatic PDAC. They reported a gradual increase in the levels of proangiogenic factors, and a gradual decrease in anti-angiogenic factors as samples progressed from normal, to inflamed and to cancerous tissue. These authors also believe that there is an 'angiogenic switch' that arises after PDAC could have been lying in a microscopic, dormant state for months or years. They propose that after prompting this switch, the dormant cancer becomes rapidly proliferative and develops the potential to disseminate [20].

The growth factors which stimulate the 'angiogenic switch' can emanate from cancer cells, PSCs, fibroblasts, the ECM, in addition to endothelial cells themselves [106]. Furthermore, TME components including mast cells, monocytes and tumour cells have demonstrated secretion of VEGF-A, VEGF-C and bFGF in culture [36].

Angiogenic receptors are not only expressed on vascular cells, but also on cancer cells. For example, VEGF-RI is found in PDAC cell lines, and once activated encourages their migration and invasion. Therefore, theoretically, anti-angiogenic therapies will not only inhibit angiogenesis, but will also stop the autocrine stimulation of pancreatic cancer cells [20].

Promising results have been elicited in vivo when VEGF receptor blockers combined with gemcitabine therapy reduced tumour volume in metastatic pancreatic cancer [107]. However, other studies have demonstrated that targeting VEGF with inhibitory agents causes the tumour to adapt and begin to produce a wider array of angiogenic molecules. For example, if VEGF is blocked then tumours can secrete other angiogenic molecules instead, such as IL-8 or bFGF. Moreover, COX-2 and NRP-1 are additional angiogenic factors, whose expression is linked to a poor prognosis in pancreatic cancer.

1.4 MicroRNA

MicroRNAs (miRNA) are a class of small (~22 nt) non-coding RNA molecules with gene-regulating functions, discovered under two decades ago. They have been implicated in a whole host of cellular processes including the epigenetic regulation of cancer related genes [108]. This has earned them a great deal of attention from the scientific community. Their importance has been further emphasised by recent evidence that each miRNA may control hundreds of gene targets. Therefore, it is staggering to consider the number of already recognised genetic pathways that miRNAs could affect [109].

1.4.1 Biogenesis, functions and targets

The first step of miRNA maturation takes place in the nucleus where the long primary transcript (pri-miRNA) is cleaved into a shorter stem-loop intermediate around 60-70 nucleotides in length, known as a precursor miRNA molecule (pre-miRNA) [110]. This processing is performed by Drosha and Pasha, an RNase III endonuclease and a double-stranded RNA binding protein respectively [111;112]. The pre-miRNA is transported from the nucleus to the cytoplasm by a molecule named Exportin-5. It is here that the pre-miRNA is cleaved by an RNase III enzyme called dicer to form mature miRNA. Mature miRNA is then loaded onto a multi-protein complex called an RNA-induced silencing complex (RISC) which acts as a guide for the miRNA. RISC binds to the 3' untranslated region of mRNA by imperfect base pairing. Once bound, the RISC molecule causes gene silencing by either cleaving the target mRNA, or by inhibiting the translational process [108].

The primary target recognition determinant known as the seed region is only 7/8 nucleotides in length, thus a single miRNA can potentially regulate hundreds of gene targets [113;114]. It is surprising that miRNAs have only recently been discovered considering that they also comprise one of the more abundant classes of gene regulatory molecules [110].

MiRNAs are grouped into families if they share an identical sequence in the seed region. As such, those from the same family bind to and regulate the expression of essentially the same set of target mRNAs.

Researchers at the University of Manchester and the Wellcome Trust Sanger institute have created a comprehensive online database of all the miRNAs discovered to date. This is a rapidly developing area of research as evidence by the exponential growth in the number of mature miRNAs identified over the past few years. The most recent database was uploaded in April 2011 (miRBase 17 release) and contains 16,772 mature miRNAs originating from over one hundred different species. This compares to only 703 mature human miRNAs reported in the miRBase 13 release in March 2009 [115-118].

Computational approaches can be used to identify regulatory targets of miRNAs. If we know the functional role of these targets, this provides clues to the function of the miRNA [108]. However, there are few mRNA molecules with near-perfect complementary base pairs to miRNAs, thus making false positives common. Accordingly, prediction algorithms can only provide a list of their likely targets but cannot be assumed to be correct, and need to be followed up with experimental evaluation [110].

1.4.2 MicroRNAs and human cancer

The potential of miRNAs to act as biomarkers for disease has also been identified. Unlike most other biomarkers currently available, this group of molecules appears to be disease and cell type specific [119]. PDAC is a disease resulting from epigenetic alterations, and conceivably has its own specific miRNA expression profile. Their central role in cellular regulation, as well as their inherent stability especially in patient serum at room temperature represent further reasons why these molecules would make useful biomarkers [120].

Lu and colleagues [121] performed miRNA expression profiling for different types of human cancers. They described that miRNA profiles not only revealed the developmental lineage of the tumour but also the state of differentiation. In general, they observed miRNA expression to be down-regulated in tumours compared to normal tissues. Messenger RNA (mRNA)

profiling was also carried out in conjunction with these experiments but mRNAs were highly inaccurate in differentiating samples.

Several miRNAs have been labelled as oncomiRs due to their capacity to down-regulate tumour suppressor genes and promote tumour oncogenes. Alternatively, other miRNAs have been shown to negatively regulate oncogenes, for example miR-15 down-regulates BCL2. Therefore, gene therapies using the latter may be an effective approach to inhibiting oncogenes and blocking tumour progression [109].

1.4.3 The microRNA-29 family

An important area of research which has not been addressed to date is the involvement of miRNAs in the regulation of pancreatic stellate cells. Identifying miRNAs which control the behaviour of PSCs is essential, since this may hold the key to reversing their activity, thus inhibiting the growth and dissemination of cancer cells.

Indications that miRNAs are important in regulating PSCs emerge from studies relating to liver fibrosis. Roderberg and colleagues [122] recently profiled miRNAs in mouse livers made fibrotic through carbon tetrachloride treatment and bile duct ligation. They found several miRNAs to be differentially expressed including all three members of the miR-29 family. In vitro analyses of resident hepatic cells revealed that miRNA-29 levels were normally expressed at very high levels in hepatic stellate cells, when compared with hepatocytes, Kupffer cells, and endothelial cells.

In subsequent experiments, isolated Hepatic stellate cells (HSC) were activated with TGFβ or lipopolysaccharide, which significantly reduced miRNA-29 levels through NFκB signalling. Up-regulation of this miRNA was also associated with a reduction in the expression of the ECM collagen genes, Col1a1, Col4a5, and Col5a3. This suggests that activated HSCs increase their secretion of collagen through the down-regulation of miRNA-29. This notion is further supported by their serum analyses showing miRNA-29 to be reduced in patients with advanced liver cirrhosis compared to healthy controls or patients with early cirrhosis.

HSCs and PSCs not only appear the same morphologically, but also possess similar functions including their mediation of fibrosis through production of collagen and other ECM proteins. Transcriptomic analysis of the two cell types displayed similar gene expression profiles, although distinct differences in expression patterns were observed [113]. The similarities between these two cell types represent further indications that miRNAs are important in the regulation of PSCs.

CHAPTER 2:

STUDY AIMS

2.1 Study aims

1. To isolate and characterise pancreatic stellate cells derived from tissue specimens of patients with a variety of pancreatic diseases.

2. To conduct a preliminary investigation to compare microRNA-29 expression between cancer-derived and inflammatory-derived primary pancreatic stellate cells.

3. To cryopreserve stocks of pancreatic stellate cells and other pancreatic stromal cell types for use in future experiments including microRNA analysis.

4. To determine optimal experimental techniques for the isolation and characterisation of pancreatic stellate cells to provide guidelines for future researchers in Dr Costello's laboratory.

CHAPTER 3:

MATERIALS & METHODS

3.1 Cell lines and cell culture

Four human Pancreatic ductal adenocarcinoma (PDAC) cell lines (MIA PaCa-2, Panc-1, BXPC-3, Suit-2) were cultured in RPMI 1640 media (Sigma, Poole, UK) supplemented with 10% FBS (PAA, Pasching, Austria), 1% L-glutamine (200mM) and 1% penicillin-streptomycin (100U/mL) (Sigma, Poole, UK). Primary PSCs were cultured in IMDM media (Sigma, Poole, UK) supplemented with FBS, L-glutamine and penicillin-streptomycin solution as above.

We also received an immortalised pancreatic stellate cell line named 'RLT-PSC' as a kind gift from Dr Ralf Jesenofsky [89], University of Heidelberg, Germany. These cells were isolated from human pancreatic tissue affected by chronic pancreatitis using an outgrowth method. They were then characterised and immortalised by transfection with SV40 large T antigen and human telomerase (hTERT). These cells were cultured in DMEM/F-12 + Glutamax media (Invitrogen, Paisley, UK) supplemented with 10% FBS, 1% L-glutamine (200 nM) and 1% penicillin-streptomycin solution (100U/mL).

All cell lines were cultured as a monolayer in 10mL media in T75 flasks (Fisher Scientific, Loughborough, UK) at 37°C in 5% CO_2. Once the cells reached 80-90% confluence they were washed with Dulbecco's PBS and passaged using 3mL of Trypsin-EDTA solution (0.5% porcine trypsin, 0.2% EDTA in Hank's Balanced Salt Solution with Phenol Red).

3.2 Sample collection

3.2.1 Protocols for sample collection

We requested protocols for stellate cell isolation from Dr Phoebe Phillips, a postdoctoral fellow with expertise in pancreatic stellate cell culture at the University of New South Wales, Australia. These were kindly sent by electronic mail, and formed the basis of the explant method, that we adopted to isolate activated pancreatic stellate cells from pathological pancreatic tissue.

The Liverpool Experimental Cancer Medicine Centre (LECMC) had formerly established protocols for the collection of human pancreatic tissue following surgical resection at the Royal Liverpool University Hospital. These procedures were performed to the standard of good clinical laboratory practice (GCLP).

The protocols received from Dr Phillips for stellate cell isolation were not compatible with the sample collection methods already in place. The previous Departmental standard operating procedure (SOP) stated that the resected pancreatic specimen should be transported from theatre to the Pathology Department in a dry specimen pot with no specified urgency. Alternatively, the PSC isolation protocol emphasised the importance of both, keeping the specimen at freezing temperatures during transportation, and placing the tissue into culture as soon as possible. Therefore, in compliance with GCLP, the SOP for the collection and transport of pancreas tissue samples from theatre was adjusted accordingly.

3.2.2 Kit building

The sample collection methods already in place utilised kits to obtain tissue from patients for research purposes. Each kit consisted of around 40 components including micro-centrifuge tubes, cryotubes, syringes, needles, consent forms and a urine pot. Samples of blood, urine, and pancreatic juice, along with tru-cut biopsies and pieces of normal and tumour tissue excised during surgery were obtained from the patient. Tissue samples were also gathered from organs surrounding the pancreas such as the duodenum and common bile duct.

In order to collect extra human tissue for PSC culture, a new type of kit was designed with three additional components to those contained in the regular pancreas collection kit. The new components comprised of two cryotubes, one for snap freezing pancreatic tissue in liquid nitrogen, and another containing 'RNA later' reagent to preserve tissue for RNA analysis at a later date. Thirdly, a viable sample sticker with a printed bar code was also added to the kit components. If PSCs were successfully cultured from a pancreas tissue sample then this sticker would be affixed to my laboratory notebook, corresponding with any information regarding subsequent stellate cell culture. All kits manufactured were recorded on the Laboratory information management system (LIMS) system and were subject to quality assurance checks in compliance with GCLP regulations. Each of the kit components was labelled with a unique barcode so that their storage locations could be tracked.

3.2.3 Sample collection day

In preparation for a sample collection day, PBS was poured into 1 litre glass bottles which were sterilised by autoclaving. Plastic specimen pots which were to be used to contain the specimen and PBS during transportation were also sterilised. This involved washing with bleach, followed by rinsing with water to wash the bleach off, and a subsequent wipe with 70% ethanol.

On the morning of a resection a 1 litre batch of sterile PBS was poured into an empty specimen pot and stored in the GCLP freezer room refrigerator at 4°C. Throughout the rest of the day, we awaited a telephone call from the theatre staff to inform us whether the tissue specimen was soon to be, or had already been resected. Occasionally, we were notified that the sample was non-resectable due to local advancement or distant metastases. If the sample was ready for collection, the specimen pot was placed into a rubber ice bucket containing ice cold freezer bags and transported from the GCLP freezer room to theatre, along with 2 cryotubes (one for snap freeze and one for RNA later) and a liquid nitrogen container.

On arrival in theatre the resected specimen was transferred from a dry pot into ice cold PBS. It was important to minimise the amount of time that the specimen was left in the dry pot by arriving to theatre as quickly as possible after the sample was declared ready for collection.

A telephone call was made to the Pathology Department informing them that the resection had taken place and that we would soon arrive there with the specimen. The ice bucket containing the specimen immersed in ice cold PBS was transported to Pathology as quickly as possible.

As long as the pathologist deemed there to be a sufficient amount of tissue for histological diagnosis, surplus tissue could be excised from the specimen for research purposes. If this was the case, the pathologist would dissect a fibrous piece of cancerous or inflamed tissue.

The pathologist sliced the dissected tissue sample into two pieces. The first was destined for snap freezing in a Dewar liquid nitrogen container, and the second was immersed into a Falcon tube containing 20mL of sterile ice cold PBS supplemented with 1% Pencillin-Streptomycin solution. A tissue sample was considered to be fibrous if it sank to the bottom of the Falcon tube. Unwanted excess fatty tissue would cause it to float in the PBS.

The sample to be snap frozen was wrapped in aluminium foil, inserted into a cryotube and immersed in liquid nitrogen. This cryotube was temporarily stored in the Dewar container until it was transferred to the -150°C freezer in the GCLP facility biobank later that day.

The other piece of tissue was transported to the primary culture laboratory for processing. This was then further dissected into three pieces, the first for PSC outgrowth, the second immersed in 'RNA later' reagent, and the third immersed in 4% formalin (Sigma, Poole, UK) to be later examined by Haematoxylin and Eosin staining.

The tissue destined for 'RNA later' reagent was diced into tiny pieces, approximately 1-2mm^3 in size before being dropped into the solution. This cryotube was stored in the GCLP facility at 4°C overnight, and then transferred to -80°C the following day. The freezer locations for both the snap freeze and 'RNA later' cryotubes were recorded on the LIMS system.

3.3 Pancreatic stellate cell outgrowth

The dissected tissue sample was swiftly transported from Pathology to our laboratory, where it was diced into tiny pieces (<1mm^3) using a sterile scalpel and sterile tweezers (Sigma, Poole, UK).

The culture medium used for stellate cell outgrowth was Iscove's modified Dulbecco's medium (IMDM) (Sigma, Poole, UK) supplemented with 20% FBS (PAA, Pasching, Austria), 1% L-glutamine (2mM), and 1% penicillin-streptomycin solution (100U/mL) (Sigma, Poole, UK).

Half a millilitre of IMDM media was added to a 40 mm diameter petri dish. Five pieces of diced tissue were placed into the dish with sufficient space between them, using sterile tweezers. The dish was then placed into the incubator for culture at 37°C in 5% CO_2. Care was taken when transporting it to the incubator, ensuring that it was held flat to prevent the tissue pieces from being displaced. This process was repeated using the remainder of the diced tissue sample.

Over the next few days the dishes were monitored for any sign of contamination such as turbid media. In the absence of obvious infection, a further 0.5 mL of media was added to each dish after 3 days of culture. From here onwards, media was exchanged once every 3 days.

According to Dr Phillip's protocols, PSCs were expected to grow out from the tissue pieces after 1-2 weeks of culture. Moreover, following the initiation of PSC outgrowth in the dish, it was recommended that the tissue pieces should be removed as soon as 'empty zones' began to appear in the spaces immediately surrounding them. The term 'empty zone' simply referred to an area lacking in cell growth.

3.4 Pancreatic stellate cell culture

After reaching confluence in the dish, stellate cells were passaged into a T-25 or T-75 flask (Fisher Scientific, Loughborough, UK). A volume of 1mL Trypsin-EDTA solution (0.05%, 0.02%) was added to the petri dish which was incubated for 3 min. After this time period the trypsin was neutralised with 2mL IMDM media supplemented as described above.

Occasionally cells would cease to grow before they reached full confluence in the petri dish. In my experience, only cells with a greater confluence than 50% would manage to survive and proliferate after propagation into a new flask.

IMDM media used to culture primary cells in T25/T75 flasks was supplemented with 10% instead of 20% FBS. Cells that reached confluence in a T25 were passaged using 1.5mL trypsin, and incubated for 3min as above. Trypsin was neutralised with 3.5mL media. Three millilitres of trypsin was used to passage cells cultured in a T75 flask, and this was neutralised with 7mL of media.

3.5 Pancreatic stellate cell cryopreservation

Once stellate cells reached confluence in a T75 flask (usually passage 2) they were ready for cryostorage. Cells were washed twice with 10 mL PBS. Three millilitres of trypsin was added and the flask incubated at 37°C for 2-4 min. The degree of cell detachment was determined by observation under the microscope, and the flask was tapped several times to aid detachment. Seven mL of IMDM culture medium was added to stop the action of trypsin. The cell suspension was mixed by gentle pipetting, and the sides and surface of the flask were rinsed. The suspension was transferred to a falcon tube and centrifuged at 1500 rpm, 4°C for 5 min. All of the supernatant was removed and the tube flicked several times to break up the cell pellet. A solution consisting of 5% DMSO dissolved in IMDM media (20% FBS) was removed from ice, and 1.5mL of this was added to the cell pellet. This was mixed by gentle pipetting. The resulting solution was transferred into a cryotube and kept on ice. The PSCs were stored at -80°C for 24 h, before being transferred to the -150°C freezer located in the GCLP facility. The location of all cryopreserved cells was logged onto the LIMS.

3.6 Characterisation of Pancreatic stellate cells by Immunofluorescence staining

3.6.1 Immunofluorescence experiment protocol

Glass coverslips 13mm in diameter (Fisher Scientific, Loughborough, UK) were sterilised by autoclaving in advance of the immunofluorescence staining experiment. They were subsequently stored in a petri dish containing 70% ethanol solution so as to maintain their sterility.

Mounting medium was also prepared in advance in the following way. Six grams of glycerol, 2.4g Mowiol 4-88 (Sigma, Poole, UK), 6mL ddH_20, and 12mL 0.2M Tris buffer pH 8.5 was mixed for 12 h on the shaker. This was left to sit for 2 h. The mixture was incubated at 50°C for 10 min and then centrifuged at 5000g for 15 min. Finally, the supernatant was removed, aliquoted and freezed at -20°C until use.

When stellate cells reached confluence in a T75 flask they were trypsinised. Three millilitres of the resultant 10 mL cell suspension were kept in the flask and topped up with media. The other 7 mL was transferred into a 15 mL Falcon tube, and cell clumps removed by gentle pipetting. Twenty five microlitres of this cell suspension was pipetted into a haemocytometer chamber, cells were counted, and the number of cells per mL calculated.

Whilst working in the cell culture hood, coverslips were transferred into the wells of a 24 well plate using sterile forceps. One millilitre of the cell suspension at the appropriate cell density was dispensed into each well. Cell densities varied according to cell type but ranged between $3x10^4$ and $8\ x10^4$ cells per well.

Immortalised PSCs and PDAC cell lines were plated at lower cell densities to the primary stellate cells due to their more rapid rate of growth. Cells were left in the incubator to proliferate and adhere properly to the coverslips.

Forty-eight hours later, cells were rinsed twice with PBS before fixation in 4% formalin (Sigma, Poole, UK). Fixation was achieved through the addition of 1 mL of formalin solution per well, and incubation for 20-30 min at 4°C.

The formalin was aspirated and cells were rinsed with PBS. Cells were permeabilised by incubating with PBS+0.5% Triton X-100 (Sigma, Poole, UK) for 3-5 min at 4°C. Three washes, each lasting 5 min, were carried out with PBS whilst gently shaking the plate.

All blocking solutions were prepared using PBS. Goat serum (Invitrogen, Paisley, UK) diluted to a concentration of 10% was usually used for blocking. However, when staining for vimentin expression, BSA at a concentration of 2% was utilised instead because our vimentin antibody is raised in goat species. Protein aggregates were removed by passing the blocking solution through a 0.2µm filter. Blocking was carried out for at least 1 h using 1mL per well, ensuring coverslips were entirely covered.

All antibodies were diluted in blocking solution. Depending on which agent was used for blocking, goat serum was reduced from 10% to 2% for the antibody incubation step, whereas BSA was reduced from 2% to 1% for the antibody incubation step. Prior to treatment with the antibody, the plate lid was labelled and parafilm adhered to the lid. Twenty-five microlitres of antibody solution was pipetted onto the parafilm over each corresponding well.

Coverslips were lifted out from the wells using fine tip forceps, and then laid cell face down onto the drop of antibody solution. Care was taken to make sure that the entire surface of the coverslip was immersed in the drop of fluid. The plate lid was left in a humidified chamber (plastic container containing paper towels soaked in warm water) for 1 h at room temperature or alternatively overnight at 4°C.

Coverslips were transferred back into the wells of the 24-well plate and washed 3 times with PBS for 5 min each with gentle shaking.

Secondary antibody treatment was carried out using the same technique as for the primary. From this point onwards the coverslips were protected from the light whenever possible using aluminium foil to cover the plate.

Subsequent to another 2 washes lasting 5 min each, the coverslips were treated with DAPI (4′,6-Diamidino-2-phenylindole dihydrochloride) solution (Sigma, Poole, UK) for 5 min and then placed back into PBS. DAPI was applied at a concentration of 0.5 µg/mL.

Five microlitres of Mowiol 4-88 (Sigma, Poole, UK) mounting medium was dispensed onto a glass slide (VWR, Lutterworth, UK). The coverslip was lifted from the 24 well plate and excess moisture aspirated by gentle contact against a paper towel. The coverslip was then

layered slowly onto the drop of mounting medium cell face down, whilst ensuring that no bubbles of air were trapped beneath the coverslip.

Mounting medium was left to set for a minimum of 3 h. Glass slides were stored at 4°C in the dark.

Due to the delicate nature of this procedure, occasionally a glass coverslip would be dropped whilst transferring them back and forth with forceps. In such as scenario one must then determine which side of the coverslip has the adherent cells. This can be identified by one of the following two methods. Firstly, if one hand is used to hold the coverslip, the other hand is used to scratch the surface of the coverslip gently with forceps, observing whether any cells are removed in the process. Alternatively, the coverslip can be transferred back into the well of the 24 well plate and examined under the microscope. If the coverslip happens to be cell side up then the cells growing on the coverslip will focus at a different magnification to the cells growing directly on the plate around the coverslip.

The antibodies used to stain for stellate cells are listed in Table 3.1 below.

Antibody	Species raised in	Marker	Supplier
GFAP	Rabbit polyclonal	Stellate cell / astrocyte	Abcam, Cambridge, UK
GFAP	Rabbit polyclonal	Stellate cell / astrocyte	DAKO, Stockport, UK
Desmin	Rabbit polyclonal	Stellate / smooth muscle cell	Abcam, Cambridge, UK
Desmin	Mouse monoclonal	Stellate / smooth muscle cell	DAKO, Stockport, UK
Alpha smooth muscle actin	Mouse monoclonal	Stellate cell / myofibroblast	Abcam, Cambridge, UK
Vimentin	Goat polyclonal	Mesenchymal cell	Santa Cruz Biotech, USA
Pan-cytokeratin	Mouse monoclonal	Epithelial cell	Abcam, Cambridge, UK
Isotype control	mouse	Normal mouse IgG	Santa Cruz Biotech, USA
Isotype control	rabbit	Normal rabbit IgG	Santa Cruz Biotech, USA
Alexa fluor 488	mouse	Green fluorescent tag	Invitrogen, Paisley, UK
Alexa fluor 488	rabbit	Green fluorescent tag	Invitrogen, Paisley, UK
Cy3	mouse	Red fluorescent tag	Jackson ImmunoResearch, West Grove, USA
Cy3	rabbit	Red fluorescent tag	Jackson ImmunoResearch, West Grove, USA
Cy3	goat	Red fluorescent tag	Jackson ImmunoResearch, West Grove, USA

Table 3.1 Antibodies used for the characterisation of stellate cells in this project.

3.6.2 Immunofluorescence image analysis

Immunostained cells were visualised using the 100x oil immersion lens of a fluorescent microscope (Nikon TE 300). Images were captured with an attached Zeiss camera.

The coverslips were wiped using a cotton bud soaked in analytical reagent grade methanol. A drop of Carl Zeiss Immersol 518N immersion oil (Fisher Scientific, Loughorough, UK) was placed onto each coverslip. It was imperative that slides removed from the refrigerator were allowed to warm to room temperature before observation under the microscope to avoid condensed water mixing with the immersion oil.

In order to observe the cells, the slide was slotted upside down on the microscope platform, and the lens raised high enough so that it gently touched against the coverslip.

Simple PCI 6 software was utilised for image interpretation and processing. Images were recorded in 'tif' format and were later converted to 'png' files using ImageJ software. Gain, exposure and binning settings were constant between cells stained within the same immunofluorescence experiment to allow for accurate comparisons. However, these measures could be adjusted between different experiments.

3.7 MicroRNA-29 analysis

3.7.1 Cell plating and TGFβ treatment

Primary PSCs, RLT-PSCs and the BXPC3 cancer cells were seeded in 6 well plates as shown in the tables below. Cells were starved in 2% FBS and either:

- Stimulated for 48 h with 20ng/mL recombinant human TGF-β or
- Left untreated for 48 h

They were lysed immediately after this treatment and underwent RNA purification.

Plate 1

Pt 1 Stellate with TGF-β	Pt 2 Stellate with TGF-β	RLT PSC with TGF-β
Pt 1 Stellate without TGF-β	Pt 2 Stellate without TGF-β	RLT PSC without TGF-β

Plate 2

BXPC3 cancer cell line with TGF-β		
BXPC3 cancer cell line without TGF-β		

3.7.2 RNA purification

RNA molecules ranging in size from 18 to 200 nucleotides were purified from cultured cells using the miRNeasy mini kit (Qiagen, Crawley, UK). The cells were lysed directly in the 6 well plates using 700 µl of QIAzol lysis reagent. A cell scraper was used to aid transfer of the lysate into microcentrifuge tubes (Eppendorf, Cambridge, UK). From this point onwords, reactions were carried out on ice unless otherwise stated.

The lysates were homogenised by vortexing for 1 min, then allowed to stand on the benchtop at room temperature for 2-3 min. One hundred and forty microlitres of chloroform was added to each tube and shaken vigorously for 15 s before being left on the benchtop again for 2-3 min. This suspension of lysate mixed with chloroform was centrifuged for 15 min at 13,000 rpm at 4°C, separating the sample into 3 phases: an upper, colourless, aqueous phase containing RNA; a white interphase; and a lower, red, organic phase. The upper aqueous phase was pipetted into a new eppendorf tube. One and a half volumes of 100% ethanol was added to each tube and mixed thoroughly by pipetting. Continuing without delay, 700 µl of the sample was transferred into an RNeasy Mini spin column in a 2 mL collection tube. This was centrifuged at 10,000 rpm for 15 s at room temperature and the flow-through discarded.

DNase digestion was also performed. Three hundred and fifty microlitres of miRNeasy mini kit buffer RWT was pipetted into the RNeasy Mini spin column and centrifuged for 15 s at 10,000 rpm. The flow-through was discarded. Eighty microlitres of DNase I incubation mix was pipetted directly onto the RNeasy Mini spin column membrane, and the tube placed on the benchtop for 15 min. Three hundred and fifty microlitres of the RWT buffer was then pipetted into the RNeasy Mini spin column which was centrifuged for 15 s at 10,000 rpm. The flow-through was discarded.

Five hundred microlitres of miRNeasy mini kit RPE buffer was pipetted onto the RNeasy Mini spin column which was centrifuged for 15 s at 10,000 rpm to wash the column. The flow-through was discarded. Another 500 µl of RPE buffer was added to the RNeasy Mini spin column and this time centrifuged for 2 min to dry the RNeasy Mini spin column membrane. This ensured that no ethanol was carried over during RNA elution which could interfere with downstream reactions.

Following centrifugation, the RNeasy Mini spin column was removed from the collection tube containing flow-through and placed into a new 2 mL collection tube and centrifuged at full speed for 1 min. This step eliminated any possible carryover of Buffer RPE. The RNeasy Mini spin column was transferred to a new 1.5 mL collection tube. Forty microlitres of RNase-free water was pipetted directly onto the RNeasy Mini spin column membrane and the tubes centrifuged for 1 min at 10,000 rpm. This resulted in elution of RNA and the tubes were stored at -80°C.

2.7.3 Reverse Transcription

RNA was reverse transcribed into cDNA using the miScript reverse transcription kit (Qiagen, Crawley, UK).

The purified RNA samples and miScript reverse transcriptase mix were thawed on ice. RNase free water and 5x miScript RT Buffer were thawed at room temperature. The individual solutions were mixed and centrifuged briefly to collect residual liquid from the sides of the tubes.

The reverse transcription master mix was prepared on ice. The 5x RT buffer (containing Mg^{2+}, dNTPs and primers), RNase free water and reverse transcriptase mix were added together in 0.5 mL PCR tubes. The resulting solutions were mixed by gently flicking the tubes. The template RNA (up to 1 µg) was then added and the tubes were centrifuged briefly at 5,000 rpm. The mixtures were then incubated for 1 h at 37°C followed by 5 min at 95°C.

After this incubation the quantity of cDNA in each sample was determined using a ND-1000 nanodrop spectrophotometer along with ND1000 v3.5.2 software.

3.7.4 Real-time PCR

Mature microRNA was quantified by real-time PCR using the miScript SYBR Green PCR kit, miScript Primer Assays, and miScript PCR control set (Qiagen, Crawley, UK).

Before starting the procedure the 10x miScript Primer assays and PCR control set primers were thawed on ice. The primers were reconstituted by centrifuging the vial briefly, then adding 550 µl of TE buffer. The resulting solution was mixed by vortexing.

The template cDNA was also thawed on ice. Each sample was diluted with TE buffer to give a concentration at which it was possible to load 1-3 ng in a volume of less than 5 µl. These volumes were calculated according to the cDNA concentrations detected by the nanodrop.

The 2x QuantiTect SYBR Green PCR Master Mix was thawed along with the 10x miScript Universal Primer and RNase-free water. The individual solutions were mixed by gently inverting the tubes.

Twenty-five microlitres of the SYBR green master mix and 5 µl of the universal primer were pipetted into the wells of the 96 well plate giving a volume of 30 µl per well. Variable volumes of the RNase free water were then added to the wells, followed by 5 µl of the specific primer or PCR control primer (RNU6B is recommended).

Finally, the cDNA was added to the wells, and the plate was sealed with a plastic sheet and centrifuged briefly. It was placed into the plate holder of the real-time cycler (Roche Lightcycler 480) and programmed as shown in Table 3.2 below. Real-time PCR data was analysed using LightCycler 480 Software, Version 1.5.

Step	Time	Temperature
PCR Initial activation step	15 min	95ºC
3-step cycling:		
Denaturation	15 s	94ºC
Annealing	30 s	55ºC
Extension	30 s	70ºC
Cycle number	45 cycles	

Table 3.2 PCR programme used for the amplification of micro-RNAs

CHAPTER 4:

RESULTS

4. 1 Sample collection and primary cell culture

4.1.1 Sample collection from theatre

A significant delay was experienced during the first sample collection. Having arrived at the Pathology Department with a Whipple's resection specimen, there were no pathologists available to process the sample. Almost an hour had passed before any tissue had been dissected. During this wait the resected tissue remained in a specimen pot containing PBS which gradually warmed to room temperature. The dissected tissue was transported back to the laboratory and diced before being plated into culture in a 6-well plate. This plate was observed for 2 weeks before it was discarded due to the absence of cell outgrowth.

In order to reduce the delays experienced during the first sample collection, arrangements were made with the Pathology Department to ensure that future resected samples for the purposes of stellate cell research would be attended to immediately upon arrival from theatre. As part of these new arrangements, the Pathology Department requested notification of any resection from which pancreatic cells were to be cultured, at least 24 h in advance. Also, a second notification was to be made to the on-call pathologist during the operation, informing them that the sample would arrive to their Department within 30 min.

4.1.2 Primary cell culture

During the collection of the second sample, the time taken to transfer resected tissue from theatre and into culture was significantly reduced to approximately 30 min. Three 6-well plates were prepared, each containing 5 pieces of diced pancreatic tissue per well.

After 1 week in culture, spindle and stellate-shaped cells began to grow out from the tissue in some of the wells. Cell growth continued for one more week before many of the outgrowing cells died or ceased proliferating. Dr Phillips' protocols for stellate cell culture (See Section 3.4 Materials and Methods) stated that the appearance of 'empty zones' in the space immediately surrounding the tissue signifies the appropriate time to remove them from culture. However, the appearance of such 'empty zones' was difficult to interpret. Moreover, protocols from Dr Phillips lacked any information regarding the time period after which these 'empty zones' are expected to appear.

Many of the outgrowing cells died after only one week of proliferation, and it was hypothesised that this could have been avoided through earlier removal of tissue. This is because tissue left in the culture plate for too long could possibly have become necrotic thus inhibiting surrounding growth. In order to test this hypothesis, the tissue was removed from one of the few wells which still contained proliferating cells, and the cells were extracted into the well of a new 6-well plate. These cells were observed 24 hours later. Only a few of the extracted cells adhered to the plate and began to proliferate. Subsequently, a few days later all the cells had died and therefore the plate was discarded. The reason for the cell death may have been that the trypsin reagent was poorly tolerated by the primary cells. Alternatively, there may have been insufficient cell numbers to allow for proliferation in the new dish.

After 3 weeks in culture, cells had once again begun to proliferate in around half of the wells. It was now imperative to determine the appropriate time period after which to remove the tissue pieces from culture, and also when to extract the cells from the well. Hence, over the coming weeks tissue was removed at different times in the various wells and the effect on cell viability was observed by carefully examining the cells daily using a light microscope. Rarely did a clear space or 'empty zone' appear between the tissue and cells. In fact, several wells became confluent with cells and still no space appeared adjacent to the tissue. Hence,

the appearance of ‘empty zones’ next to the tissue did not prove to be a useful guide for when to remove the explanted tissue.

After over a month in culture, from a total of eighteen wells for this patient sample, only wells 3 and 5 were successfully passaged into cell culture flasks. In addition to removing tissue pieces too late, it appeared that cell death occurred if tissue was removed too early, perhaps related to a reduction in the quantities of growth factors which accompanies the removal of explanted tissue. Furthermore, as well as removing cells too early from culture as mentioned above, leaving cells to culture in the wells for too long also led to fungal contamination in some cases.

The correct balance was achieved whereby tissue removal was carried out as soon as cell proliferation had ceased for more than 2 weeks. This was measured by observing the cells daily and monitoring the edges of the growth perimeter, which were indicated on the plate lid using marker pen. Also, transferring the cells to a new flask or passaging of cells was only performed once the well was more than 50% confluent with cells. This seemed to facilitate sufficient proliferation in the T25 flask into which the cells were transferred.

The use of 6-well plates for primary culture as recommended by Dr Phillips’ protocols was later discontinued. Although they are easier to handle during transfer in and out of the incubator, the appearance of fungal contamination in one of the plate wells would swiftly spread to the other wells. Instead, 40mm diameter petri dishes were utilised as pictured in Figure 4.1.

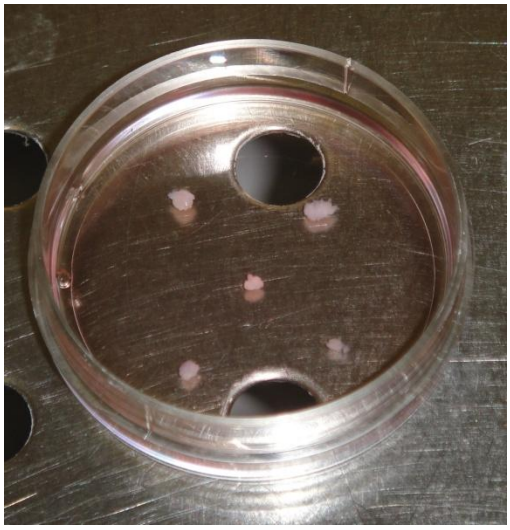

Figure 4.1 A 40mm diameter petri dish showing five pieces of tissue, as they appear immediately after placing in culture.

4.1.3 Primary cultured cell passage

In Dr Costello's laboratory the reagent typically used to detach adherent cells from the cell culture plate is Trypsin-EDTA solution, specifically comprising of 0.5% porcine trypsin and 0.2% EDTA. This solution causes minimal cell death when used to passage pancreatic cancer cell lines. However, when utilised for the passage of primary cultured cells it led to loss of viability and reduced growth.

Various types of Trypsin-EDTA reagent are available for purchase, each differing in their concentration of Trypsin and EDTA. Other types of cell dissociation buffer are also available which utilise different digestive enzymes, such as collagenase buffer, or use no digestive enzymes at all.

Several research groups have previously reported their success in establishing primary cultures of human PSCs [89;123-125]. While they have mentioned the use of trypsin for cell passage, they have not specified the concentrations of Trypsin and EDTA contained within these reagents [89;123-125].

Therefore, a number of different types of cell dissociation reagent were trialled in order to elucidate which of these would be best tolerated during primary cell passage. The results are summarised in Table 3.1, and described below. Consistently in these experiments, cells cultured in T75 flasks were passaged with 3 mL of the particular cell dissociation reagent and incubated for 3 min. Cell viability was then observed 24 h later.

Trypsin-EDTA solution containing 2.5% Trypsin and 0.5% EDTA was recommended by our colleagues in Dr Andrea Varro's Physiology Research Group at the Liverpool Cancer Research UK Centre. They use this reagent to dissociate adherent primary gastric myofibroblasts, cells which possess similar characteristics to primary activated PSCs. Unfortunately, when this reagent was used to dissociate the primary cells, it resulted in even greater proportions of cell death compared with the trypsin used as standard in Dr Costello's laboratory.

Gibco cell dissociation buffer, an enzyme free reagent was also experimented with. When this was applied to the primary cells for passage it resulted in fewer dead cells than Trypsin-

EDTA (2.5% Trypsin 0.5% EDTA). However, in comparison with Trypsin-EDTA (0.5% Trypsin 0.2% EDTA), there was a greater proportion of cell death.

The fourth and final dissociation agent that was trialled for cell passage was a weaker form of Trypsin-EDTA reagent containing only 0.05% Trypsin and 0.02% EDTA. This reagent was recommended by Dr Ralf Jesenofsky of the University of Heidelberg, who utilises this reagent for passage of both primary cultured rat PSCs and the immortalised PSC line (RLT-PSC) developed by their research group. Of all the types of dissociation reagents that were investigated, this was the best tolerated reagent, with minimal cell death occurring during passage. Despite its low concentrations of trypsin and EDTA, cells dissociated from the plastic plate within 2-4 minutes of incubation, as was observed when the other reagents were used.

Product name / supplier	**Components**	**Passaged cells**	**Approximate cell death**
Trypsin-EDTA solution 1x (Sigma, Cat No: T3924)	0.5% porcine trypsin, 0.2% EDTA, 4Na per litre of Hanks′ Balanced Salt Solution with phenol red	CP 07.02.11 Dish 11	10%
Trypsin-EDTA solution 1x (Sigma, Cat No: T4049)	2.5% porcine trypsin, 0.2% EDTA, 4Na per litre of Hanks′ Balanced Salt Solution with phenol red	CP 07.02.11 Dish 6	50%
Gibco Cell dissociation buffer (Invitrogen, Cat No: 13150-016)	Enzyme-free aqueous formulation of salts, chelating agents, and cell-conditioning agents in Ca^{2+}- and Mg^{2+}-free Hanks balanced salt solution	CP 07.02.11 Dish 9	20%
Trypsin-EDTA solution 1x (Sigma, Cat No: 59417C)	0.05% porcine trypsin, 0.02% EDTA, 4Na per litre of Hanks' Balanced Salt Solution with phenol red	CP 07.02.11 Dish 12	<1%

Table 4.1 Comparison of reagents used for the dissociation of primary cells for the purposes of passaging them. Cells were cultured in T75 flasks, and passaged by incubating three minutes with 3 mL of the respective cell dissociation reagent. Cell viability was recorded 24 h later following examination of the cells using light microscopy.

4.1.4 Optimisation relating to Immunofluorescence (IF) staining

During initial IF experiments, analysis of data was sometimes inhibited because cells were absent from the coverslips when examined under the fluorescent microscope. Hence, with subsequent experiments, cells were visualised under the light microscope after each step of the procedure. This was to elicit at which point the cells were detaching from the coverslip.

It became clear that the cells were being dislodged after the addition of formalin to the wells. This is likely due to the fact that formalin is quite a dense fluid compared to the other reagents utilised in this procedure. Hence, from here on the formalin was pipetted very gently against the wall of the well, and care was taken to avoid direct pipetting onto the cells at each step of the procedure.

This scenario more commonly occurred when cells had only been plated 24 h previous to the experiment, and thus had yet to adhere securely to the glass. This problem is somewhat expected because the glass has a smooth, flat surface compared with that of a cell culture plate, which is treated to optimise the ability of cells to adhere.

4.2 Description of patients and specimens

4.2.1 Description of patients from whom primary cells were successfully cultured

Primary pancreatic cells were successfully cultured from the resected tissue of 10 patients at the RLUH. Table 4.2 lists the age and gender of these patients, along with the date of their resection, their clinical diagnosis, and the histopathological details of the excised tissue sample.

Attempts were made to culture cells from more than 10 patients but several problems were encountered during sample collection. For example, the Pathology Department at the Royal Liverpool University Hospital (RLUH) closes at 5pm in the evening. Occasionally an operation would extend past 5pm, and the specimen would be resected after this time. As a result, tissue was not dissected and no samples were available to culture. At the RLUH one cannot request a surgeon to excise tissue for research purposes, in case this action interferes with diagnosis and staging later undertaken by the pathologist.

In other cases, the pathologist having examined the specimen, confirmed that the tumour was very small and that the whole sample was required for diagnostic and staging purposes. Furthermore, preoperative investigations such as CT scans were sometimes misleading. They occasionally indicated the presence of a pancreatic tumour before the resection, which was then found to be absent during histopathological examination.

Date of sample collection	Age / Gender	Clinical diagnosis / tumour stage	Histopathology details
19.10.10	75 / F	PDAC in head of pancreas pT3 pN1 M0 pR0	Poorly differentiated tumour measuring 31 x 20 x 19 mm. Perineural invasion present but no vascular invasion. No involvement of anterior, medial or posterior margins of pancreas, although tumour does reach duodenal submucosa. Three lymph nodes resected from posterior superior location contain metastatic carcinoma. Other lymph nodes are not involved.
07.12.10	37 / F	Mucinous cystic neoplasm in tail of pancreas	Multiloculated cyst measuring 110 x 110 x 25mm. Cyst lining is smooth and shiny, and cyst content is mucoid and watery. Focal solid area present which represents around 5% of total volume. No high-grade dysplasia or stromal invasion, even in the solid areas. Background pancreas shows features of Chronic Pancreatitis.
13.12.10	45 / F	PDAC in head of pancreas T3 N1 M0 R1	Ill-defined solid grey-white lesion, up to 27mm in its maximum dimension. Tumour is poorly differentiated and invades into the ampulla and peripancreatic fat. There is florid perineural and vascular invasion. Necrosis is present within tumour. Ten of 19 lymph nodes resected contain metastatic carcinoma. Background pancreas shows features of Chronic Pancreatitis. Focal areas of squamous metaplasia and PanIN-3 present.
14.12.10	51 / F	Cholangiocarcino-ma pT3 pN1 M0 pR0	White lesion measuring 20 x 15 x 15mm. Moderately differentiated tumour arising from the intrapancreatic bile duct in the head of pancreas, and extensively involves the adjacent pancreas. Two of 29 resected lymph nodes have metastatic carcinoma. Three other lymph nodes show a granulomatous inflammatory response. Foci of perineural invasion but no vascular invasion. Pancreatic resection margin and medial margin are involved by carcinoma.
20.12.10	74 / F	Adenosquamous PDAC in head of pancreas T3 N1 M0 R0	Solid grey/white tumour, 35mm in its maximum dimension. Background pancreas appears fibrotic with multi-focal PanIN-2 and -3. It is a poorly differentiated tumour which has locally invaded into peripancreatic fat, ampulla, duodenal wall, and the intra-pancreatic bile duct. Florid perineural invasion and vascular invasion seen. There is necrosis within the tumour. One of the 32 lymph nodes resected contains metastatic adenocarcinoma.

19.01.11	71 / M	PDAC in head of pancreas pT3 pN0 M0 pR1	Firm, white tumour measuring 50 x 45 x 25mm. It is a moderately, and focally poorly differentiated tumour. There is focal invasion of the muscularis propria of the duodenum, extensive perineural and intramural invasion as well, but no vascular invasion. Twelve lymph nodes contain reactive changes only.
25.01.11	52 / M	Chronic alcoholic pancreatitis. No clinical suspicion of malignancy	There is florid peri-tubular and intralobular fibrosis, loss of acinar tissue, mild chronic inflammation, islet cell hyperplasia, and neutrophil polymorphs within dilated ducts and ductules. There is PanIN-1A but no dysplasia or malignancy. Twelve lymph nodes have reactive changes only.
28.01.11	61 / F	PDAC in head of pancreas pT3 pN0 M0 pR0	White tumour with dimensions of 30 x 20 x 20mm. It is well/moderately differentiated and there is no vascular invasion, but extensive perineural invasion is present. Carcinoma extends to the duodenal wall. Foci of PanIN1b also present. Chronic Pancreatitis is present elsewhere in the pancreas, including in the excision margins. Twenty-seven lymph nodes show no evidence of metastatic carcinoma.
07.02.11	36 / F	Hereditary pancreatitis. No clinical suspicion of malignancy	There is extensive fibrosis and calcification with dilated pancreatic duct measuring up to 10mm in diameter and dilated branch ducts. Also, there is marked lobular atrophy with most lobules showing only residual ductules and scanty remaining acinar tissue. Large ducts are dilated, disrupted, and show squamous metaplasia. There are abundant foci of PanINs-1A & 1B, and a single focus of PanIN-2. There is no evidence of malignancy. Twenty lymph nodes resected show reactive changes only.
10.02.11	68 / F	Ampullary carcinoma pT4 pN1 M0 R0	Ulcerated tumour measuring 20 x 15 x 20mm. Poorly-differentiated and extending into adjacent pancreas, duodenal wall and peripancreatic fatty tissue. Vascular and perineural invasion are present. Two of the resected lymph nodes contain metastatic carcinoma.

Table 4.2 Clinical diagnosis and histopathology details of 10 patients from whom primary cells were successfully cultured

4.2.2 Nomenclature for pancreatic primary cell cultures

Flasks of primary pancreatic cells in culture have been named according to the resection date of the specimen from which they were derived, the pathology of the explanted tissue, the dish/well number that they were extracted from, and the number of passages which they have undergone in culture.

For example, a flask of cells named ‘PDAC 19.01.11 well 2 passage 1’ would represent cells in their first passage having been extracted from well number 2 of a 6-well plate (or dish no. 2), which contained explanted tissue constituting PDAC, from a patient who underwent resection on 19.01.11.

It is essential to distinguish between the different dishes/wells of primary cells from the same patient, due to the potential heterogeneity of these cells.

4.2.3 Haematoxylin and Eosin (H/E) staining of resected tissue

Photographs were taken of H/E stained tissue of two patients from whom cultures of primary cells were derived. The photographs displayed immediately below (Figure 4.2) are those of a PDAC tissue sample resected 28th January 2011.

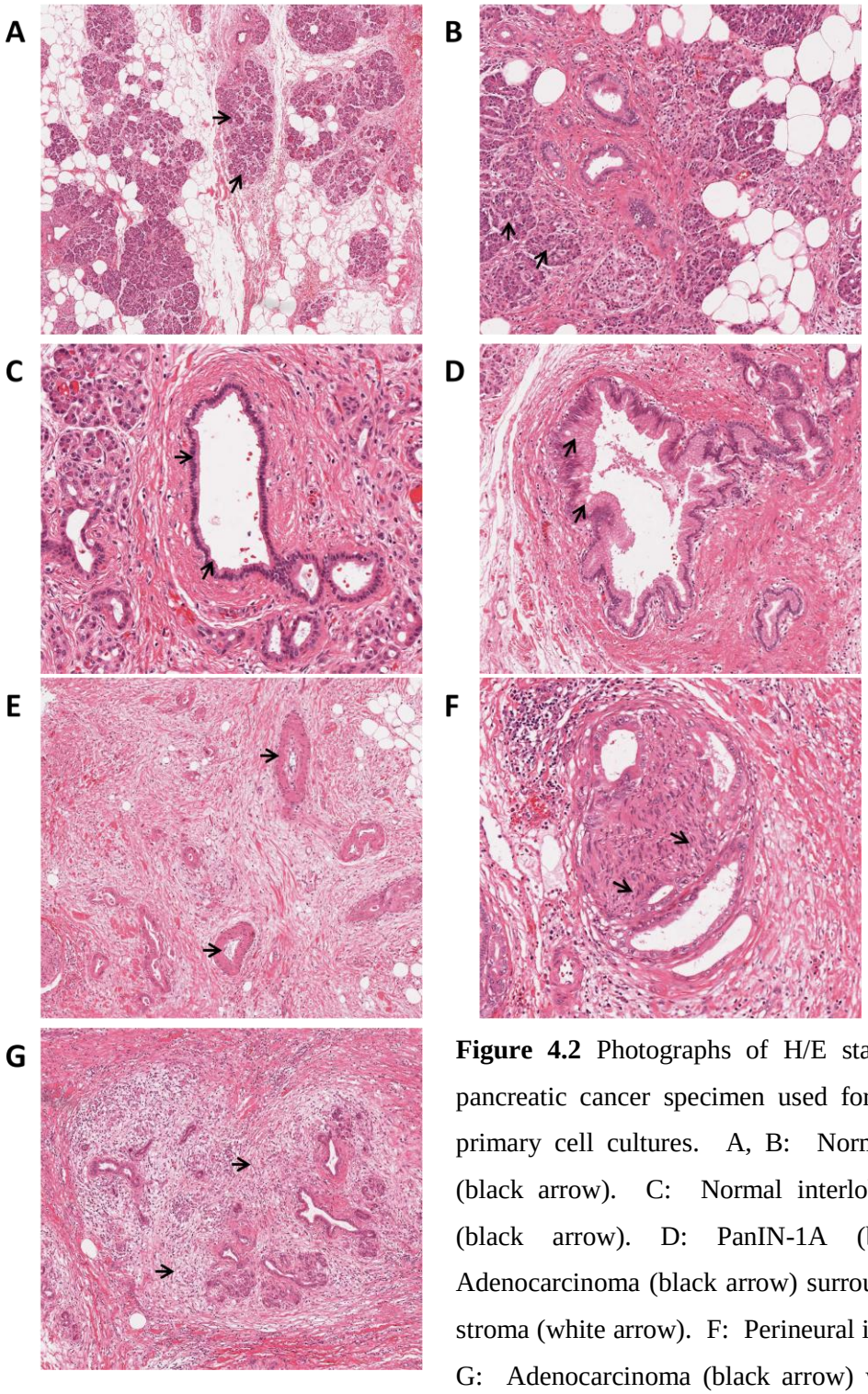

Figure 4.2 Photographs of H/E stained sections from a pancreatic cancer specimen used for the establishment of primary cell cultures. A, B: Normal pancreatic lobules (black arrow). C: Normal interlobular duct epithelium (black arrow). D: PanIN-1A (black arrow). E: Adenocarcinoma (black arrow) surrounded by desmoplastic stroma (white arrow). F: Perineural invasion (black arrow). G: Adenocarcinoma (black arrow) with adjacent Chronic Pancreatitis (white arrow).

Figure 4.3 below shows H/E stained tissue from a chronic pancreatitis sample resected 25th January 2011.

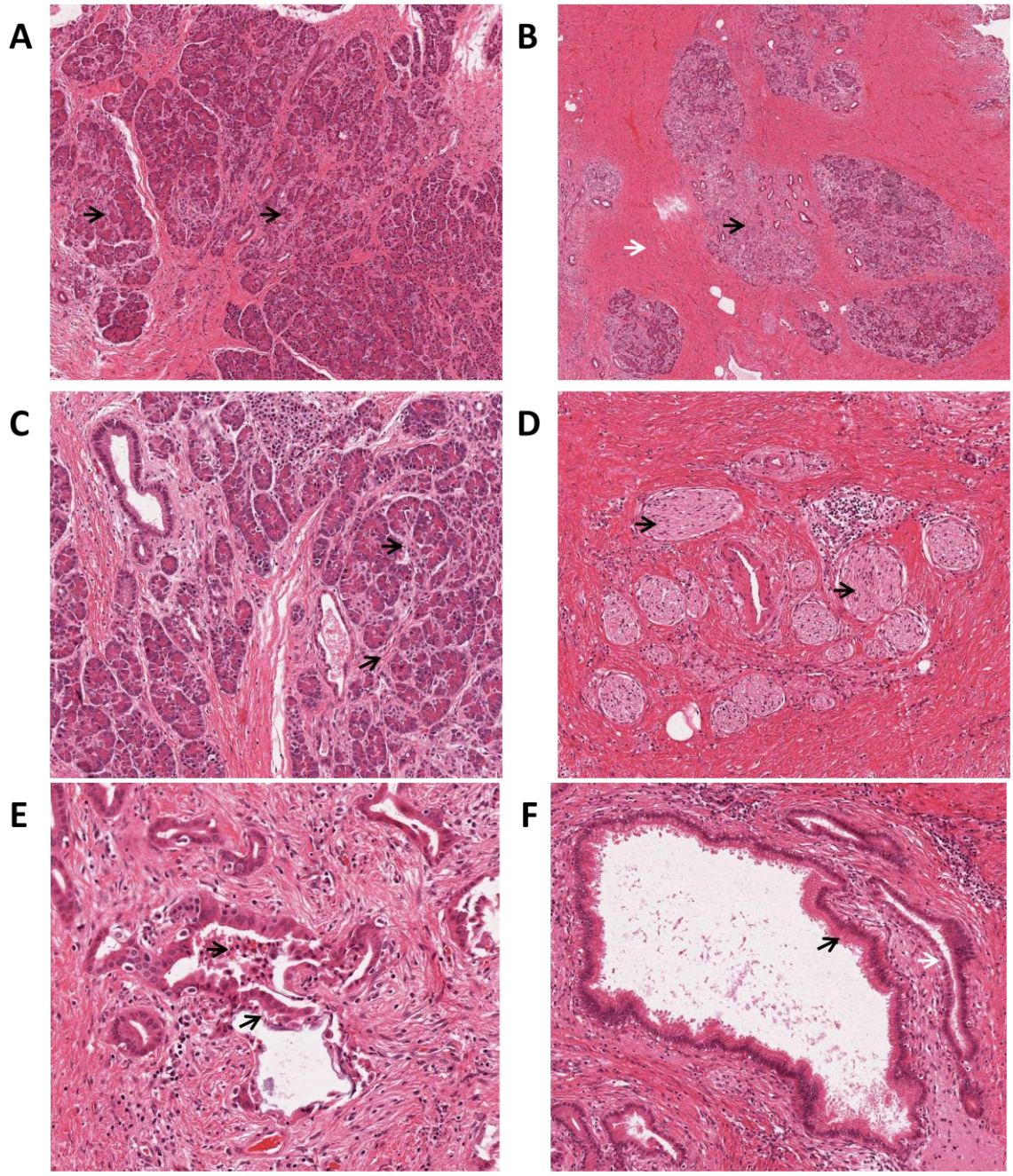

Figure 4.3 Photographs of H/E stained sections from a chronic pancreatitis sample used to establish of primary cell cultures. A: Intralobular fibrosis (black arrow). B: Intralobular (black arrow) and perilobular (white arrow) fibrosis. C: Intralobular fibrosis (black arrow). D: Neuronal hyperplasia (black arrow). E: Scanty neutrophils within disrupted duct (black arrow). F: PanIN-1A (black arrow) and adjacent normal duct (white arrow)

4.3 Description of pancreatic primary cell morphology

4.3.1 Light microscopy of primary cultured cells

Phase-contrast images were taken of primary cultured cells once they had been transferred from the original dish/well into T25 flasks. Cells with different morphologies were sometimes identified between the different flasks of cells, despite having originated from the same patient tissue sample.

All of the cells observed by microscopy appeared mesenchymal in shape, with long cytoplasmic processes extending outwards from the cell body. Several different cell morphology types were observed and are arbitrarily referred to here as types A, B and C. Type A, were the most commonly seen cells, which were large with a myofibroblast-like phenotype as pictured in Figure 4.4.

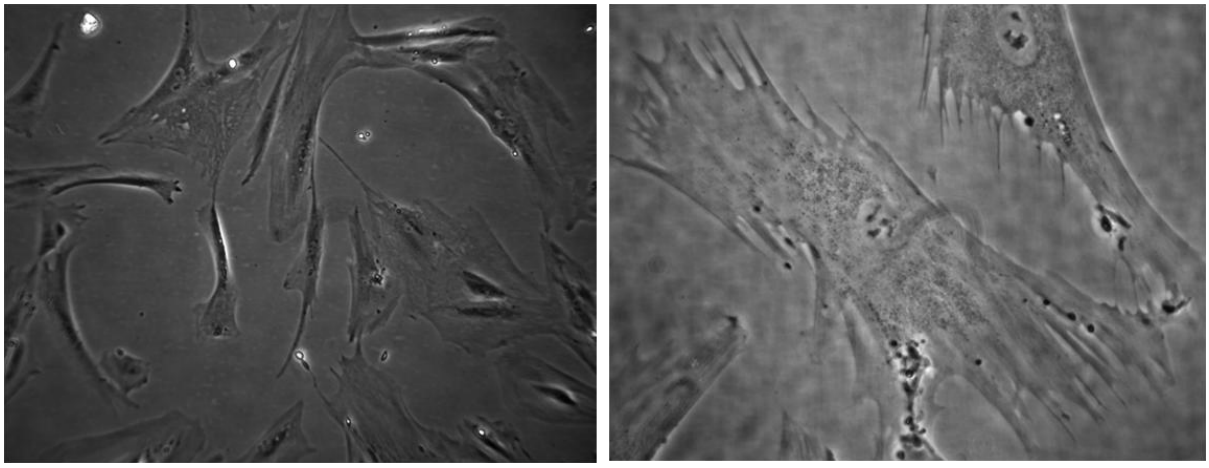

Figure 4.4 Light microscopy images of cells with Type A morphology. Left panel: Cells from sample CP 25.01.11 Dish 9 passage 3 taken at 10x magnification; Right panel: Cells from sample PDAC 28.01.11 Dish 7 passage 3 taken at 40x magnification.

Type B cells, as displayed in Figures 4.5 and 4.6 were less commonly observed. These were similar shaped cells but smaller in size, and possessing thinner cellular processes. Their shape seemed to differ according to the length of time they had adhered to the cell culture

plate. Having only adhered to the plate 48 h previously the cells appear compact as shown in Figure 4.5.

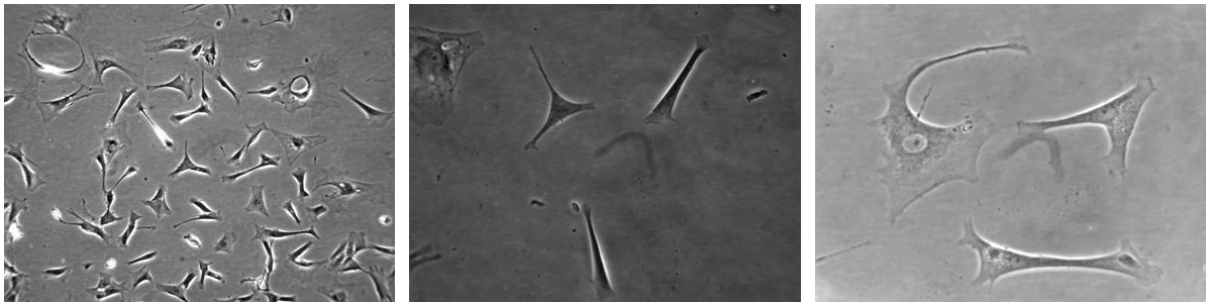

Figure 4.5 Light microscopy images of cells with Type B morphology. PDAC 28.01.11 Dish 4 passage 2. Left panel: 10x magnification; Middle panel: 20x magnification; Right panel: 40x magnification.

However, after another 3d in culture the cell shape developed with the cellular processes extending into the surrounding environment as shown in Figure 4.6 below.

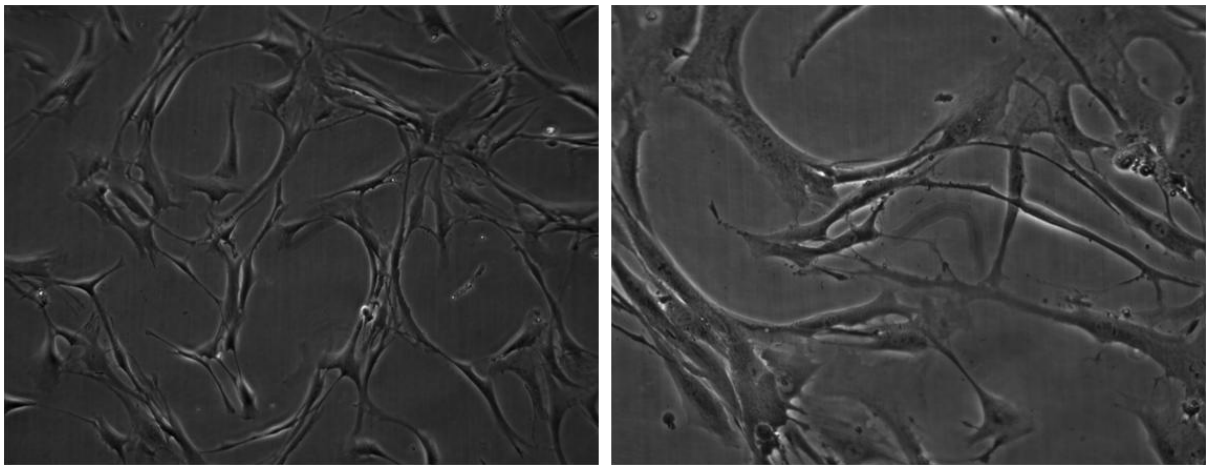

Figure 4.6 Light microscopy images of cells with Type B morphology. Left panel: Cells from sample PDAC 28.01.11 Dish 4 passage 2 taken at 10x magnification; Right panel: Cells from sample PDAC 28.01.11 Dish 4 passage 2 taken at 20x magnification.

Finally, there appeared to be a third cell type, referred to as type C which were characterised by an even more slender morphology, with longer and thinner cellular processes to the

aforementioned cells. However, these cells were much more rarely encountered, and were only discovered in three of the wells/dishes cultured with explanted tissue from the various samples. These cells were propagated into T25 flasks and were pictured as displayed in Figure 4.7.

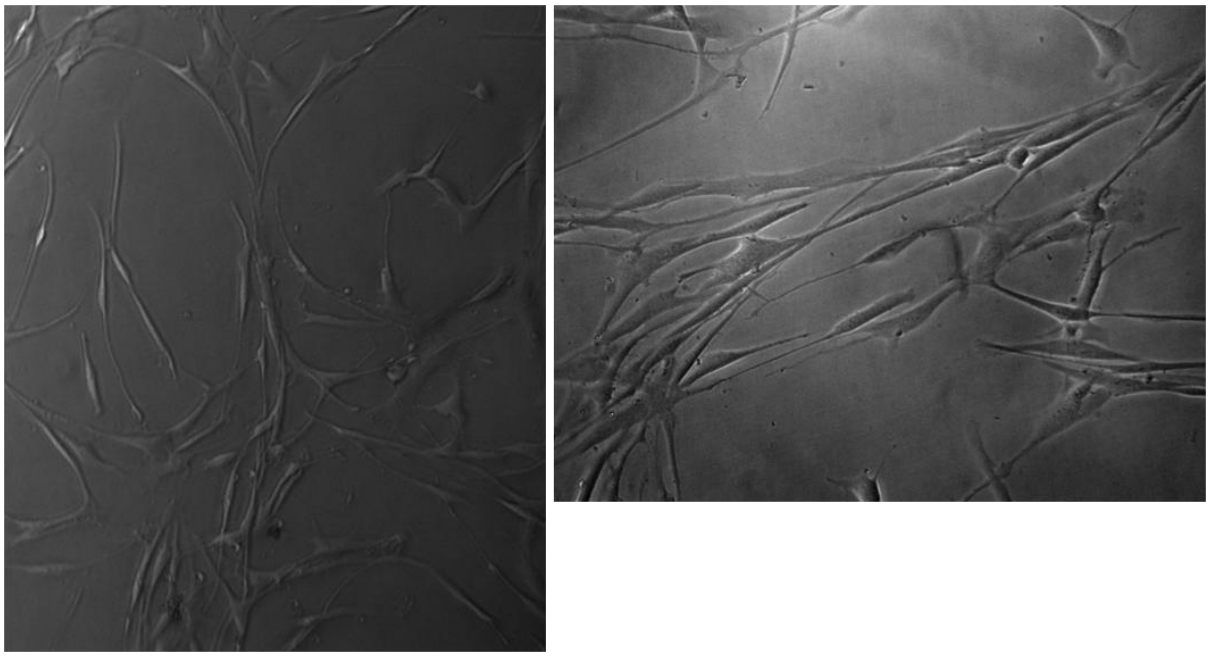

Figure 4.7 Light microscopy images of cells with Type C morphology. CP 25.01.11 Dish 14 passage 3 cells. Left panel: 10x magnification; Right panel: 20x magnification.

Hence, several different types of primary cell seem to have grown out of the explanted tissue. The majority of the primary cells were of the phenotype illustrated in Figure: 4.4.

These cells could not be characterised from morphology alone, thus immunofluorescence staining/microscopy was used in an attempt to differentiate between the various cell populations, and to elicit the expression of stellate cell markers.

4.4 Immunofluorescence characterisation of primary cultured cells

In a series of experiments, the expression of the four stellate cell markers were quantified, namely alpha SMA, GFAP, desmin and vimentin (See Section 1.3.2). This expression was measured in the various types of primary cultured cell, the immortalised pancreatic stellate cell line (RLT-PSC) and the numerous cancer cell lines.

4.4.1 Evaluation of alpha SMA and GFAP expression

Initial attempts at characterisation of primary cultured cells were performed on cells derived from the explanted pancreatic tissue of a patient who underwent resection for PDAC on 18th October 2010. The RLT-PSCs and the pancreatic cancer cell line, MiaPaCa-2 were also stained to act as positive and negative cell controls respectively.

Prior to fixation with formalin, the primary cells having been cultured on glass coverslips for 48 h, appeared like the cells displayed in Section 4.3.1 Figure 4.4 i.e. they displayed 'type A' morphology.

All cells were blocked in a PBS-based solution containing 2% BSA and antibodies were diluted in a PBS-solution containing 1% BSA (see Materials and Methods section 3.6.1). The primary antibodies used to stain the cells were rabbit polyclonal GFAP and mouse monoclonal αSMA antibody (Abcam). Each of the cell types were also stained with an isotype control antibody. The secondary antibodies utilised were cy3 anti-rabbit (red) and FITC anti-mouse (green) both diluted to 1:100.

<u>Isotype</u>

As shown in Figure 4.8 below, both rabbit and mouse isotype control antibodies displayed negative binding in both the primary cell sample and the Mia-PaCa-2 cells. Therefore, subsequent staining in this experiment is considered to be specific to the antibody of interest.

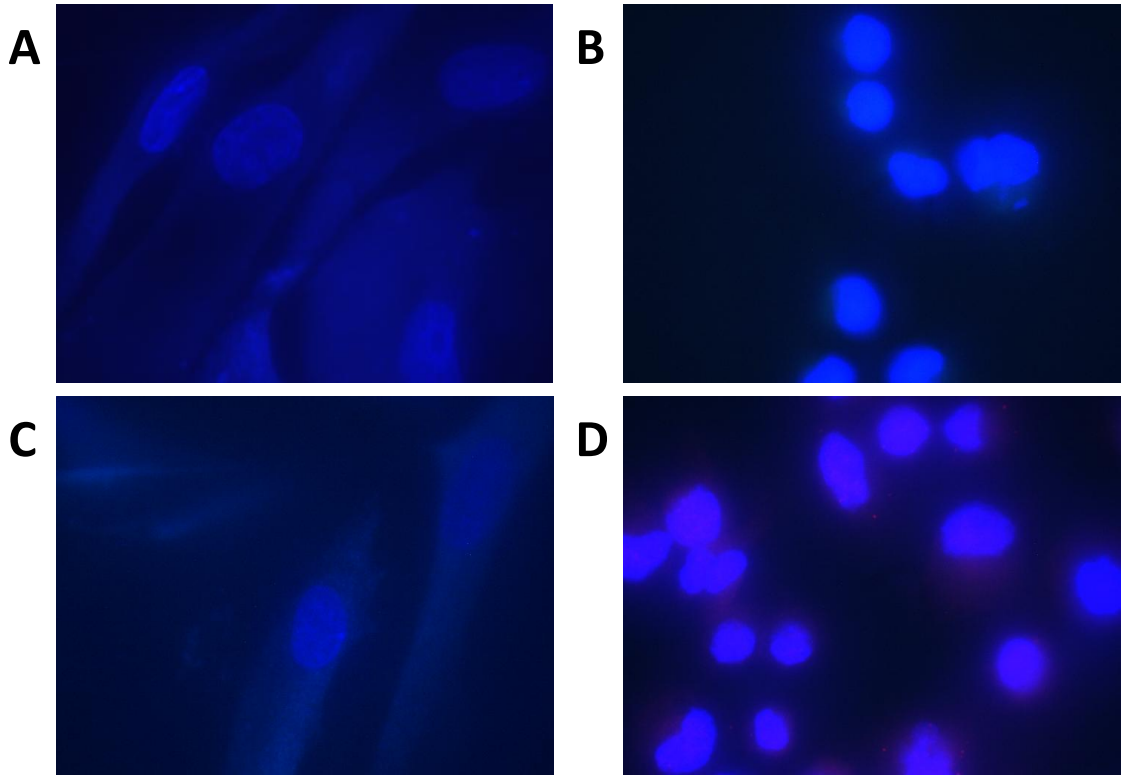

Figure 4.8 Immunofluorescence images. A: PDAC 18.10.10 well 3 passage 2 stained with isotype mouse 1:500. B: MiaPaCa-2 cells stained with isotype mouse 1:500. C: PDAC 18.10.10 well 3 passage 2 stained with isotype rabbit 1:500. D: MiaPaCa-2 stained with isotype rabbit 1:500. All images taken at 100x magnification.

Alpha SMA

Figure 4.9A displays a primary cell with distinctive alpha SMA staining (green) at a dilution of 1:500, although Figure 4.9B illustrates that while a proportion of these cells expressed alpha SMA, some also lacked expression. However, the primary cells did not express alpha SMA when the antibody was diluted to 1:1000 (Figure 5.0 left panel). MiaPaca-2 cells (Figure 4.9C, and Figure 5.0 right panel) and RLT-PSC cells (Figure 4.9D) did not express alpha SMA at either dilution.

GFAP

GFAP expression (red) was positive in all cells when the antibody was utilised at a dilution of 1:500 (Figure 4.9), but was absent at an antibody dilution of 1:1000 (Figure 5.0). Staining was even positive in the MiaPaCa-2 cells which were a negative cell control (Figure 4.9C).

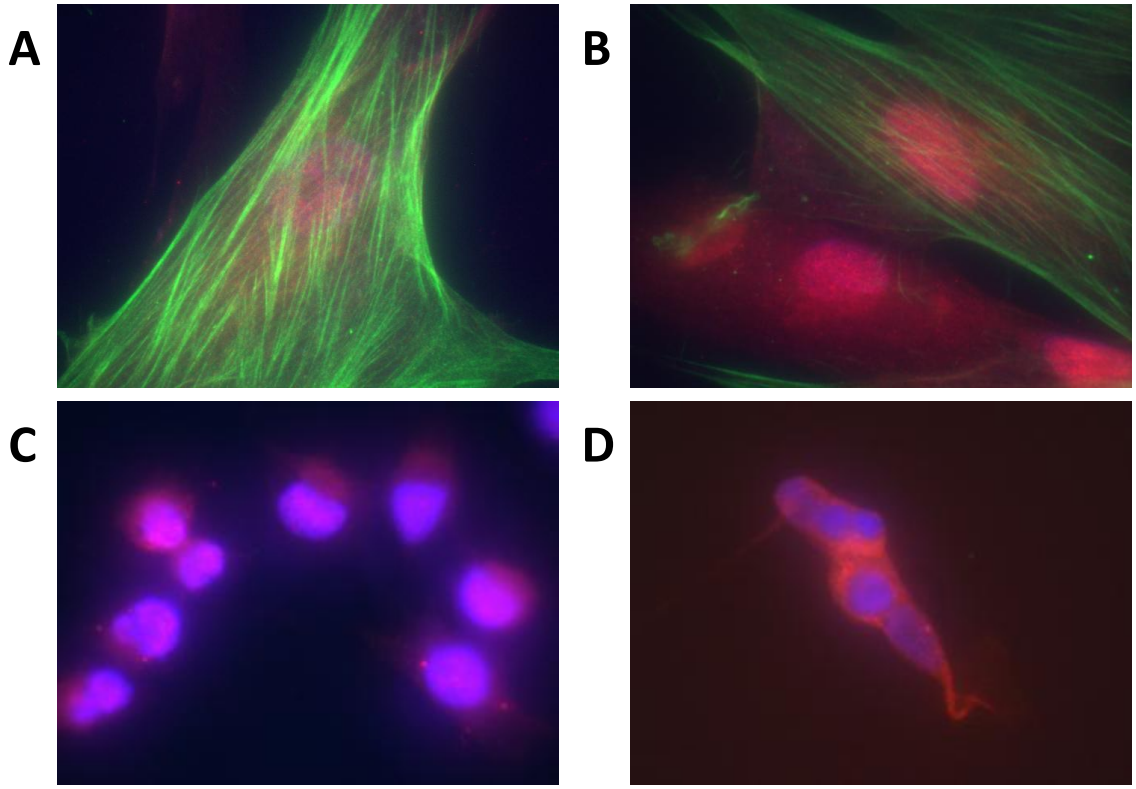

Figure 4.9 Immunofluorescence images. Cells double-stained with GFAP (red) & αSMA (green) 1:500. A & B: PDAC 18.10.10 well 3 passage 2. C: MiaPaCa-2. D: RLT-PSC. All images taken at 100x magnification.

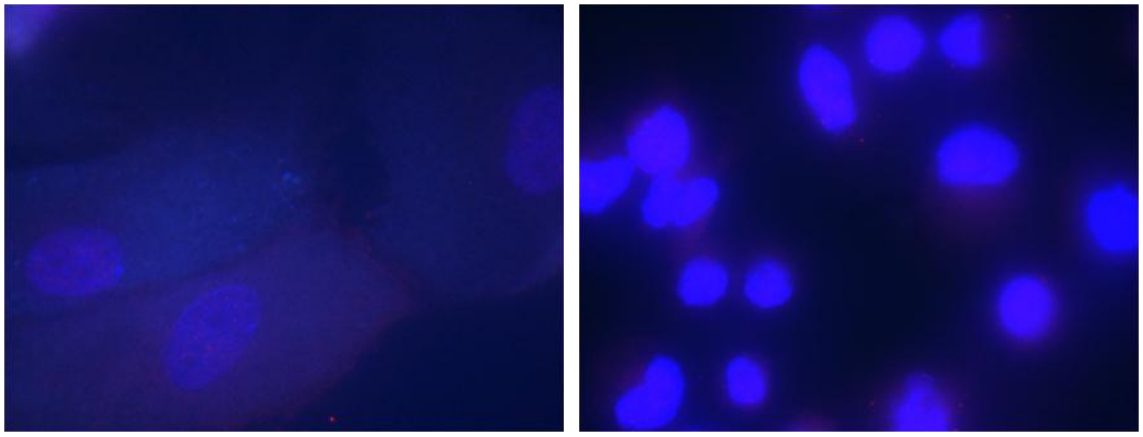

Figure 5.0 Immunofluorescence images. Cells double-stained with GFAP (red) & αSMA (green) 1:1000. Left panel: PDAC 18.10.10 well 3 passage 2. Right panel: MiaPaCa-2. All images taken at 100x magnification.

4.4.2 Evaluation of Desmin and Vimentin expression

Two cell samples, both derived from the explanted pancreatic tissue of a patient who underwent resection for an adenosquamous variant of PDAC on 20th December 2010, were evaluated for the expression of desmin and vimentin. Unfortunately, the primary cells used in the previous section had not yet reached full confluency at the time of performing this experiment. Hence, a different sample of primary cells had to be utilised. Once again, both of these samples displayed a 'type A' morphology as described in Section 4.3.1.

The expression of desmin and vimentin was evaluated using a rabbit polyclonal desmin antibody (Abcam) and a goat polyclonal vimentin antibody (Santa Cruz) respectively as described in the Materials and Methods Section 3.6.1. Cells were blocked with the same method as in Section 4.4.1. The desmin antibody was applied in serial dilutions to find the optimal concentration for use in IF staining. Only one dilution (1:50) was used for vimentin due to the low numbers of primary cells available for staining.

The concentrations of both secondary antibodies were reduced to a 1:400 dilution in this experiment, compared to 1:100 in the previous experiment. This was a precaution taken to prevent non specific binding and to stop the MiaPaCa-2 cancer cells from staining positively again (please see Section 4.4.1), cells which were supposed to be acting as a negative control. Furthermore, the green fluorescent tag, FITC was exchanged for an Alexa Fluor-488 antibody. The fluorescence of the latter is reported to last much longer than that of the former i.e. months as opposed to days. The red cy3 anti-mouse antibody was continued. Figure 5.1 below displays the findings from this experiment.

Isotype

As displayed in the top row of Figure 5.1, the isotype control antibody exhibited an intense fluorescence in all three cell samples, and this was even brighter than the green stain elicited when the same cells were stained with desmin. Hence, any green stain associated with the desmin antibody is invalid, and should be considered to be non-specific binding. Vimentin expression was positive and equal in intensity between all cells. However, no goat isotype control antibody was utilised, and thus non-specific binding cannot be ruled out for the red stain.

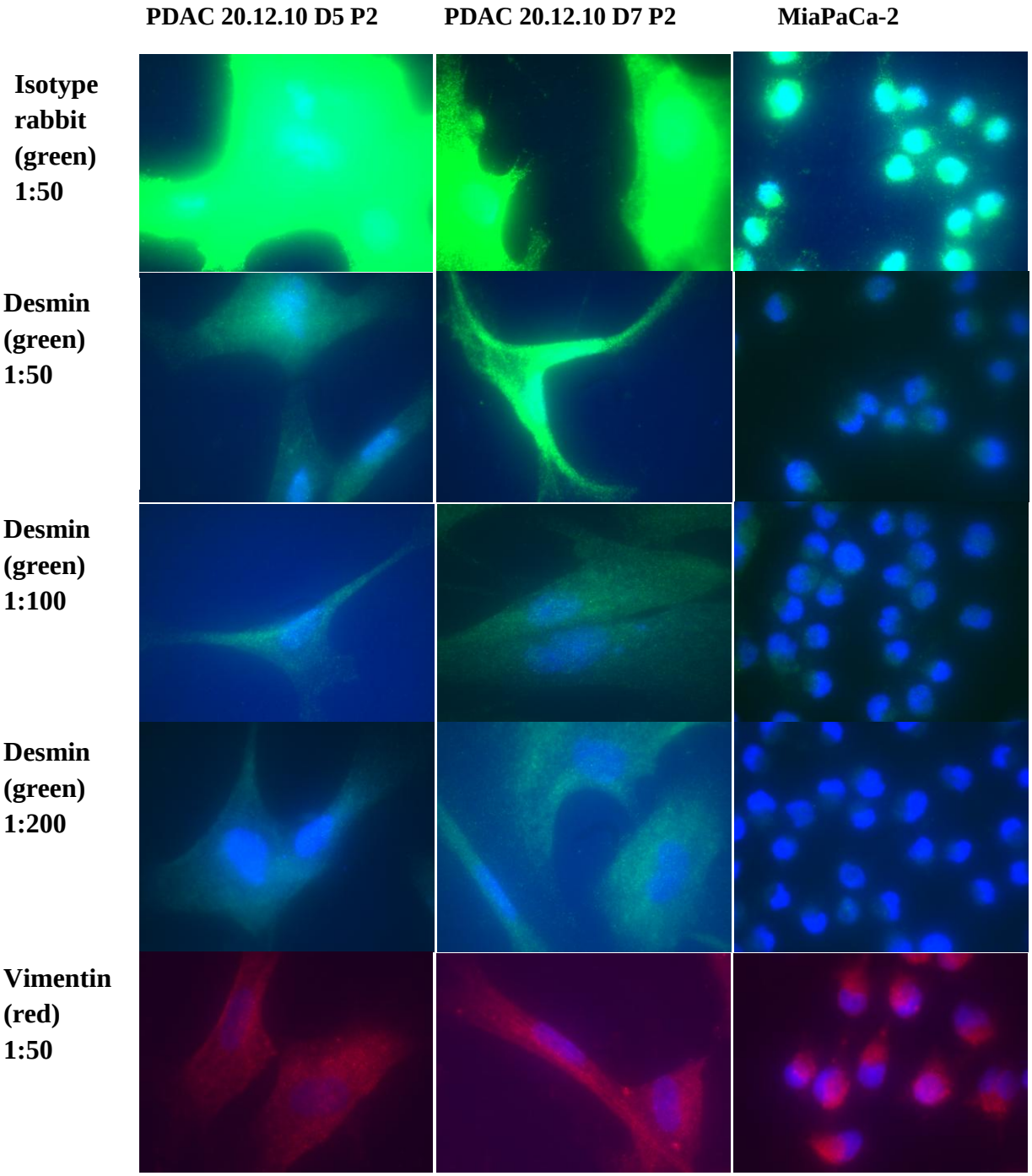

Figure 5.1 Immunofluorescence images. Left panel: PDAC 20.12.10 Dish 5 passage 2. Middle panel: PDAC 20.12.10 Dish 7 passage 2. Right panel: MiaPaCa-2. Cells were stained with isotype rabbit 1:50, desmin (rabbit) at serial dilutions 1:50, 1:100, 1:200, and vimentin (goat) 1:50. DAPI stain (blue) represents cell nuclei.

4.4.3 Further evaluation of Desmin, GFAP and alpha SMA expression

Mouse monoclonal desmin and rabbit polyclonal GFAP antibodies were purchased from DAKO and were used to stain another set of primary cultured cells. These results would be compared with the previous stains that were undertaken with the antibodies purchased from Abcam, to deduce whether the antibodies from Abcam were binding non-specifically to cells (See Sections 4.4.1 and 4.4.2). In addition, expression of alpha SMA was measured, and some cells were incubated with the secondary antibody alone to elicit whether secondary antibodies were binding non-specifically.

Instead of using BSA for blocking as in Sections 4.4.1 and 4.4.2, a PBS based solution containing 10% goat serum was used both for blocking cells and dilution of antibodies (See Materials and Methods section 3.6.1). This alternative method of blocking may have been better at preventing non-specific binding if any was taking place. Cells were double stained with serial dilutions of all three primary antibodies. AlexaFluor-488 anti-rabbit and cy3 anti-mouse antibodies were used as secondary tags and were both diluted to 1:1000, a higher dilution than in the two previous experiments (See Sections 4.4.1 and 4.4.2). The higher dilution of secondary was used to elucidate whether the cancer cell lines were previously staining positively for stellate cell markers non-specifically because of too high a concentration of secondary antibody.

For the first time, primary cells with different morphologies were stained alongside one another. These included PDAC 20.12.10 dish 5 passage 4 cells (type A morphology) and CP 25.1.11 dish 8 passage 2 cells (type B morphology). The aim was to see whether any difference in marker expression could be elicited between the cells types. If such differences were present this could indicate two distinct cell types. RLT-PSCs and Panc-1 cancer cells were utilised as positive and negative control cells respectively.

Figure 5.2 displays the results when the four different cell types were double-stained with isotype controls, and serial dilutions of GFAP, desmin and alpha SMA.

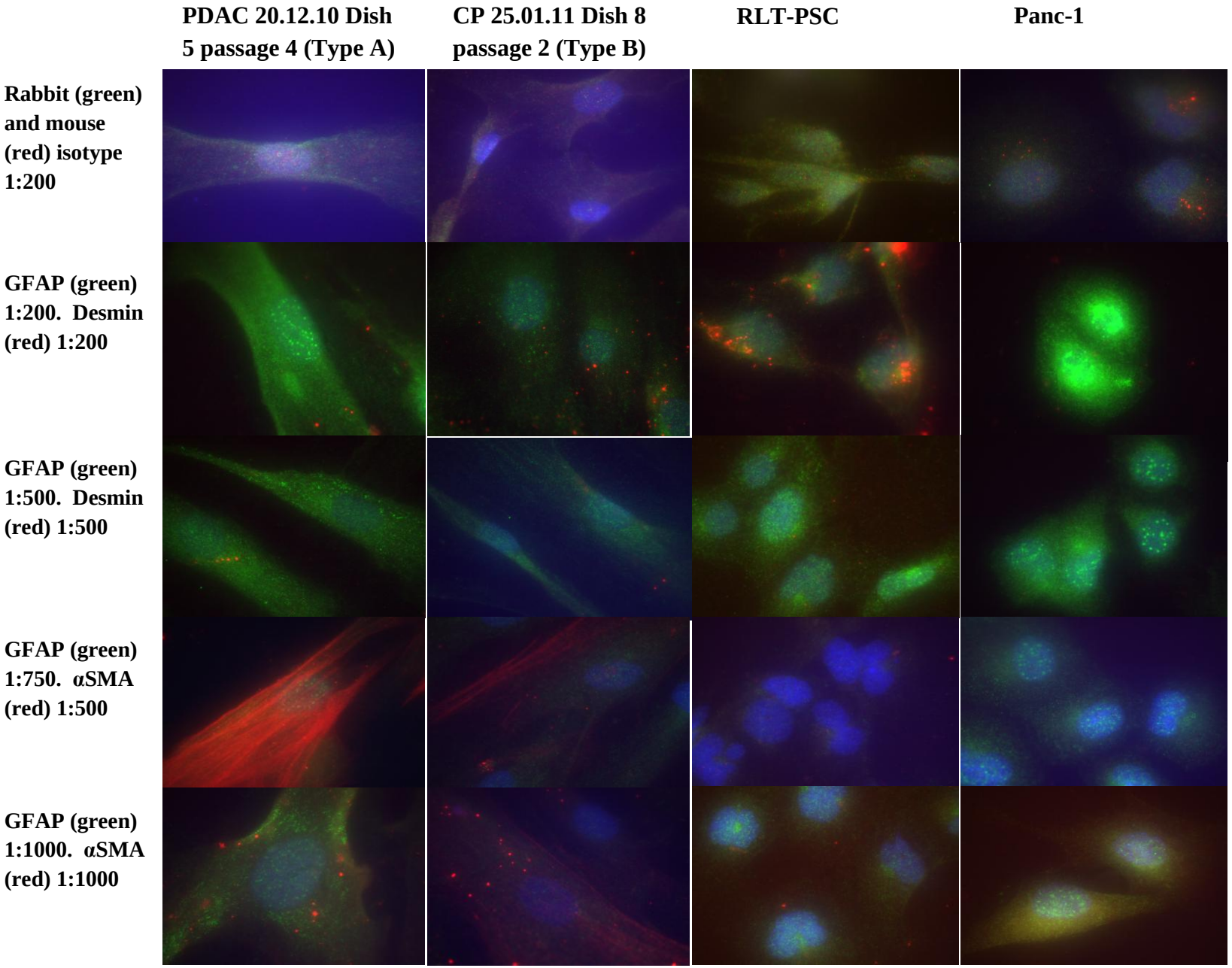

Figure 5.2 Immunofluorescence images. PDAC 20.12.10 Dish 5 passage 4, CP 25.01.11 Dish 8 passage 2, RLT-PSC, Panc-1 stained with rabbit and mouse isotype (1:200), and serial dilutions of GFAP (rabbit), Desmin (mouse), and αSMA (mouse).

Isotype

The rabbit isotype control antibody stained weakly for all cell types, unlike the bright green stain displayed in the previous experiment (See Section 4.4.2). This is probably related to the increased dilution of the isotype control (1:200) in this experiment, compared to 1:50 in the previous experiment. Mouse isotype antibody expression was negative in all the cell types, apart from the Panc-1 cells in which there was very faint red fluorescence.

GFAP

As shown in Figure 5.2, the PDAC 20.12.10 Dish 5 passage 4 cells (Type A morphology) stained more brightly green against GFAP than with the rabbit isotype control, especially when GFAP was used at dilutions of 1:200 and 1:500. Hence, the green fluorescence emitted by these cells is considered to be specific for GFAP, and non-specific binding can be ruled out.

Unfortunately, Panc-1 cells also fluoresced bright green with the GFAP marker despite using a new antibody from DAKO, and also despite the drop in concentration of secondary antibody to 1:1000 from 1:400 in the previous experiment. Therefore, an alternative cancer cell line to Panc-1 and MiaPaCa-2 will be used in the subsequent investigations.

CP 25.01.11 dish 8 passage 2 (Type B morphology) cells expressed GFAP very faintly, and this was clearly much weaker than the green fluorescence emitted by the PDAC 20.12.10 Dish 5 passage 4 cells. The RLT-PSC cells displayed some green fluorescence when stained with GFAP, although this was comparable in intensity to the green fluorescence emitted for the rabbit isotype stain and hence could be non-specific. For all four cell types, the optimal dilution for GFAP appeared to exist somewhere between 1:200 and 1:500, and so subsequent experiments will utilise dilutions of GFAP within this range.

Desmin

The new desmin antibody from DAKO was utilised. Most of the cell samples did not express desmin (Figure 5.2). The RLT-PSCs did produce some weak patchy staining when the desmin antibody was applied at a dilution of 1:200, although this was not very convincing.

Alpha SMA

Alpha SMA expression was observed in both primary cultured cell samples. However, the fluorescent red stain was higher in intensity for the PDAC 20.12.10 dish 5 passage 4 (Type A morphology) cells compared to the CP 25.01.11 Dish 8 passage 2 (Type B morphology) cells. A dilution of 1:1000 for the alpha SMA antibody was too high, whereas 1:500 seemed to work well. It is yet unknown whether this is the optimal dilution, so the antibody will be trialled in subsequent experiments at lower dilutions. The RLT-PSC cells and Panc-1 cells did not express alpha SMA at either of the two antibody dilutions.

In a similar scenario to that of Section 4.4.1, there were variations in the expression of alpha SMA between primary cells originating from the same sample. Approximately 20% of the PDAC 20.12.10 Dish 5 passage 3 (Type A) cells expressed this marker. However, under 5% of the CP 25.01.11 Dish 8 passage 2 (Type B) cells stained positively. These approximations were determined by calculating the proportion of cells that stained positively in 40 different fields of view on the microscope at 100x magnification. A total of 71 PDAC 20.12.10 dish 5 passage 4 cells were counted, of which 14 stained positive for alpha SMA (19.7%). A total of 129 CP 25.01.11 dish 8 passage 2 cells were counted of which only 3 showed expression of alpha SMA (2.3%).

Secondary antibody only

The images in Figure 5.3 were taken from cells double-stained with secondary antibody alone. Very faint red staining was observed in all of the cells indicating that the cy3 anti-mouse antibody displays some non-specific binding. However, this red expression was very weak and thus not significant enough to warrant the use of different secondary antibody in subsequent experiments. The green fluorescence of the AlexaFluor-488 anti-rabbit antibody was absent as expected.

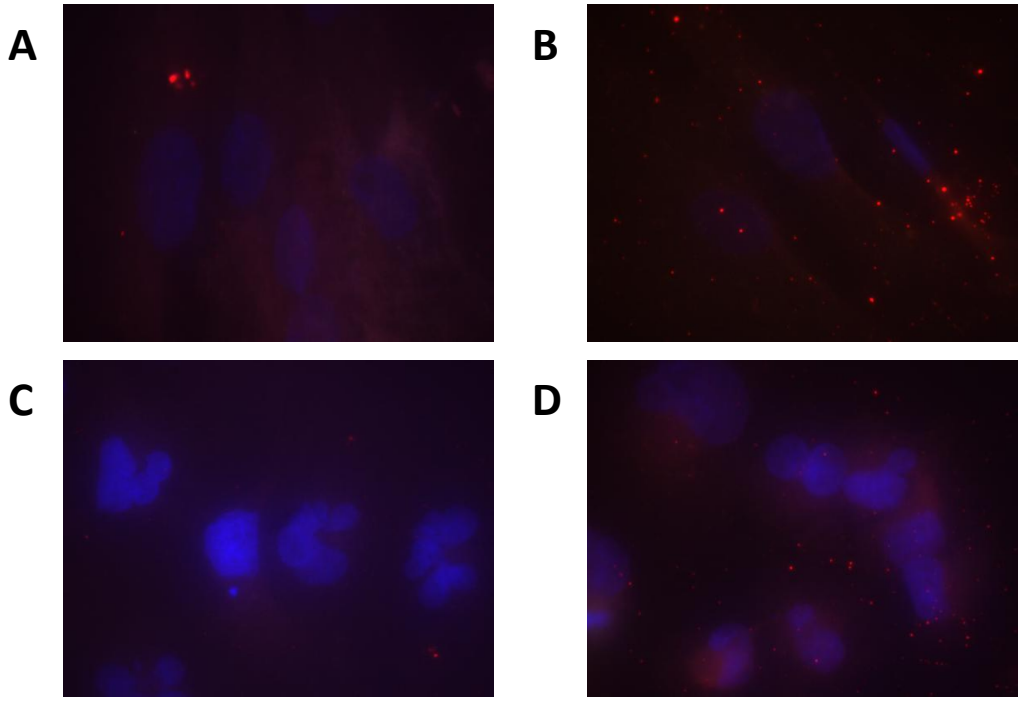

Figure 5.3 Immunofluorescence images. Secondary antibody stain only: Alexa Fluor-480 anti-rabbit (green), Cy3 anti-mouse (red) both 1:1000. A: PDAC 20.12.10 Dish 5 passage 4. B: CP 25.01.11 Dish 8 passage 2. C: RLT-PSC. D: Panc-1

4.4.4 Further evaluation of desmin and alpha SMA expression

It has already been established that the Type A morphology cells express alpha SMA and GFAP (See Sections 4.4.1, and 4.4.3). Ideally the results for GFAP expression need to be supported by negative control cell data.

In this experiment, two more samples of primary cells (Type A morphology) were characterised for desmin expression using the new antibody from DAKO. This antibody has been previously applied at dilutions of 1:200 and 1:500 but no fluorescence was emitted by any of the cells (See Section 4.4.3). In the following experiment the desmin antibody was utilised at a dilution of 1:50. RLT-PSCs were not utilised as a positive control cell considering their lack of expression of stellate cell markers in previous experiments. Thus far, MiaPaCa-2 and Panc-1 cells have expressed mesenchymal and stellate cell markers (See Sections 4.4.1 to 4.4.3). Hence, an alternative cancer cell line, the BXPC3 cell line, was trialled as a negative control cell in the following experiment. As yet no negative control cell has been found.

A PBS based solution containing 10% goat serum was used to block cells and a solution containing 2% goat serum was employed for antibody dilution. The green staining was elicited by Alexa Fluor-488 anti-rabbit and anti-mouse, and the red staining by cy3 anti-goat all diluted to 1:500.

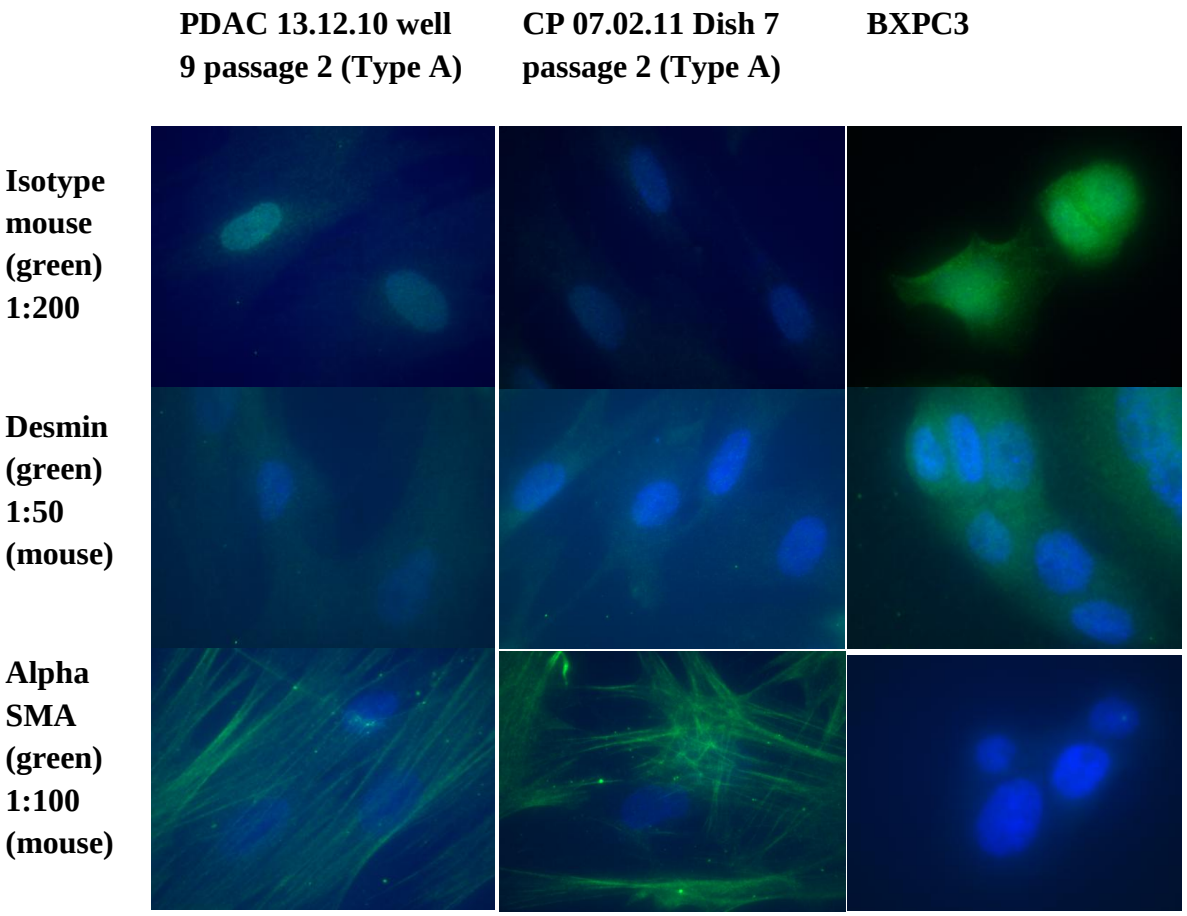

Figure 5.4 Immunofluorescence images. Primary cultured cells with 'type A' morphology characterised for alpha SMA and desmin expression. Left panel: PDAC 13.12.10 well 9 passage 2. Middle panel: CP 07.02.11 Dish 7 passage 2. Right panel: BXPC3

As expected, alpha SMA expression was positive in both samples of primary cells (Type A), and more than 90% of the cells expressed this protein. BXPC3 cells however did not exhibit alpha SMA. The mouse isotype stains were negative in the primary cells, and desmin expression was positive but very faint. Hence, these primary cells could possibly express a low level of desmin although the data is not very convincing due to the very faint stains. The positive fluorescence for desmin in the BXPC3 cells is invalid considering that the mouse isotype stained even brighter.

4.4.5 Comparison of marker expression between different morphology types

PDAC 28.01.11 dish 4 passage 3 (type B) cells and PDAC 19.01.11 dish 12 passage 3 (type C) cells were stained with alpha SMA, GFAP and desmin antibodies. RLT-PSC and Suit-2 cancer cells were also stained. The latter were trialled as a potential negative cell control.

For this experiment the concentration of mouse monoclonal alpha SMA was increased to 1:300, from a concentration of 1:500 that was used previously in Section 4.4.3. The increase in antibody concentration was to elucidate whether a greater proportion of cells would stain positively for alpha SMA at this higher concentration. Rabbit polyclonal desmin (Abcam) was utilised at 1:100, and rabbit polyclonal GFAP (DAKO) at 1:400. As mentioned in Section 4.4.3 the optimal dilution for GFAP (DAKO) seemed to exist somewhere between 1:200 and 1:500, thus 1:400 was the chosen dilution on this occasion.

All primary antibodies were incubated overnight at 4°C. Cy3 anti mouse, alexa fluor-488 anti rabbit and alexa fluor-488 anti mouse antibody were utilised at 1:500. Prior experiments demonstrated that an increased dilution of the secondary antibody to 1:1000 had no effect on non-specific binding (See Section 4.4.3). All cells were blocked in a PBS based solution containing 10% goat serum, and antibodies were diluted in a solution containing 2% goat serum (see Materials and Methods section 3.6.1).

The results of these experiments are illustrated in Figure 5.5.

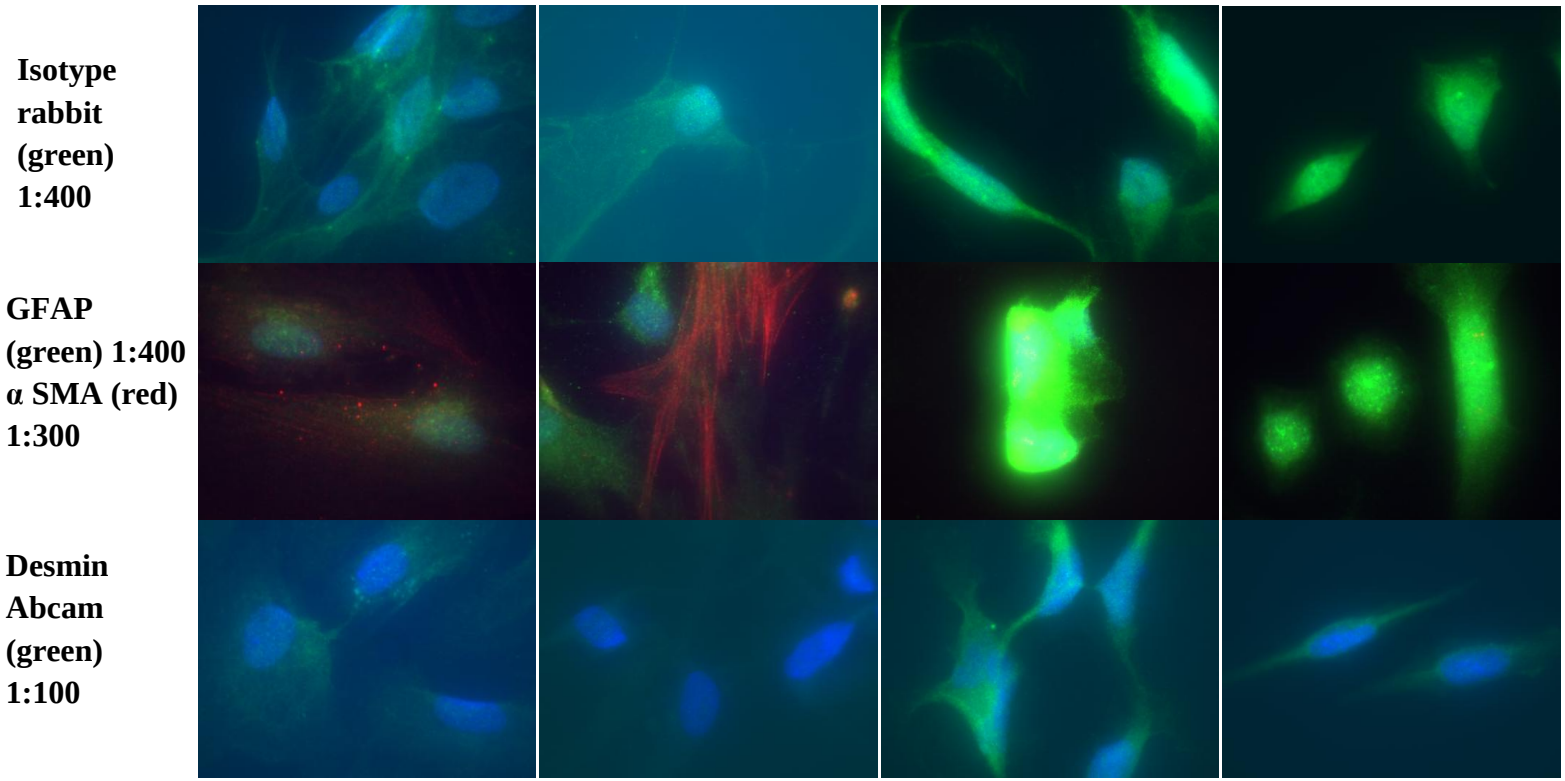

Figure 5.5
Immunofluorescence images. 3 different cell morphology types stained with rabbit isotype control, GFAP (rabbit), αSMA (mouse), desmin/Abcam (rabbit)

Isotype, GFAP, desmin

The rabbit isotype antibody (1:400) produced positive fluorescence in all four cell types, similar to the scenario in Section 4.4.2. For the majority of the cells, the fluorescence associated with the isotype control was exhibited at an equal or a higher intensity to the fluorescence produced by the other antibodies (GFAP, and desmin from Abcam). Hence, the results for GFAP and desmin expression are considered invalid, and the green fluorescence is considered to be a result of non-specific binding. The only exception to this was the RLT-PSC cells which stained for GFAP at a brighter intensity than that of the rabbit isotype control, thus providing evidence that the RLT PSC cells express this marker.

Alpha SMA

As was the case in a previous alpha SMA stain (see Section 4.4.3), the number of type B morphology cells expressing this marker was under 5%. Interestingly, around 50% of the type C morphology cells expressed alpha SMA (Figure 5.5). The same method of cell counting was used here as in section 4.4.3, where 40 fields of view were analysed on the microscope at 100x to determine the proportion of cells staining positive. A total of 148 PDAC 28.01.11 dish 4 passage 3 cells were counted, of which 6 stained positive for alpha SMA (4.1%). A total of 124 PDAC 19.01.11 dish 12 passage 3 cells were counted, and 70 of these cells exhibited the alpha SMA marker (56.4%).

The Suit-2 cells stained negatively for alpha SMA. This was also true for the RLT-PSC cells, despite the antibody concentration being increased from 1:500 to 1:300 compared to the last experiment in which they were stained (See Section 4.4.3).

4.4.6 The effect of TGFβ treatment on alpha SMA expression

The proportion of primary cells within each sample exhibiting alpha SMA has been rather low in previous sections. Hence, TGFβ was applied to both 'type A' and 'type B' morphology cell types (See Section 3.7.1) to determine whether the number of cells expressing this protein would increase. The reason for this being that TGFβ has been shown in the literature to stimulate inactivated fibroblasts, myofibroblasts and stellate cells into alpha SMA expressing cells in vitro [49;82;126;127].

The two primary cell samples utilised in this experiment were PDAC 28.01.11 dish 7 passage 4 cells (type A) and PDAC 28.01.11 dish 4 passage 5 cells (type B). RLT-PSC and cancer cells were not included in the experiment because both fail to express the alpha SMA marker.

A PBS based solution containing 10% goat serum was used to block cells and a solution containing 2% goat serum was used to dilute antibodies. Isotype mouse was used at a dilution of 1:300 and alpha SMA at serial dilutions of 1:200 and 1:400. Alexa Fluor-488 anti mouse, which represented the secondary antibody was diluted 1:500.

As shown in Figure 5.6 (below), there was no positive staining to the mouse isotype control in either of the primary cultured cells. Surprisingly, the majority of the type A morphology cells expressed alpha SMA at both dilutions, with or without TGFβ treatment. Expectedly, very few type B cells expressed alpha SMA at either dilution. However, over 90% of the cells that were exposed to TGFβ displayed expression of alpha SMA afterwards. This increase in number of cells expressing alpha SMA was observed at both dilutions. PDAC 28.01.11 dish 4 passage 5 cells that were stained with alpha SMA (1:200) were counted as described in section 4.4.4. Of the cells treated with TGFβ, a total of 113 cells were counted from 40 different fields of view. Of these, 105 expressed the characteristic strand-like staining of alpha SMA (93%). However, alpha SMA was expressed by very few cells in the untreated cells stained at the same dilution (1:200). From a total of 96 cells, only 2 of these displayed green staining (2%).

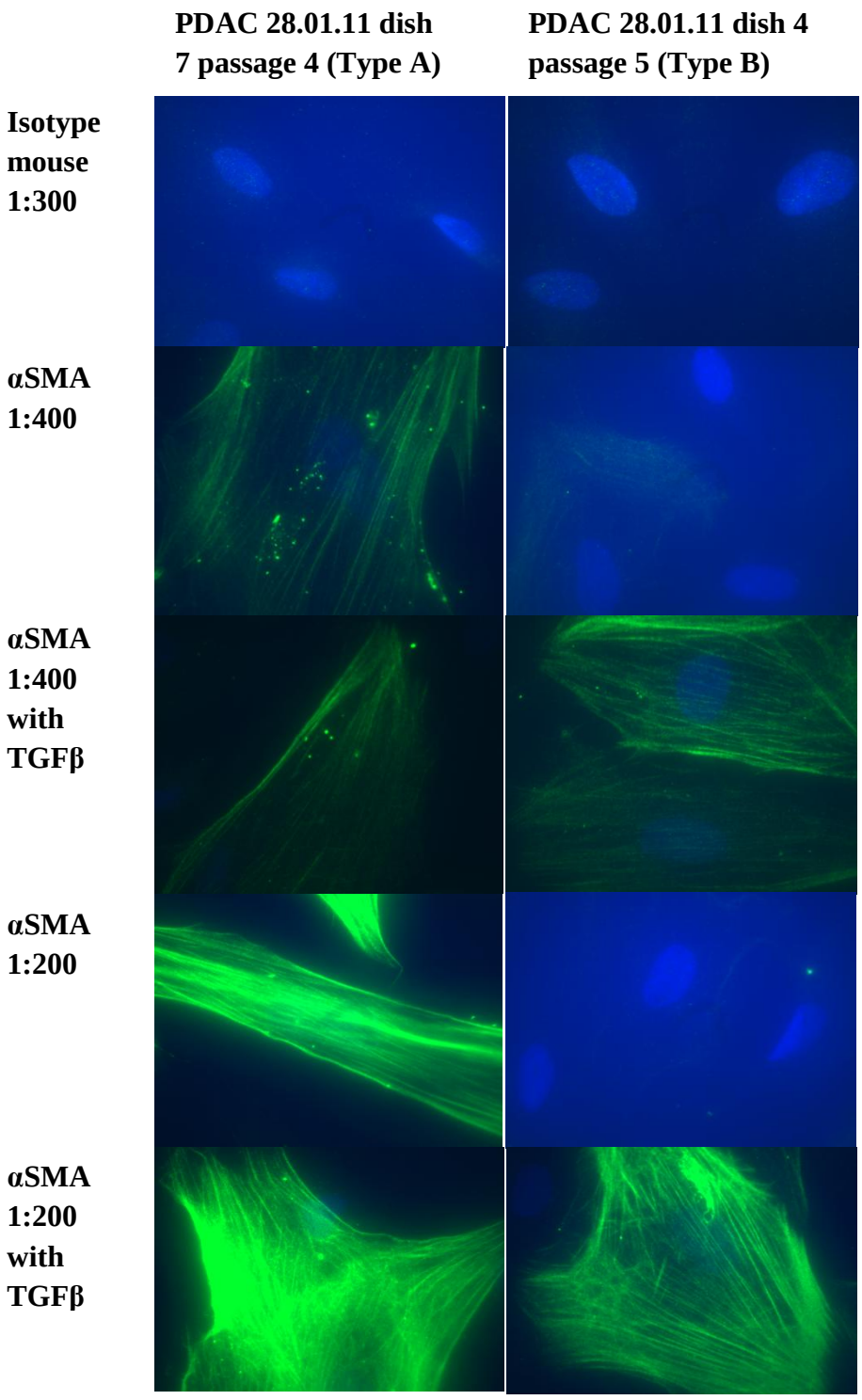

Figure 5.6 Immunofluorescence images. Alpha SMA stain (green) for Type A and Type B morphology cells with or without prior TGFβ stimulation

4.4.7 Evaluation of Cytokeratin expression

Pancreatic stellate cells are expected to have absent or low expression of cytokeratin, an epithelial cell marker. Mouse monoclonal pan-cytokeratin antibody was used to stain PDAC 28.01.11 dish 4 passage 7 (Type B) cells and CP 25.01.11 dish 14 passage 4 (type C) cells in order to determine whether these cultures were contaminated with epithelial cells. BXPC3 cancer cells were chosen to represent a positive cell control for cytokeratin expression.

Cells were blocked in a PBS based solution containing 10% goat serum, and antibodies incubated in a PBS based solution containing 2% goat serum. The pan-cytokeratin antibody was used at dilutions of 1:100 and 1:300. AlexaFluor-488 anti-mouse antibody was the chosen secondary antibody and was diluted to 1:500.

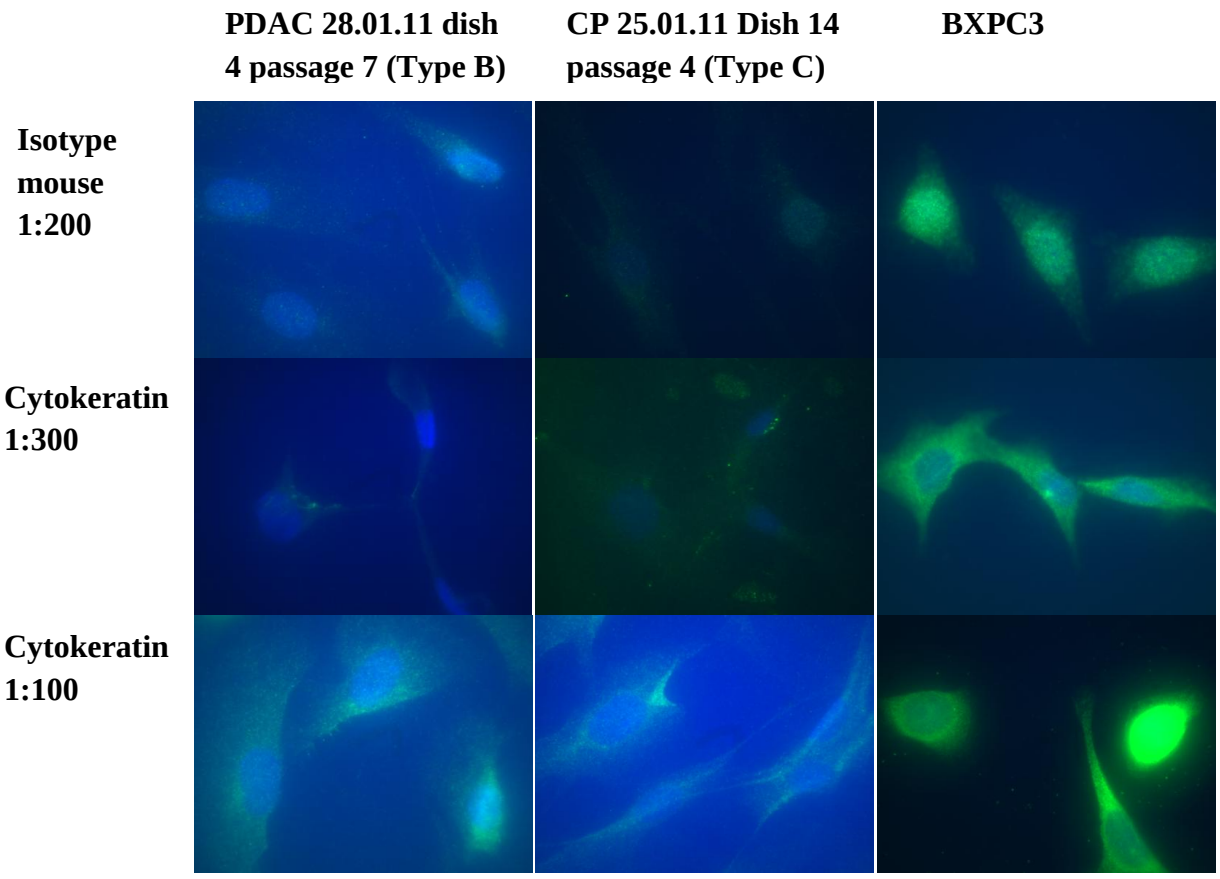

Figure 5.7 Immunofluorescence images. Primary cultured cells and BXPC3 epithelial cancer cells stained with cytokeratin antibody (green).

Figure 5.7 illustrates that isotype stains (1:200) of the primary cells were negative or very weak. Cytokeratin staining in the primary cells was either absent or very weak at 1:300 and slightly more intense at 1:100. The BXPC3 cells displayed positive cytokeratin expression, which was very intense at the 1:100 dilution. However, the mouse isotype control was also positive in the BXPC3 cells, albeit at a lower intensity in comparison with the fluorescence elicited by the cytokeratin antibody. Hence, one can conclude that the BXPC3 cells display positive cytokeratin expression whereas the primary cells do not.

4.5 MicroRNA analysis

Along with RLT-PSC cells, two samples of primary cultured cells were taken forward for use in miRNA quantification experiments. These were PDAC 28.01.11 dish 7 passage 5 and CP 07.02.11 dish 7 passage 2 cells, both of which possessed the Type A morphology (See Section 4.3.1). From here on these cells will be referred to as 'PDAC' and 'CP' respectively. The symbols '+' and '-' are used to demonstrate whether or not the cells were pre-treated with TGFβ. As mentioned earlier, cells with the type A morphology may possibly comprise pancreatic stellate cells in view of their positive expression of alpha SMA and GFAP in previous experiments (See Section 4.4).

4.5.1 RNA purification from primary cultured cells and RLT-PSCs

A nanodrop spectrophotometer was used to quantify the RNA purified from cultured cells (Table 4.3) using the miRNeasy kit from Qiagen (See Section 3.7). The technique used to extract miRNA is also described in this section.

Sample	Reading 1 (ng/µl)	Reading 2 (ng/µl)	Average reading (ng/µl)
PDAC +	1.5	2.5	2
PDAC -	4.0	4.5	4.25
CP +	21.8	21.8	21.8
CP -	7.5	8.7	8.1
RLT-PSC+	50.0	47.3	48.65
RLT-PSC-	47.0	49.6	48.3

Table 4.3 Total RNA quantification in primary cultured cells and RLT-PSC samples

4.5.2 Reverse transcription

Reverse transcription was conducted on the RNA samples purified in the previous section. Table 4.4 displays the concentrations of cDNA that were yielded during this procedure. These were quantified using a nanodrop spectrophotometer as described in the materials and methods section 3.7.3.

Sample	**cDNA content (ng/µl)**
PDAC +	916.2
PDAC -	1469.6
CP +	1139.8
CP -	1456.7
RLT-PSC+	873.8
RLT-PSC-	879.1

Table 4.4 Quantification of cDNA in primary cultured cells and RLT-PSC samples

4.5.3 Real–time PCR quantification of the miRNA-29 family

4.5.3.1 Loading concentrations of sample cDNA

The miScript PCR kit from Qiagen (see Material and Methods section 3.7.4) recommend a loading amount cDNA approximately 1-3ng in a volume of less than 5µl. Hence, samples of cDNA created by reverse transcription were too concentrated (Table 4.4) and were diluted 1 in 1000 in RNase free water. These were then quantified one more time using the nanodrop spectrophotometer (Table 4.5).

Sample	**cDNA reading 1 (ng/µl)**	**cDNA reading 2 (ng/µl)**	**cDNA reading 3 (ng/µl)**	**cDNA average reading (ng/µl)**
PDAC +	7.3	7.6	8.2	7.7
PDAC -	6.6	6.1	6.3	6.33
CP +	6.0	5.8	6.1	6.0
CP -	5.0	6.7	8.4	6.94
RLT-PSC+	6.8	7	6.8	6.87
RLT-PSC-	5.8	5.5	6.1	5.8

Table 4.5 cDNA quantification in primary cultured cells and RLT-PSC samples

It was essential to load the amount of cDNA recommended by the kit manufacturer i.e. 1 to 3 ng dissolved in less than 5 µl. Therefore, samples were each diluted to provide a final concentration of 2 ng per 3 µl for each PCR reaction. These dilutions were calculated on the basis that 2 ng per 3 µl is equivalent to 0.66 ng per 1 µl. Therefore, the cDNA concentrations were divided by 0.66 to provide the necessary dilution ratio. These are listed in Table 4.6.

cDNA sample	Average cDNA reading (ng/µl)	Dilution ratio of cDNA to RNase free water	Volume of RNase free water to add to 10 µl of cDNA
PDAC +	7.7	1:11.66	106.6
PDAC -	6.33	1:9.59	85.9
CP +	6.0	1:9	80
CP -	6.94	1:10.5	95
RLT-PSC+	6.87	1:10.4	94
RLT-PSC-	5.8	1:8.79	77.9

Table 4.6 Volume of dilutent needed to provide 2 ng/ 3 µl of cDNA per PCR reaction

The cycling conditions required for the amplification of miRNA are described in the Material and Methods section 3.7.4. Real-time PCR was performed with the six samples shown in Table 4.6 above. Each sample was incubated with four different primers. The miRNA-29 primers included a, b and c subtypes. RNU6B was a PCR control and would act as the fourth primer. It is an endogenous reference RNA and its use would allow for normalisation of quantities of miRNA-29a, b, and c.

Control wells in triplicate were also included for each of the four primers. These wells contained the specific primers as well as the other components of the kit (See Section 3.7.4), but importantly lacked any cDNA.

4.5.3.2 Relative miRNA-29 quantification

MicroRNA-29a, b and c were each quantified in triplicate from the two different primary cell samples, PDAC 28.01.11 dish 7 passage 4, and CP 07.02.11 dish 7 passage 4.

Of the twelve control samples that were set up without cDNA, one of these showed contamination with cDNA, and produced a cp (crossing point) value of more than 40 cycles.

The Tm melting curve for all of the samples is displayed in Figure 5.8 below.

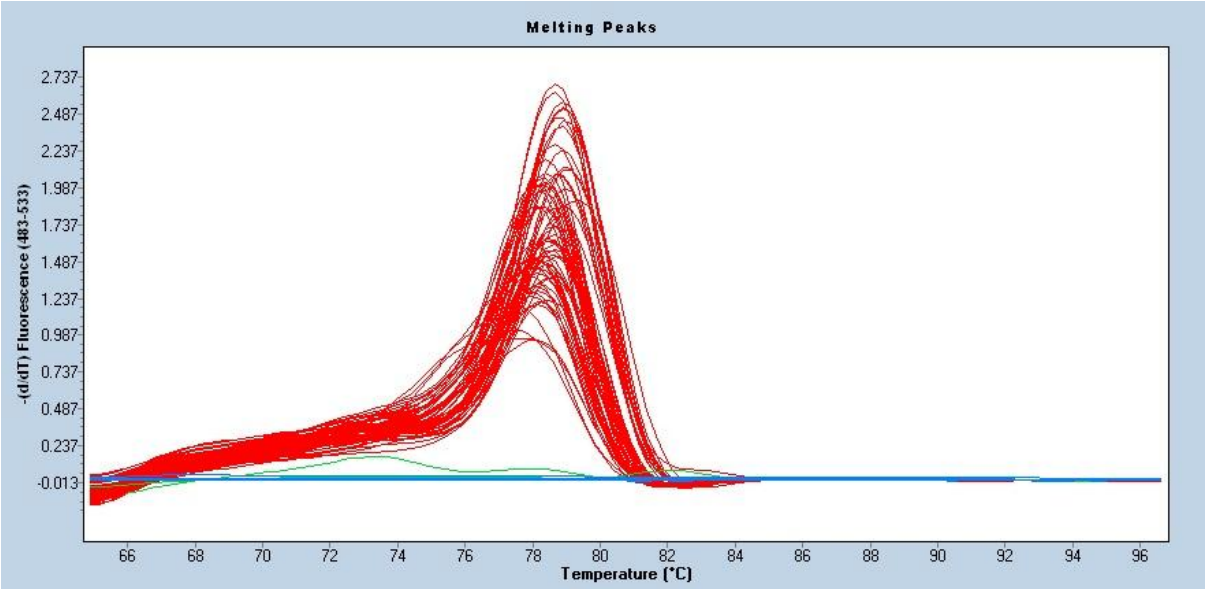

Figure 5.8 Melting curve analysis for all samples

Table 4.7 below displays the Cp values when real-time PCR was performed on the primary cell samples with the RNU6B control primer. For each sample, an average Cp value of the triplicate readings was taken. The net difference was then calculated between the average Cp value for the TGFβ treated (+) cells and that of the TGFβ untreated (-) cells for RNU6B control primer. These values are also listed in Tables 4.8, 4.9, and 5.0 and were later used to normalise the Cp values to any variations in the loading of the cDNA.

Sample cDNA	Cp values for RNU6B	Average of triplicate Cp values	Net difference between +/- samples for RNU6B
PDAC +	31.52	31.23	-2.38
PDAC +	30.9		
PDAC +	31.28		
PDAC -	32.94	33.62	
PDAC -	33.89		
PDAC -	34.03		
CP +	29.11	29.16	+0.76
CP +	29.17		
CP +	29.2		
CP -	28.32	28.4	
CP -	28.55		
CP -	28.33		
RLT-PSC+	26.43	26.42	+0.15
RLT-PSC +	26.33		
RLT-PSC +	26.49		
RLT-PSC –	26.28	26.27	
RLT-PSC –	26.26		
RLT-PSC –	26.27		

Table 4.7 Cp values for RNU6B control for real-time PCR performed on primary cultured cells and RLT-PSC samples treated +/-TGFβ

Figure 5.9 displays the real-time PCR data for all of the cell samples which were incubated with the RNU6B control primer. It is clear that there is variation in loading of cDNA between the different samples. The least difference was observed between TGF-beta treated and untreated RLT-PSC cells, with a Cp difference of just 0.15 (Table 4.7). The Cp difference of 0.76 for TGF-beta treated and untreated stellate 2 approaches a single cycle difference between the detection of RNU6B amplicon. The data for 'PDAC' cells (Cp difference of 2.38) indicate a greater than two cycle difference in the detection of RNU6B.

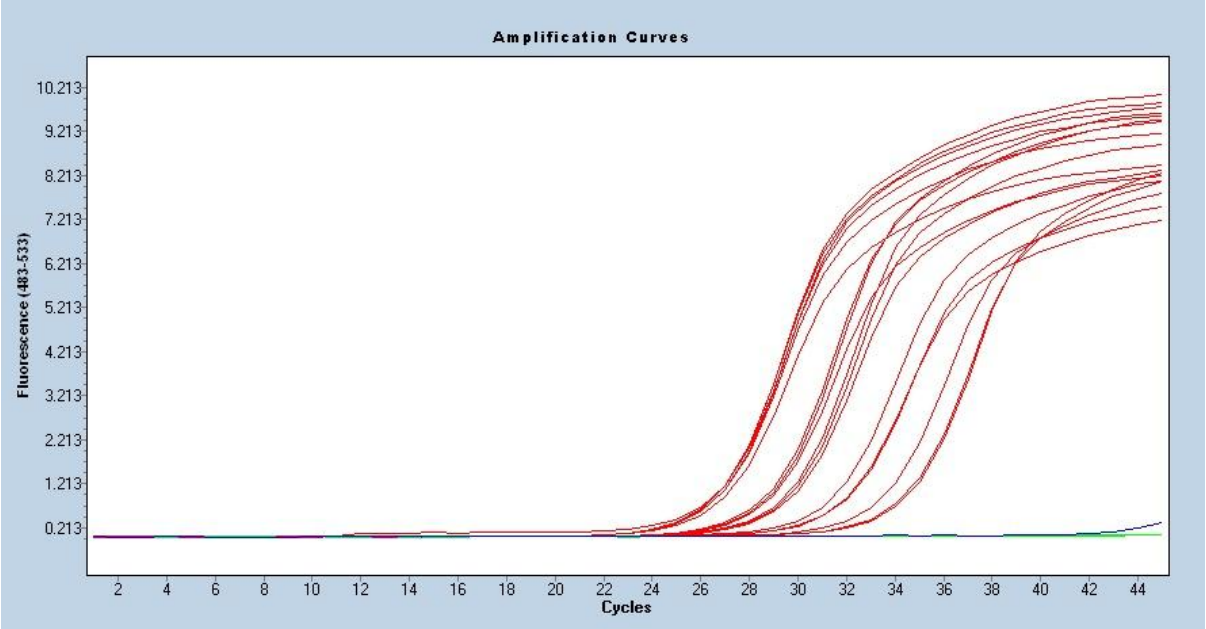

Figure 5.9 PCR curve for primary cultured cells and RLT-PSC samples with RNU6B control primer

The real-time PCR data are listed for miRNA-29a, b, and c in Tables 4.8, 4.9, and 5.0 respectively. The average Cp value was calculated for each primary cell sample using the triplicate values. The net difference between the average Cp value for the TGFβ treated (+) cells and the average Cp value for the TGFβ untreated (-) cells was calculated to provide an overall value of the expression for the particular miRNA-29.

Due to the variation in cDNA loading, as measured by differences in the Cp values between the detection of the control miRNA RNU6B in the untreated and TGF-beta treated setting for each cell type, the net Cp values for the RNU6B control were subtracted from the net Cp values for the miRNA-29 primers. This provided an approximate estimation yielding a Cp value for each miRNA normalised to variations in loading according to the RNU6B control primer. These calculations were performed for each of the miRNA-29 family subtypes.

Following these estimates, little difference in the levels of miRNA-29a and c between untreated and TGF-beta treated cells could be deduced, with the detection of these prospective micro-RNAs occurring within less than a single cycle difference of each other in the treated and untreated scenario. The only finding that showed promise was the apparent downregulation of miRNA-29b in the 'CP +' cells treated with TGFβ (Table 4.9). Here the Cp value for the TGFβ treated cells was almost one cycle higher than in the untreated cells.

This same micro RNA showed no difference in level in treated and untreated RLT-PSC cells, and unfortunately the data from 'PDAC' cells were inconclusive, with only a single reading obtained in TGF-beta treated state.

Sample cDNA	**Cp values for miRNA-29a**	**Average of triplicate Cp values**	**Net difference between +/- samples for miRNA-29a**	**Net difference between +/- samples for RNU6B (See Table 3.4)**	**Net difference between net miRNA-29a value and net RNU6B value**
PDAC +	34.57	35.4	-1.9	-2.38	-0.48
PDAC +	35.34				
PDAC +	36.22				
PDAC -	36.46	37.3			
PDAC -	38.22				
PDAC -	37.17				
CP +	31.99	32.0	+1.0	+0.76	+0.24
CP +	32.06				
CP +	31.82				
CP -	30.87	31.0			
CP -	31.16				
CP -	31.07				
RLT-PSC+	30.84	31.0	-0.6	+0.14	-0.45
RLT-PSC +	31.13				
RLT-PSC +	30.86				
RLT-PSC -	31.58	31.6			
RLT-PSC -	31.82				
RLT-PSC -	31.46				

Table 4.8 Cp values for miRNA-29a primer for real-time PCR performed on primary cell samples and RLT-PSCs treated +/-TGFβ.

Sample cDNA	Cp values for miRNA-29b	Average of triplicate Cp values	Net difference between +/- samples for miRNA-29b	Net difference between +/- samples for RNU6B (See Table 3.4)	Net difference between net miRNA-29b value and net RNU6B value
PDAC +	36.13	36.21	-0.90	-2.38	-1.48
PDAC +	37.4				
PDAC +	35.12				
PDAC -	37.12	37.12			
PDAC -	-				
PDAC -	-				
CP +	35.46	36.33	+1.74	+0.76	+0.98
CP +	36.67				
CP +	36.86				
CP -	34.74	34.58			
CP -	35.13				
CP -	33.89				
RLT-PSC+	34.83	34.96	+0.06	+0.15	+0.09
RLT-PSC+	34.58				
RLT-PSC +	35.49				
RLT-PSC -	34.24	34.90			
RLT-PSC -	35.36				
RLT-PSC -	35.12				

Table 4.9 Cp values for miRNA-29b primer for real-time PCR performed on primary cultured cell samples and RLT-PSCs treated +/-TGFβ.

Sample cDNA	Cp values for miRNA-29c	Average of triplicate Cp values	Net difference between +/- samples for miRNA-29c	Net difference between +/- samples for RNU6B (See Table 3.4)	Net difference between net miRNA-29c value and net RNU6B value
PDAC +	35.14	35.20	-2.31	-2.39	-0.08
PDAC +	34.86				
PDAC +	35.61				
PDAC -	40	37.51			
PDAC -	36.14				
PDAC -	36.4				
CP +	33.71	33.09	+1.02	+0.76	+0.26
CP +	32.8				
CP +	32.78				
CP -	32.31	32.07			
CP -	32.02				
CP -	31.89				
RLT-PSC+	31.53	31.75	-0.45	+0.14	-0.30
RLT-PSC +	31.89				
RLT-PSC +	31.85				
RLT-PSC -	32.11	32.21			
RLT-PSC -	32.32				
RLT-PSC -	32.2				

Table 5.0 Cp values for miRNA-29c primer for real-time PCR performed on primary cultured cell samples and RLT-PSCs treated +/-TGFβ.

4.6 Pancreatic primary cell cryopreservation

Table 5.1 provides details for all the primary cultured cells that have been cryopreserved. These samples are stored in freezer 2 of the GCLP biobank.

Primary cultured cell sample	Box location	Date frozen	No of times thawed	Morphology (Type A/B/C): refer to section 3.3	Recommended size flask for thawing (T75/T25)
PDAC 28.01.11 D4 P4	1 x 5	25.06.11	None	B	T75
CP 25.01.11 D14 P5	1 x 1	25.06.11	None	C	T75
PDAC 20.12.10 D15 P1	1 x 2	07.05.11	None	B	T75
PDAC 20.12.10 D7 P4	1 x 3	25.06.11	None	A	T75
PDAC 20.12.10 D5 P5	1 x 4	03.06.11	None	A	T75
PDAC 20.12.10 D7 P4	1 x 6	10.05.11	None	A	T75
Ampul 10.02.11 D5 P3	1 x 7	14.05.11	None	A	T75
PDAC 20.12.10 D5 P3	1 x 8	27.04.11	None	A	T25
PDAC 20.12.10 D7 P4	2 x 1	07.05.11	None	A	T25
CP 25.01.11 D3 P2	2 x 2	07.05.11	None	B	T75
PDAC 20.12.10 D7 P5	2 x 4	03.06.11	None	A	T75
CP 07.02.11 D20 P2	2 x 6	10.05.11	None	A	T25
PDAC 28.01.11 D4 P4	2 x 5	03.06.11	None	B	T75
CP 25.01.11 D8 P4	2 x 7	10.05.11	None	A	T75
CP 25.01.11 D8 P3	2 x 8	27.04.11	None	B	T75
PDAC 28.01.11 D4 P4	3 x 1	25.06.11	None	B	T75
Ampul 10.02.11 D5 P2	3 x 2	07.05.11	None	B	T75
CP 07.02.11 D6 P2	3 x 3	07.05.11	None	A	T75
PDAC 20.12.10 D7 P5	3 x 4	03.06.11	None	A	T75
CP 07.02.11 D11 P3	3 x 5	10.05.11	None	A	T75
CP 07.02.11 D14 P2	3 x 6	10.05.11	None	A	T75
Ampul 10.02.11 D5 P3	3 x 7	14.05.11	None	A	T75
PDAC 28.01.11 D4 P7	4 x 1	25.06.11	None	B	T75
CP 25.01.11 D14 P3	4 x 2	07.05.11	None	C	T75
PDAC 20.12.10 D5 P6	4 x 3	03.06.11	None	A	T75

CP 25.01.11 D7 P3	4 x 4	07.05.11	None	A	T75
CP 07.02.11 D3 P2	4 x 6	10.05.11	None	A	T75
PDAC 28.01.11 D10 P2	4 x 7	14.05.11	None	A	T75
PDAC 28.01.11 D14 P2	5 x 1	22.06.11	None	B	T75
CP 25.01.11 D9 P3	5 x 3	03.06.11	None	A	T75
CP 25.01.11 D7 P3	5 x 4	07.05.11	None	A	T75
PDAC 20.12.10 D5 P4	5 x 5	07.05.11	None	A	T25
CP 07.02.11 D5 P2	5 x 7	10.05.11	None	A	T25
CP 25.01.11 D14 P5	6 x 1	25.06.11	None	C	T75
CP 25.01.11 D14 P3	6 x 2	07.05.11	None	C	T75
CP 25.01.11 D3 P6	6 x 3	25.06.11	None	B	T75
PDAC 18.10.10 D3 P5	6 x 4	07.05.11	None	A	T75
PDAC 13.12.10 D11 P2	6 x 5	10.05.11	None	A	T25
PDAC 20.12.10 D8 P1	6 x 6	10.05.11	None	A	T75
PDAC 28.01.11 D4 P3	6 x 7	27.05.11	None	B	T75
PDAC 20.12.10 D5 P7	7 x 1	22.06.11	None	A	T75
PDAC 19.01.11 D12 P3	7 x 2	07.05.11	None	B	T75
PDAC 28.01.11 D4 P4	7 x 3	03.06.11	None	B	T75
PDAC 20.12.10 D5 P5	7 x 4	21.06.11	None	A	T75
CP 25.01.11 D9 P2	7 x 5	10.05.11	None	A	T75
CP 25.01.11 D6 P3	7 x 7	10.05.11	None	A	T75
PDAC 19.01.11 D12 P3	8 x 1	07.05.11	None	B	T75
CP 25.01.11 D14 P3	8 x 2	07.05.11	None	C	T75
CP 25.01.11 D3 P6	8 x 3	25.06.11	None	B	T75
PDAC 28.01.11 D10 P2	8 x 4	21.06.11	None	B	T75
PDAC 20.12.10 D7 P3	8 x 5	10.05.11	None	A	T75
CP 07.02.11 D21 P4	8 x 6	14.05.11	None	A	T75
CP 07.02.11 D16 P2	8 x 7	10.05.11	None	A	T25
CP 07.02.11 D21 P3	9 x 1	07.05.11	None	B	T75
CP 25.01.11 D6 P2	9 x 2	07.05.11	None	A	T25
PDAC 20.12.10 D9 P1	9 x 3	03.06.11	None	A	T75
PDAC 19.01.11 D12 P5	9 x 4	21.06.11	None	C	T75
CP 07.02.11 D19 P2	9 x 5	10.05.11	None	A	T25
Ampul 10.02.11 D7 P2	9 x 7	10.05.11	None	A	T25
CP 07.02.11 D21 P3	5 x 2	-	None	-	-

CP 25.01.11 D14 P5	5 x 6	01.07.11	none	C	T75
PDAC 28.01.11 D17 P1	7 x 6	04.07.11	none	A	T75
PDAC 28.01.11 D4 P8	2 x 3	01.07.11	none	B	T75
CP 07.02.11 D9 P3	4 x 5	04.07.11	none	A	T75
PDAC 20.12.10 D5 P5	9 x 6	10.07.11	none	A	T75
PDAC 20.12.10 D5 P4	3 x 8	10.07.11	none	A	T75

Table 5.1 Details of primary cultured cells stored in freezer 2 of the GCLP biobank.

CHAPTER 5:

DISCUSSION, PROSPECTS

FOR FUTURE STUDIES

5.1 Discussion

Two decades ago the pancreatic stellate cell was identified as the cell type predominantly responsible for the 'desmoplastic reaction' [123;128]. Since then, the number of PubMed cited reports investigating these cells has grown exponentially. Pancreatic stellate cells exhibit a great deal of interaction with cancer cells in vitro and in vivo. This feature, along with their contribution to the stromal reaction, has led to this cell type being proposed fundamental to pancreatic cancer progression [36;49].

As a result of the work described in this thesis, there are now approximately eighty vials of primary cultured cells that have been cryopreserved in Dr Costello's laboratory. Characterisation of these primary cells has revealed three distinct cell types. Whilst it is highly likely that one of these three cell types represents the pancreatic stellate cell, various difficulties encountered during characterisation meant that this was unconfirmed. According to the light microscopy and immunofluorescence data, which is discussed in more detail below, the cells with the Type A morphology (See Section 4.4) are the most likely candidates to be stellate cells. They displayed positive expression of alpha SMA, one of the four stellate cell markers. GFAP expression in these cells was also positive, along with negative or less intense isotype stains. However, the experiments lacked a control cell to stain negatively for GFAP (See Section 5.1.2.1). Hence, unfortunately it could not be stated with complete certainty that these primary cells do exhibit the GFAP protein.

Other than stellate cells, the primary cultured cells may instead represent another pancreatic stromal cell type, such as a cancer-associated fibroblast or myofibroblast. Either way, once fully characterised these primary cells can be utilised in experiments in Dr Costello's laboratory, as an adjunct to the epithelial cancer cell lines that are frequently used for pancreatic cancer research.

5.1.1 Isolation and culture of primary cells

The protocols for pancreatic stellate cell culture (See Material and Methods Section 3.0 to 3.5) were kindly shared by Dr Phoebe Phillips, an internationally recognised expert in this field. Her colleagues, led by Professor Apte were amongst the first researchers in the world to isolate stellate cells from the pancreas [43;123]. It proved necessary to adapt the methods in order to suit research practices here at the Royal Liverpool University Hospital (See Section 4.1). Measures for collecting pancreas samples were already in place. These were performed to GCLP standards, thus limiting inter-sample variation attributed to inconsistent collection or processing methods. Having adjusted standard operating procedures (SOP) and information management tools (LIMS), all of the necessary procedures were in place to collect tissue samples for the purposes of PSC culture, and to cryopreserve cultured cells within the GCLP facility.

As explained in section 4.1.1, Dr Phillips' protocols were refined to cater for the differences in the way surgical samples are collected between our two institutions. The main problem encountered here was the diversion of samples from Theatre to Pathology immediately after resection, due to diagnostic purposes. Hence for reasons beyond my control, precious time was being lost transporting the specimen back and forth, thus delaying its passage into culture. Despite these obstacles, increased liaison with pathologists, surgeons and theatre staff ensured this inevitable time period in transport was minimised.

Additional problems I encountered related to the timing of 'explant' removal from the culture dish and passaging or subculturing of cells. I quickly deduced that the primary cells I had plated in culture exhibited poor tolerability to many types of cell dissociation agent. Literature searches relating to PSC culture methods on Medline unfortunately yielded only a few resources, none of which included detailed protocols for their explant culture [89;124;125;128].

Many of the early primary cell cultures perished for the reasons mentioned above. Section 4.1.2 describes the problems associated with fungal contamination, which was exacerbated by the use of 6-well plates, where the infection could potentially spread between the wells leading to the loss of all the cells from a patient sample. This is the reason why 40 mm diameter dishes were utilised in later cultures. In my experience fungal contamination was best avoided by removing tissue once cell proliferation had ceased for more than 2 weeks.

Necrotic tissue left in the well was perhaps the reason for contamination. Furthermore, the fact that the cells had ceased to proliferate, was a possible indication that the tissue was no longer viable and had stopped providing the cells with growth factors, although I have no formal proof that this is the case.

Having experienced additional difficulties with the timing of cell passage, I concluded that the primary cells could not proliferate and remain viable in a T25 flask, unless they were extracted from a 40mm dish that was more than 50% confluent. This was perhaps due to the fact that the cells needed to be plated at a sufficiently high density to avail of paracrine stimulation that would facilitate growth in the new flask. Again, this was an observation I made through trial and error, and not one that I specifically set out to test.

Finally, passaging these cells, as eluded to above, was initially problematic. Eventually, having trialled a number of different cell dissociation reagents, a relatively weak form of trypsin reagent was purchased (see section 4.1.3) which was well tolerated by the primary cells. At this stage in my research, having acquired more experience in the primary culture and passage of these cells, I was in a position to devote greater amounts of time to characterising them.

5.1.2 Characterisation of primary cultured cells.

Early primary cultures of cells were examined with light microscopy at 10x, 20x, and 40x magnifications. Clear differences in morphology were observed between cells derived from the various dishes of the same patient sample (See Section 4.3). There was some confusion as to whether these differences in morphology represented alternative cell types, such as fibroblasts or myofibroblasts, or rather corresponded to variations in cell behaviour e.g. recent adherence, apoptosis, or senescence (See Section 4.3 Figures 4.5 and 4.6).

Therefore, cells were characterised for the detection of the four PSC markers: GFAP, desmin, alpha SMA and vimentin. Dr Phillips' protocols recommended the use of immunofluorescence staining for characterisation, and this staining method was also used by other research groups who have previously characterised PSCs [89;124;125]. Prior to beginning

characterisation, we received an immortalised pancreatic stellate cell line (RLT-PSC) [89] as a kind gift from Dr Ralf Jesenofsky, University of Heidelberg, to use as positive control cell in our experiments. Several epithelial cancer cell lines were being cultured in Dr Costello's laboratory and were utilised as potential negative cell controls.

5.1.2.1 The search for a negative control cell

As shown in Section 4.4.1, MiaPaCa-2 cells unexpectedly stained positively for GFAP (Figure 4.9C). The rabbit isotype control stained negatively in these cells (Figure 4.8D), suggesting that GFAP antibody binding was specific. Despite this, certain precautionary measures were taken to reduce the chance of non-specific binding in subsequent IF experiments. For instance, in Section 4.4.2, the secondary antibodies were increased in dilution from 1:100 to 1:400. A high concentration of secondary antibody such as 1:100 could have caused non-specific binding in the first experiment. In addition, different types of secondary antibody were used in Section 4.4.2 to ensure that none of the previous antibodies were faulty.

In Section 4.4.2 positive fluorescence was again observed in the supposed negative control cell. This time the MiaPaCa-2 cells had been stained for desmin and vimentin (Section 4.4.2 Figure 5.1). However, the results were discounted following the analysis of the rabbit isotype images. Bright fluorescence was observed in these images thus indicating that non-specific binding was taking place (Figure 5.1).

In section 4.4.3 MiaPaCa-2 cells were replaced with another cancer cell line named Panc-1 cells. Other changes included a variation of the blocking method in order to reduce the chances of background staining, and a reduction in the concentration of secondary antibody from 1:400 to 1:1000. All of these changes were made in an attempt to achieve a negative stain in the Panc-1 cancer cells. Furthermore, another set of GFAP and desmin antibodies were purchased from DAKO, the reason for this being that the pattern of staining in the MiaPaCa-2 cells in previous experiments could have been attributed to the low specificity of the primary antibodies from Abcam.

Unfortunately, the Panc-1 cells did stain positively for GFAP with the new antibody from DAKO (Section 4.4.3 Figure 5.2), thus probably ruling out primary antibody non-specificity as the cause of these cells expressing stellate cell markers. No desmin expression was detected in PDAC 20.12.10 dish 5 passage 4, CP 25.01.11 dish 8 passage 2, RLT-PSC, or Panc-1 cells, perhaps because the antibody was used at too high a dilution (1:200, 1:500). Secondary antibody was also used independently to stain these four cell types to discover any non-specific binding (Figure 5.3). A very faint red fluorescence was noticed in all of these images, indicating that the cy3 antibody was giving rise to a weak signal, despite the absence of primary antibody. However, this is unlikely to be the reason for the more intense red staining observed in the cancer cells, as it is very low in intensity compared to the red stain observed in those images (Section 4.4.1 Figure 4.9 and Section 4.4.2 Figure 5.1).

Thus far, MiaPaCa-2 and Panc-1 cancer cells had both expressed mesenchymal markers which was an unexpected finding (Sections 4.4.1 to 4.4.3). Therefore, a literature search was performed in order to explore whether this characteristic of cancer cell lines had been reported elsewhere. In a recent study, Collisson et al [3] described different subtypes of PDAC. They found that both Panc-1 and MiaPaca-2 cells have what they termed a 'quasi-mesenchymal' phenotype (Figure 6.0), and expressed some mesenchymal markers. These findings provided an explanation for the results observed in the first three IF characterisation experiments described above. Collisson et al [3] also labelled Suit-2 cancer cells as having a 'classical' phenotype, meaning that they do not express mesenchymal markers. Hence, Suit-2 cancer cells were subsequently trialled as a negative control cell in Section 4.4.5.

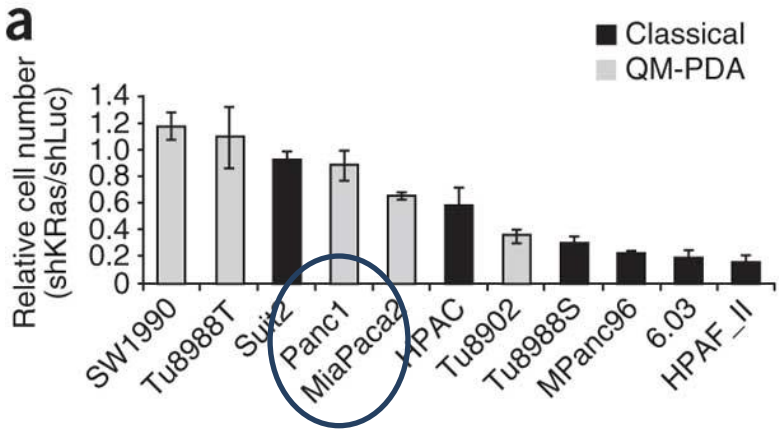

Figure 6.0 Collisson et al [3] reported subtypes of PDAC. Panc-1 and MiaPaca-2 cells have a QM (quasimesenchymal) phenotype.

Surprisingly, the Suit-2 cells also exhibited mesenchymal markers. Hence, the data from Collisson et al [3] did not correlate with the results in this thesis. The only plausible explanation for these results is that the Suit-2 cells in our laboratory might be contaminated with a different type of cancer cell line. Ideally, this experiment would be repeated after rigorous genotyping analysis of the Suit-2 cells in order to validate their identity.

A different study conducted by Arumugam and colleagues [129] discussed the occurrence of EMT in pancreatic cancer cell lines cultured in vitro. They later demonstrated that both MiaPaCa-2 cells and Panc-1 cells were able to express vimentin after several years in culture. A third study by Zhang and colleagues [130] revealed that breast cancer cell lines showed neuronal marker expression in addition to their usual epithelial markers. Hence, the expression of mesenchymal markers in MiaPaCa-2 and Panc-1 cells has been observed by others. From these findings, and the negative results of the secondary antibody only stain (Section 4.4.3 Figure 5.2), it is probable that nonspecific binding is not taking place, and that the methods and reagents currently being used for blocking and staining are working sufficiently.

However, there still remains the unexplained finding of intense staining displayed by the rabbit isotype (Section 4.4.2 Figure 5.1) which initially suggested that non-specific binding had taken place. As displayed in Section 4.4.3 Figure 5.2, both rabbit and mouse isotypes were used at a dilution of 1:200, although only the rabbit isotype was positively stained. In fact, the rabbit isotype is consistently staining positive throughout the IF stains (Figure 5.1, 5.2, 5.5), whilst the mouse isotype has been negative. This could indicate a problem with the rabbit isotype control antibody. Therefore, an alternative rabbit isotype should be purchased for future experiments, or the mouse isotype should be utilised where possible.

5.1.2.2 GFAP, desmin, and vimentin expression

Having established that antibodies were seemingly working effectively and binding specifically despite the existence of positive staining in the cancer cell lines, the other cells could now be analysed for their expression of GFAP, desmin, and vimentin.

The Type A morphology cells, RLT-PSCs, MiaPaCa-2, and Panc-1 cells all demonstrated expression of GFAP (See Sections 4.4.1, 4.4.3, and 4.4.5). These cells were also treated with an isotype control antibody, which stained either negatively, or less intensely than the GFAP antibody. Hence, this was an indication that non-specific binding was not taking place. Furthermore, two different GFAP antibodies were utilised successfully in these experiments to ensure that neither of the primary antibodies were binding non-specifically.

Desmin expression was assessed in sections 4.4.2 to 4.4.4. Positive fluorescence for desmin was detected in section 4.4.2, although this was associated with bright staining for the rabbit isotype control antibody. Once again, I am unsure whether this was non-specific binding associated with the desmin antibody, or there was a problem with the rabbit isotype antibody which has repeatedly stained positively under different experimental conditions as described above. A desmin antibody from a different provider (DAKO) was utilised in section 4.4.3, though the staining of all cells was negative at dilutions of 1:200 and 1:500. Hence, in section 4.4.4 this desmin antibody was reapplied at a dilution of 1:50, which demonstrated very weak expression of desmin in the primary cells (Type A morphology). The BXPC3 cancer cells did not show desmin expression, and the mouse isotype was negative for the primary cells, thus ruling out non-specific binding. Therefore, in conclusion there possibly was a some degree of desmin expression, yet this was of a low intensity and it is debatable as to whether it should be considered as positive or negative expression. A similar result was produced for the two different samples of Type A morphology cells.

Vimentin expression was assessed in Section 4.4.2. This was positive in two samples of Type A morphology cells and in the MiaPaCa-2 cells. However, no goat isotype antibody was utilised and so one cannot be sure whether this fluorescence was specific to vimentin expression.

5.1.2.3 Alpha SMA expression

As expected, the MiaPaCa-2, Panc-1, BXPC3, and Suit-2 cancer cell lines all lacked expression of the alpha SMA protein. Surprisingly, the immortalised pancreatic stellate cell line (RLT-PSC) also stained negatively for alpha SMA (Section 4.4.1 Figure 4.9D). This is despite a report from Jesnowski et al [89] displaying fluorescent images of these cells with

positive expression. This paper was published in 2005. Perhaps these cells have differentiated in some way during this time or due to conditions in culture in our laboratory in Liverpool, resulting in absent expression of this cytoskeletal protein. Hence, no positive control cell was available to represent alpha SMA expression. Despite this, the distinctive strand-like staining (Section 4.4.1 Figure 4.9A), coupled with the lack of expression in the cancer cell lines (Section 4.4.1 Figure 4.9C), meant that the positive staining was unlikely to represent non-specific binding.

As shown in Section 4.4.1 Figure 4.9B, some of the PDAC 18.10.10 well passage 2 cells (type A) did not exhibit alpha SMA expression. In fact, during this experiment only around 20% of the cells displayed this protein. Similar findings were made in section 4.4.3 when the PDAC 20.12.10 dish 5 passage 3 cells (type A) were stained. Bachem and colleagues [128] have successfully cultured human pancreatic stellate cells. They reported that the proportion of their cells exhibiting alpha SMA stain is more than 70% per flask.

This low proportion of alpha SMA expression amongst 'type A' morphology cells was not a universal finding however. For example, PDAC 28.01.11 Dish 7 passage 4 cells (Section 4.4.6), and PDAC 13.12.10 well 9 passage 2 cells together with CP 07.02.11 dish 7 passage 2 cells (Section 4.4.4) were stained with alpha SMA at various dilutions. More than 90% of the cells exhibited positive expression in these three samples of Type A morphology primary cells.

Therefore, the low quantity of cells expressing alpha SMA in some of the cell samples may be due to contamination with non alpha SMA expressing cells, such as inactivated fibroblasts or myofibroblasts. In fact Bachem at el [128] also reported that the most commonly observed contaminating cells in their primary cultures were non alpha SMA expressing myofibroblasts.

Alternatively, the low quantity of cells expressing alpha SMA in some of the cell samples may be due to the variable dilution of the alpha SMA antibody between experiments. Of the samples mentioned above, the PDAC 28.01.11 dish 7 passage 4 cells were stained at 1:400 and 1:200 (Section 4.4.6 Figure 5.6), and the PDAC 13.12.10 well 9 passage 2 cells and CP 07.02.11 dish 7 passage 2 cells at 1:100 (Section 4.4.4 Figure 5.4). These three samples displayed greater than 90% positive expression for alpha SMA. Conversely, the PDAC 18.10.10 well 3 passage 2 (Section 4.4.1 Figure 4.9), and PDAC 20.12.10 dish 5 passage 2 cells (Section 4.4.3 Figure 5.2) which were both 20% positive, were stained at 1:500. It cannot be ruled out that this small difference in antibody dilution caused the large increase in

the proportion of antigen expression detected, and this should be tested formally in future work.

The alpha SMA protein was also exhibited by 'type B' and 'type C' morphology cells (Sections 4.4.3, 4.4.6, and Section 4.4.5 respectively). Less than 5% of the PDAC 28.01.11 dish 4 passage 5 cells (Type B) displayed alpha SMA expression at dilutions of both 1:400 or 1:200 (Section 4.4.6 Figure 5.6). Interestingly, over 90% of the cells that were exposed to TGFβ treatment (Material and Methods Section 3.7.1) displayed expression of alpha SMA (1:200) afterwards. The fact that these 'type B' morphology cells began to express alpha SMA when exposed to TGFβ, coupled with their lack of GFAP expression, could indicate that they are inactivated fibroblasts that transformed into an activated state by exposure to TGFβ.

PDAC 19.01.11 dish 12 passage 3 cells, which had the type C morphology (Section 4.3 Figure 4.7) were also stained with alpha SMA and over 50% of the cells showed positive expression (Section 4.4.5 Figure 5.5). However, as mentioned above, these cells lacked GFAP and desmin expression which implies that they cannot be activated PSCs.

Due to the pure populations of alpha SMA-positive cells found in the PDAC 28.01.11 dish 7 passage 4 flask (90%), along with the myofibroblast-like appearance of the cells (type A morphology), these are likely to be either activated stellate cells or cancer-associated myofibroblasts. If this data is considered along with the positive expression of GFAP, this suggests that these 'type A' morphology cells are more likely to represent activated PSCs than myofibroblasts.

5.1.2.4 Conclusions and further characterisation

There is solid evidence that the primary cultured cells with 'Type A' morphology exhibit alpha SMA protein expression. Corresponding negative isotype stains signified that antibody binding was specific. Furthermore, all of the other cell types failed to exhibit this marker.

No negative control cell was established for GFAP, desmin or vimentin expression. However, there was convincing evidence for positive GFAP expression in the primary cells due to a combination of positive GFAP antibody stains and negative or weak isotype stains.

These results were corroborated in two separate experiments (See Sections 4.4.1 and 4.4.3). Despite this, the lack of a negative control cell means that one cannot say with absolute certainty that the primary cells do express the GFAP protein.

Desmin expression in these cells was unconvincing and remains to be proven. Due to time restrictions, desmin expression was only measured on one occasion at the optimal dilution for the antibody. Thus, ideally this experiment would be repeated to reveal whether the 'type A' morphology cells exhibit the desmin protein. Vimentin expression has been shown to be positive, although the lack of an isotype control means that this expression could have been a result of non-specific binding.

Further characterisation experiments should incorporate the use of other cell lines to act as control cells, including fibroblasts or smooth muscle cells to represent negative controls. As mentioned in Section 5.1.2.1 several studies suggest cancer cells are able to express mesenchymal markers, thus concurring with the findings in this thesis. Moreover, an alternative immortalised pancreatic stellate cell line to 'RLT-PSC' should be utilised as a positive cell control in subsequent experiments, for the reason that the 'RLT-PSC' cell line failed to exhibit any alpha SMA or desmin expression.

5.1.3 Evaluation of microRNA expression in primary cultured cells

A preliminary investigation was undertaken into the regulation of miRNA-29 in primary cultured cells derived from two patients (Type A morphology) and the RLT-PSC cell line. As mentioned earlier, cells with the type A morphology may possibly comprise pancreatic stellate cells in view of their positive expression of alpha SMA and GFAP in previous experiments (See Section 3).

The idea to investigate the aforementioned particular family of microRNAs was gleaned from a recent report into liver fibrosis [131]. The authors found levels of miRNA-29 to be significantly raised in HSCs compared to other resident liver cells. Exposure of these cells to TGFβ elicited a significant reduction in their miRNA-29 expression. Up-regulation of this miRNA was also associated with a reduction in the expression of several ECM collagen genes.

PSCs and HSCs display an almost identical gene expression profile which is 99% similar at the mRNA level, and there has also been speculation of whether these cells could share a common origin in the bone marrow [60]. Therefore, it would be interesting to elucidate whether the same mechanisms of miRNA regulation highlighted by the study above are also being mediated in our cells.

Eventually, we plan to analyse the expression of all known microRNAs in both disease associated and quiescent pancreatic stellate cells. However, with the recent publication of this report into liver fibrosis, we took the opportunity to take a preliminary examination of microRNA expression in our primary cells, starting with the miRNA-29 family.

Two primary cultured cell samples, one derived from a patient with PDAC, the other from a patient with CP were utilised in these experiments, along with the immortalised pancreatic stellate cell line (RLT-PSC). As explained in the Material and Methods Section 3.7.1, some of the cells from each of these samples were exposed to TGFβ, and others were left untreated thus resulting in six different samples from which RNA was purified.

Unfortunately, the results of the preliminary experiment shown here were rather inconclusive. Despite cDNA samples being quantified using a nanodrop spectrophotometer beforehand (See Section 4.5.3.1 Table 4.5), the loaded cDNA concentration varied between the different

samples (Figure 5.9). These variations were revealed from the use of an endogenously expressed RNA molecule named RNU6B, which acted as the PCR control primer. RNU6B is a widely used endogenous reference RNA in many miRNA quantification studies because of its small size (45 nt).

Several calculations were performed using the Cp values for the control primer and the miRNA primers, in an attempt to normalise the cDNA loading between samples (Tables 4.8, 4.9, and 5.0). Following these estimates, little difference in the levels of miRNA-29a and c between untreated and TGF-beta treated cells could be deduced. The only finding that showed promise was the apparent downregulation of miRNA-29b in the 'CP' primary cells treated with TGFβ (Table 4.9). Here the Cp value for the TGFβ treated cells was almost one cycle higher than in the untreated cells. However, the downregulation of this miRNA was not corroborated in any of the other cell samples.

Clearly, solid conclusions cannot be drawn from these results because the normalisation calculations that were carried out were only an estimate. The experiment would have to be repeated, this time ensuring that cDNA is loaded equally between the different samples. Furthermore, the real-time PCR data would benefit from the use of another primer control, in addition to RNU6B, just in case this control is actually being regulated under the experimental conditions.

5.2 Prospects for Future Study

We propose to analyse the expression of all known microRNAs in human pancreatic stellate cells. Apart from utilising disease associated stellate cells, attempts will also be made to culture quiescent cells from the normal pancreas to provide a control cell in the forthcoming experiments.

The stocks of primary cultured cells in our laboratory which were isolated and characterised in this thesis are likely to be stellate cells, but require further characterisation before they can be utilised in such microRNA investigations.

The analysis of microRNAs will be carried out using an array-based approach, which will highlight significant microRNA targets that will subsequently be validated using techniques such as quantitative real-time PCR.

MicroRNAs are implicated in a whole host of cellular processes including the epigenetic regulation of cancer related genes [108]. Exploration of identified targets in pancreatic stellate cells should provide more insight into the behaviour of these cells. More understanding is required of what mediates the transformation of PSCs from their quiescent to an activated state, and whether this process can be halted or even reversed.

Reference List

(1) Greenfield LJ, Mulholland MW, Ovid Technologies I. Greenfield's surgery scientific principles and practice. 5th ed ed. Philadelphia: Wolters Kluwer Health/Lippincott Williams & Wilkins; 2010.

(2) Gray H, Carter HV. Anatomy descriptive and surgical. 1995.

(3) Collisson EA, Sadanandam A, Olson P, Gibb WJ, Truitt M, Gu S et al. Subtypes of pancreatic ductal adenocarcinoma and their differing responses to therapy. Nat Med 2011; 17(4):500-503.

(4) Morris PJ, Wood WC. Oxford textbook of surgery. 2nd ed ed. Oxford: Oxford University Press; 2000.

(5) Moore KL, Dalley AF, Agur AMR. Clinically oriented anatomy. 5th ed ed. Philadelphia: Lippincott Williams & Wilkins; 2006.

(6) Guyton AC, Hall JE. Textbook of medical physiology. 11th ed ed. Philadelphia: Elsevier Saunders; 2006.

(7) Castellanos E, Berlin J, Cardin DB. Current treatment options for pancreatic carcinoma. Curr Oncol Rep 2011; 13(3):195-205.

(8) Saif MW. Pancreatic neoplasm in 2011: an update. JOP 2011; 12(4):316-321.

(9) Hidalgo M. Pancreatic cancer. N Engl J Med 2010; 362(17):1605-1617.

(10) Blackford A, Parmigiani G, Kensler TW, Wolfgang C, Jones S, Zhang X et al. Genetic mutations associated with cigarette smoking in pancreatic cancer. Cancer Res 2009; 69(8):3681-3688.

(11) Vincent A, Herman J, Schulick R, Hruban RH, Goggins M. Pancreatic cancer. Lancet 2011; 378(9791):607-620.

(12) Grocock CJ, Vitone LJ, Harcus MJ, Neoptolemos JP, Raraty MG, Greenhalf W. Familial pancreatic cancer: a review and latest advances. Adv Med Sci 2007; 52:37-49.

(13) Hahn SA, Greenhalf B, Ellis I, Sina-Frey M, Rieder H, Korte B et al. BRCA2 germline mutations in familial pancreatic carcinoma. J Natl Cancer Inst 2003; 95(3):214-221.

(14) Ghaneh P, Costello E, Neoptolemos JP. Biology and management of pancreatic cancer. Gut 2007; 56(8):1134-1152.

(15) Brugge WR, Lauwers GY, Sahani D, Fernandez-Del CC, Warshaw AL. Cystic neoplasms of the pancreas. N Engl J Med 2004; 351(12):1218-1226.

(16) Maitra A, Fukushima N, Takaori K, Hruban RH. Precursors to invasive pancreatic cancer. Adv Anat Pathol 2005; 12(2):81-91.

(17) Matthaios D, Zarogoulidis P, Balgouranidou I, Chatzaki E, Kakolyris S. Molecular pathogenesis of pancreatic cancer and clinical perspectives. Oncology 2011; 81(3-4):259-272.

(18) Crippa S, Fernandez-Del CC, Salvia R, Finkelstein D, Bassi C, Dominguez I et al. Mucin-producing neoplasms of the pancreas: an analysis of distinguishing clinical and epidemiologic characteristics. Clin Gastroenterol Hepatol 2010; 8(2):213-219.

(19) Sipos B, Frank S, Gress T, Hahn S, Kloppel G. Pancreatic intraepithelial neoplasia revisited and updated. Pancreatology 2009; 9(1-2):45-54.

(20) Kleeff J, Beckhove P, Esposito I, Herzig S, Huber PE, Lohr JM et al. Pancreatic cancer microenvironment. Int J Cancer 2007; 121(4):699-705.

(21) Jones S, Zhang X, Parsons DW, Lin JC, Leary RJ, Angenendt P et al. Core signaling pathways in human pancreatic cancers revealed by global genomic analyses. Science 2008; 321(5897):1801-1806.

(22) Yachida S, Jones S, Bozic I, Antal T, Leary R, Fu B et al. Distant metastasis occurs late during the genetic evolution of pancreatic cancer. Nature 2010; 467(7319):1114-1117.

(23) Campbell PJ, Yachida S, Mudie LJ, Stephens PJ, Pleasance ED, Stebbings LA et al. The patterns and dynamics of genomic instability in metastatic pancreatic cancer. Nature 2010; 467(7319):1109-1113.

(24) Neoptolemos JP. Adjuvant treatment of pancreatic cancer. Eur J Cancer 2011; 47 Suppl 3:S378-S380.

(25) Diener MK, Fitzmaurice C, Schwarzer G, Seiler CM, Antes G, Knaebel HP et al. Pylorus-preserving pancreaticoduodenectomy (pp Whipple) versus pancreaticoduodenectomy (classic Whipple) for surgical treatment of periampullary and pancreatic carcinoma. Cochrane Database Syst Rev 2011;(5):CD006053.

(26) Aung KL, Smith DB, Neoptolemos JP. Adjuvant therapy for pancreatic cancer. Expert Opin Pharmacother 2007; 8(15):2533-2541.

(27) Ghaneh P, Smith R, Tudor-Smith C, Raraty M, Neoptolemos JP. Neoadjuvant and adjuvant strategies for pancreatic cancer. Eur J Surg Oncol 2008; 34(3):297-305.

(28) Neoptolemos JP, Stocken DD, Bassi C, Ghaneh P, Cunningham D, Goldstein D et al. Adjuvant chemotherapy with fluorouracil plus folinic acid vs gemcitabine following pancreatic cancer resection: a randomized controlled trial. JAMA 2010; 304(10):1073-1081.

(29) Neoptolemos JP, Stocken DD, Tudur SC, Bassi C, Ghaneh P, Owen E et al. Adjuvant 5-fluorouracil and folinic acid vs observation for pancreatic cancer: composite data from the ESPAC-1 and -3(v1) trials. Br J Cancer 2009; 100(2):246-250.

(30) Conroy T, Desseigne F, Ychou M, Bouche O, Guimbaud R, Becouarn Y et al. FOLFIRINOX versus gemcitabine for metastatic pancreatic cancer. N Engl J Med 2011; 364(19):1817-1825.

(31) Moore MJ, Goldstein D, Hamm J, Figer A, Hecht JR, Gallinger S et al. Erlotinib plus gemcitabine compared with gemcitabine alone in patients with advanced pancreatic cancer: a phase III trial of the National Cancer Institute of Canada Clinical Trials Group. J Clin Oncol 2007; 25(15):1960-1966.

(32) Middleton G, Ghaneh P, Costello E, Greenhalf W, Neoptolemos JP. New treatment options for advanced pancreatic cancer. Expert Rev Gastroenterol Hepatol 2008; 2(5):673-696.

(33) Stathis A, Moore MJ. Advanced pancreatic carcinoma: current treatment and future challenges. Nat Rev Clin Oncol 2010; 7(3):163-172.

(34) Apte MV, Wilson JS. Mechanisms of pancreatic fibrosis. Dig Dis 2004; 22(3):273-279.

(35) Guturu P, Shah V, Urrutia R. Interplay of tumor microenvironment cell types with parenchymal cells in pancreatic cancer development and therapeutic implications. J Gastrointest Cancer 2009; 40(1-2):1-9.

(36) Chu GC, Kimmelman AC, Hezel AF, DePinho RA. Stromal biology of pancreatic cancer. J Cell Biochem 2007; 101(4):887-907.

(37) Bachem MG, Zhou S, Buck K, Schneiderhan W, Siech M. Pancreatic stellate cells--role in pancreas cancer. Langenbecks Arch Surg 2008; 393(6):891-900.

(38) Sawhney N, Garrahan N, Douglas-Jones AG, Williams ED. Epithelial--stromal interactions in tumors. A morphologic study of fibroepithelial tumors of the breast. Cancer 1992; 70(8):2115-2120.

(39) Vonlaufen A, Phillips PA, Xu Z, Goldstein D, Pirola RC, Wilson JS et al. Pancreatic stellate cells and pancreatic cancer cells: an unholy alliance. Cancer Res 2008; 68(19):7707-7710.

(40) Farrow B, Albo D, Berger DH. The role of the tumor microenvironment in the progression of pancreatic cancer. J Surg Res 2008; 149(2):319-328.

(41) Neesse A, Michl P, Frese KK, Feig C, Cook N, Jacobetz MA et al. Stromal biology and therapy in pancreatic cancer. Gut 2011; 60(6):861-868.

(42) Lohr M, Trautmann B, Gottler M, Peters S, Zauner I, Maillet B et al. Human ductal adenocarcinomas of the pancreas express extracellular matrix proteins. Br J Cancer 1994; 69(1):144-151.

(43) Apte MV, Park S, Phillips PA, Santucci N, Goldstein D, Kumar RK et al. Desmoplastic reaction in pancreatic cancer: role of pancreatic stellate cells. Pancreas 2004; 29(3):179-187.

(44) Haber PS, Keogh GW, Apte MV, Moran CS, Stewart NL, Crawford DH et al. Activation of pancreatic stellate cells in human and experimental pancreatic fibrosis. Am J Pathol 1999; 155(4):1087-1095.

(45) Masamune A, Watanabe T, Kikuta K, Shimosegawa T. Roles of pancreatic stellate cells in pancreatic inflammation and fibrosis. Clin Gastroenterol Hepatol 2009; 7(11 Suppl):S48-S54.

(46) Froeling FE, Feig C, Chelala C, Dobson R, Mein CE, Tuveson DA et al. Retinoic Acid-Induced Pancreatic Stellate Cell Quiescence Reduces Paracrine Wnt-beta-Catenin Signaling to Slow Tumor Progression. Gastroenterology 2011.

(47) Apte MV, Wilson JS. Mechanisms of pancreatic fibrosis. Dig Dis 2004; 22(3):273-279.

(48) Schneider E, Schmid-Kotsas A, Zhao J, Weidenbach H, Schmid RM, Menke A et al. Identification of mediators stimulating proliferation and matrix synthesis of rat pancreatic stellate cells. Am J Physiol Cell Physiol 2001; 281(2):C532-C543.

(49) Duner S, Lopatko LJ, Ansari D, Gundewar C, Andersson R. Pancreatic cancer: the role of pancreatic stellate cells in tumor progression. Pancreatology 2010; 10(6):673-681.

(50) Masamune A, Kikuta K, Satoh M, Suzuki N, Shimosegawa T. Protease-activated receptor-2-mediated proliferation and collagen production of rat pancreatic stellate cells. J Pharmacol Exp Ther 2005; 312(2):651-658.

(51) Phillips PA, Yang L, Shulkes A, Vonlaufen A, Poljak A, Bustamante S et al. Pancreatic stellate cells produce acetylcholine and may play a role in pancreatic exocrine secretion. Proc Natl Acad Sci U S A 2010; 107(40):17397-17402.

(52) Omary MB, Lugea A, Lowe AW, Pandol SJ. The pancreatic stellate cell: a star on the rise in pancreatic diseases. J Clin Invest 2007; 117(1):50-59.

(53) McCarroll JA, Phillips PA, Santucci N, Pirola RC, Wilson JS, Apte MV. Vitamin A inhibits pancreatic stellate cell activation: implications for treatment of pancreatic fibrosis. Gut 2006; 55(1):79-89.

(54) Bachem MG, Schunemann M, Ramadani M, Siech M, Beger H, Buck A et al. Pancreatic carcinoma cells induce fibrosis by stimulating proliferation and matrix synthesis of stellate cells. Gastroenterology 2005; 128(4):907-921.

(55) Schneiderhan W, Diaz F, Fundel M, Zhou S, Siech M, Hasel C et al. Pancreatic stellate cells are an important source of MMP-2 in human pancreatic cancer and accelerate tumor progression in a murine xenograft model and CAM assay. J Cell Sci 2007; 120(Pt 3):512-519.

(56) Vonlaufen A, Joshi S, Qu C, Phillips PA, Xu Z, Parker NR et al. Pancreatic stellate cells: partners in crime with pancreatic cancer cells. Cancer Res 2008; 68(7):2085-2093.

(57) Hwang RF, Moore T, Arumugam T, Ramachandran V, Amos KD, Rivera A et al. Cancer-associated stromal fibroblasts promote pancreatic tumor progression. Cancer Res 2008; 68(3):918-926.

(58) Fujita H, Ohuchida K, Mizumoto K, Egami T, Miyoshi K, Moriyama T et al. Tumor-stromal interactions with direct cell contacts enhance proliferation of human pancreatic carcinoma cells. Cancer Sci 2009; 100(12):2309-2317.

(59) Xu Z, Vonlaufen A, Phillips PA, Fiala-Beer E, Zhang X, Yang L et al. Role of pancreatic stellate cells in pancreatic cancer metastasis. Am J Pathol 2010; 177(5):2585-2596.

(60) Russo FP, Alison MR, Bigger BW, Amofah E, Florou A, Amin F et al. The bone marrow functionally contributes to liver fibrosis. Gastroenterology 2006; 130(6):1807-1821.

(61) Sparmann G, Kruse ML, Hofmeister-Mielke N, Koczan D, Jaster R, Liebe S et al. Bone marrow-derived pancreatic stellate cells in rats. Cell Res 2010; 20(3):288-298.

(62) Kallifatidis G, Beckermann BM, Groth A, Schubert M, Apel A, Khamidjanov A et al. Improved lentiviral transduction of human mesenchymal stem cells for therapeutic intervention in pancreatic cancer. Cancer Gene Ther 2008; 15(4):231-240.

(63) Direkze NC, Hodivala-Dilke K, Jeffery R, Hunt T, Poulsom R, Oukrif D et al. Bone marrow contribution to tumor-associated myofibroblasts and fibroblasts. Cancer Res 2004; 64(23):8492-8495.

(64) Zeisberg EM, Potenta S, Xie L, Zeisberg M, Kalluri R. Discovery of endothelial to mesenchymal transition as a source for carcinoma-associated fibroblasts. Cancer Res 2007; 67(21):10123-10128.

(65) Comoglio PM, Trusolino L. Cancer: the matrix is now in control. Nat Med 2005; 11(11):1156-1159.

(66) Grzesiak JJ, Bouvet M. The alpha2beta1 integrin mediates the malignant phenotype on type I collagen in pancreatic cancer cell lines. Br J Cancer 2006; 94(9):1311-1319.

(67) Armstrong T, Packham G, Murphy LB, Bateman AC, Conti JA, Fine DR et al. Type I collagen promotes the malignant phenotype of pancreatic ductal adenocarcinoma. Clin Cancer Res 2004; 10(21):7427-7437.

(68) Sethi T, Rintoul RC, Moore SM, MacKinnon AC, Salter D, Choo C et al. Extracellular matrix proteins protect small cell lung cancer cells against apoptosis: a mechanism for small cell lung cancer growth and drug resistance in vivo. Nat Med 1999; 5(6):662-668.

(69) Olive KP, Jacobetz MA, Davidson CJ, Gopinathan A, McIntyre D, Honess D et al. Inhibition of Hedgehog signaling enhances delivery of chemotherapy in a mouse model of pancreatic cancer. Science 2009; 324(5933):1457-1461.

(70) Farrow B, Albo D, Berger DH. The role of the tumor microenvironment in the progression of pancreatic cancer. J Surg Res 2008; 149(2):319-328.

(71) Chen G, Tian X, Liu Z, Zhou S, Schmidt B, Henne-Bruns D et al. Inhibition of endogenous SPARC enhances pancreatic cancer cell growth: modulation by FGFR1-III isoform expression. Br J Cancer 2010; 102(1):188-195.

(72) Kanno A, Satoh K, Masamune A, Hirota M, Kimura K, Umino J et al. Periostin, secreted from stromal cells, has biphasic effect on cell migration and correlates with the epithelial to mesenchymal transition of human pancreatic cancer cells. Int J Cancer 2008; 122(12):2707-2718.

(73) Fritz G, Just I, Kaina B. Rho GTPases are over-expressed in human tumors. Int J Cancer 1999; 81(5):682-687.

(74) Paszek MJ, Zahir N, Johnson KR, Lakins JN, Rozenberg GI, Gefen A et al. Tensional homeostasis and the malignant phenotype. Cancer Cell 2005; 8(3):241-254.

(75) Issa R, Zhou X, Constandinou CM, Fallowfield J, Millward-Sadler H, Gaca MD et al. Spontaneous recovery from micronodular cirrhosis: evidence for incomplete resolution associated with matrix cross-linking. Gastroenterology 2004; 126(7):1795-1808.

(76) Overall CM, Wrana JL, Sodek J. Transforming growth factor-beta regulation of collagenase, 72 kDa-progelatinase, TIMP and PAI-1 expression in rat bone cell populations and human fibroblasts. Connect Tissue Res 1989; 20(1-4):289-294.

(77) Shek FW, Benyon RC, Walker FM, McCrudden PR, Pender SL, Williams EJ et al. Expression of transforming growth factor-beta 1 by pancreatic stellate cells and its implications for matrix secretion and turnover in chronic pancreatitis. Am J Pathol 2002; 160(5):1787-1798.

(78) Overall CM, Kleifeld O. Tumour microenvironment - opinion: validating matrix metalloproteinases as drug targets and anti-targets for cancer therapy. Nat Rev Cancer 2006; 6(3):227-239.

(79) Coussens LM, Raymond WW, Bergers G, Laig-Webster M, Behrendtsen O, Werb Z et al. Inflammatory mast cells up-regulate angiogenesis during squamous epithelial carcinogenesis. Genes Dev 1999; 13(11):1382-1397.

(80) Neesse A, Wagner M, Ellenrieder V, Bachem M, Gress TM, Buchholz M. Pancreatic stellate cells potentiate proinvasive effects of SERPINE2 expression in pancreatic cancer xenograft tumors. Pancreatology 2007; 7(4):380-385.

(81) Radisky DC, Levy DD, Littlepage LE, Liu H, Nelson CM, Fata JE et al. Rac1b and reactive oxygen species mediate MMP-3-induced EMT and genomic instability. Nature 2005; 436(7047):123-127.

(82) Kalluri R, Zeisberg M. Fibroblasts in cancer. Nat Rev Cancer 2006; 6(5):392-401.

(83) Barnas JL, Simpson-Abelson MR, Yokota SJ, Kelleher RJ, Bankert RB. T cells and stromal fibroblasts in human tumor microenvironments represent potential therapeutic targets. Cancer Microenviron 2010; 3(1):29-47.

(84) Kuperwasser C, Chavarria T, Wu M, Magrane G, Gray JW, Carey L et al. Reconstruction of functionally normal and malignant human breast tissues in mice. Proc Natl Acad Sci U S A 2004; 101(14):4966-4971.

(85) Jones EA, Kinsey SE, English A, Jones RA, Straszynski L, Meredith DM et al. Isolation and characterization of bone marrow multipotential mesenchymal progenitor cells. Arthritis Rheum 2002; 46(12):3349-3360.

(86) Karnoub AE, Dash AB, Vo AP, Sullivan A, Brooks MW, Bell GW et al. Mesenchymal stem cells within tumour stroma promote breast cancer metastasis. Nature 2007; 449(7162):557-563.

(87) Feuerer M, Beckhove P, Garbi N, Mahnke Y, Limmer A, Hommel M et al. Bone marrow as a priming site for T-cell responses to blood-borne antigen. Nat Med 2003; 9(9):1151-1157.

(88) Schmitz-Winnenthal FH, Volk C, Z'graggen K, Galindo L, Nummer D, Ziouta Y et al. High frequencies of functional tumor-reactive T cells in bone marrow and blood of pancreatic cancer patients. Cancer Res 2005; 65(21):10079-10087.

(89) Jesnowski R, Furst D, Ringel J, Chen Y, Schrodel A, Kleeff J et al. Immortalization of pancreatic stellate cells as an in vitro model of pancreatic fibrosis: deactivation is induced by matrigel and N-acetylcysteine. Lab Invest 2005; 85(10):1276-1291.

(90) Esposito I, Menicagli M, Funel N, Bergmann F, Boggi U, Mosca F et al. Inflammatory cells contribute to the generation of an angiogenic phenotype in pancreatic ductal adenocarcinoma. J Clin Pathol 2004; 57(6):630-636.

(91) von Bernstorff W, Voss M, Freichel S, Schmid A, Vogel I, Johnk C et al. Systemic and local immunosuppression in pancreatic cancer patients. Clin Cancer Res 2001; 7(3 Suppl):925s-932s.

(92) Schmitz-Winnenthal FH, Volk C, Z'graggen K, Galindo L, Nummer D, Ziouta Y et al. High frequencies of functional tumor-reactive T cells in bone marrow and blood of pancreatic cancer patients. Cancer Res 2005; 65(21):10079-10087.

(93) Fukunaga A, Miyamoto M, Cho Y, Murakami S, Kawarada Y, Oshikiri T et al. CD8+ tumor-infiltrating lymphocytes together with CD4+ tumor-infiltrating lymphocytes and dendritic cells improve the prognosis of patients with pancreatic adenocarcinoma. Pancreas 2004; 28(1):e26-e31.

(94) Zou W. Immunosuppressive networks in the tumour environment and their therapeutic relevance. Nat Rev Cancer 2005; 5(4):263-274.

(95) Aoyagi Y, Oda T, Kinoshita T, Nakahashi C, Hasebe T, Ohkohchi N et al. Overexpression of TGF-beta by infiltrated granulocytes correlates with the expression of collagen mRNA in pancreatic cancer. Br J Cancer 2004; 91(7):1316-1326.

(96) Emmrich J, Weber I, Nausch M, Sparmann G, Koch K, Seyfarth M et al. Immunohistochemical characterization of the pancreatic cellular infiltrate in normal pancreas, chronic pancreatitis and pancreatic carcinoma. Digestion 1998; 59(3):192-198.

(97) Sato N, Maehara N, Goggins M. Gene expression profiling of tumor-stromal interactions between pancreatic cancer cells and stromal fibroblasts. Cancer Res 2004; 64(19):6950-6956.

(98) Yoshida S, Ujiki M, Ding XZ, Pelham C, Talamonti MS, Bell RH, Jr. et al. Pancreatic stellate cells (PSCs) express cyclooxygenase-2 (COX-2) and pancreatic cancer stimulates COX-2 in PSCs. Mol Cancer 2005; 4:27.

(99) Farrow B, Evers BM. Inflammation and the development of pancreatic cancer. Surg Oncol 2002; 10(4):153-169.

(100) van Heek NT, Meeker AK, Kern SE, Yeo CJ, Lillemoe KD, Cameron JL et al. Telomere shortening is nearly universal in pancreatic intraepithelial neoplasia. Am J Pathol 2002; 161(5):1541-1547.

(101) Armulik A, Abramsson A, Betsholtz C. Endothelial/pericyte interactions. Circ Res 2005; 97(6):512-523.

(102) Carmeliet P. VEGF as a key mediator of angiogenesis in cancer. Oncology 2005; 69 Suppl 3:4-10.

(103) Hanahan D, Folkman J. Patterns and emerging mechanisms of the angiogenic switch during tumorigenesis. Cell 1996; 86(3):353-364.

(104) Buchler P, Reber HA, Buchler MW, Friess H, Hines OJ. VEGF-RII influences the prognosis of pancreatic cancer. Ann Surg 2002; 236(6):738-749.

(105) Abdollahi A, Hahnfeldt P, Maercker C, Grone HJ, Debus J, Ansorge W et al. Endostatin's antiangiogenic signaling network. Mol Cell 2004; 13(5):649-663.

(106) Carmeliet P, Jain RK. Angiogenesis in cancer and other diseases. Nature 2000; 407(6801):249-257.

(107) Baker CH, Solorzano CC, Fidler IJ. Blockade of vascular endothelial growth factor receptor and epidermal growth factor receptor signaling for therapy of metastatic human pancreatic cancer. Cancer Res 2002; 62(7):1996-2003.

(108) Mardin WA, Mees ST. MicroRNAs: novel diagnostic and therapeutic tools for pancreatic ductal adenocarcinoma? Ann Surg Oncol 2009; 16(11):3183-3189.

(109) Esquela-Kerscher A, Slack FJ. Oncomirs - microRNAs with a role in cancer. Nat Rev Cancer 2006; 6(4):259-269.

(110) Bartel DP. MicroRNAs: genomics, biogenesis, mechanism, and function. Cell 2004; 116(2):281-297.

(111) Gregory RI, Yan KP, Amuthan G, Chendrimada T, Doratotaj B, Cooch N et al. The Microprocessor complex mediates the genesis of microRNAs. Nature 2004; 432(7014):235-240.

(112) Lee Y, Ahn C, Han J, Choi H, Kim J, Yim J et al. The nuclear RNase III Drosha initiates microRNA processing. Nature 2003; 425(6956):415-419.

(113) Buchholz M, Kestler HA, Holzmann K, Ellenrieder V, Schneiderhan W, Siech M et al. Transcriptome analysis of human hepatic and pancreatic stellate cells: organ-specific variations of a common transcriptional phenotype. J Mol Med (Berl) 2005; 83(10):795-805.

(114) Schickel R, Boyerinas B, Park SM, Peter ME. MicroRNAs: key players in the immune system, differentiation, tumorigenesis and cell death. Oncogene 2008; 27(45):5959-5974.

(115) Griffiths-Jones S. The microRNA Registry. Nucleic Acids Res 2004; 32(Database issue):D109-D111.

(116) Griffiths-Jones S, Grocock RJ, van Dongen S, Bateman A, Enright AJ. miRBase: microRNA sequences, targets and gene nomenclature. Nucleic Acids Res 2006; 34(Database issue):D140-D144.

(117) Griffiths-Jones S, Saini HK, van Dongen S, Enright AJ. miRBase: tools for microRNA genomics. Nucleic Acids Res 2008; 36(Database issue):D154-D158.

(118) Kozomara A, Griffiths-Jones S. miRBase: integrating microRNA annotation and deep-sequencing data. Nucleic Acids Res 2011; 39(Database issue):D152-D157.

(119) Rosenfeld N, Aharonov R, Meiri E, Rosenwald S, Spector Y, Zepeniuk M et al. MicroRNAs accurately identify cancer tissue origin. Nat Biotechnol 2008; 26(4):462-469.

(120) Mitchell PS, Parkin RK, Kroh EM, Fritz BR, Wyman SK, Pogosova-Agadjanyan EL et al. Circulating microRNAs as stable blood-based markers for cancer detection. Proc Natl Acad Sci U S A 2008; 105(30):10513-10518.

(121) Lu J, Getz G, Miska EA, Alvarez-Saavedra E, Lamb J, Peck D et al. MicroRNA expression profiles classify human cancers. Nature 2005; 435(7043):834-838.

(122) Roderburg C, Urban GW, Bettermann K, Vucur M, Zimmermann H, Schmidt S et al. Micro-RNA profiling reveals a role for miR-29 in human and murine liver fibrosis. Hepatology 2011; 53(1):209-218.

(123) Apte MV, Haber PS, Applegate TL, Norton ID, McCaughan GW, Korsten MA et al. Periacinar stellate shaped cells in rat pancreas: identification, isolation, and culture. Gut 1998; 43(1):128-133.

(124) Farrow B, Rowley D, Dang T, Berger DH. Characterization of tumor-derived pancreatic stellate cells. J Surg Res 2009; 157(1):96-102.

(125) Kruse ML, Hildebrand PB, Timke C, Folsch UR, Schafer H, Schmidt WE. Isolation, long-term culture, and characterization of rat pancreatic fibroblastoid/stellate cells. Pancreas 2001; 23(1):49-54.

(126) Ishida W, Mori Y, Lakos G, Sun L, Shan F, Bowes S et al. Intracellular TGF-beta receptor blockade abrogates Smad-dependent fibroblast activation in vitro and in vivo. J Invest Dermatol 2006; 126(8):1733-1744.

(127) Ihn H. Pathogenesis of fibrosis: role of TGF-beta and CTGF. Curr Opin Rheumatol 2002; 14(6):681-685.

(128) Bachem MG, Schneider E, Gross H, Weidenbach H, Schmid RM, Menke A et al. Identification, culture, and characterization of pancreatic stellate cells in rats and humans. Gastroenterology 1998; 115(2):421-432.

(129) Arumugam T, Ramachandran V, Fournier KF, Wang H, Marquis L, Abbruzzese JL et al. Epithelial to mesenchymal transition contributes to drug resistance in pancreatic cancer. Cancer Res 2009; 69(14):5820-5828.

(130) Zhang Q, Fan H, Shen J, Hoffman RM, Xing HR. Human breast cancer cell lines co-express neuronal, epithelial, and melanocytic differentiation markers in vitro and in vivo. PLoS One 2010; 5(3):e9712.

(131) Roderburg C, Urban GW, Bettermann K, Vucur M, Zimmermann H, Schmidt S et al. Micro-RNA profiling reveals a role for miR-29 in human and murine liver fibrosis. Hepatology 2011; 53(1):209-218.